

To the Graduate Council:

I am submitting herewith a thesis written by Jamie Manis Hudson entitled "The Resilient Response of Fine-Grained Tennessee Subgrade Soils." I have examined the final copy of this thesis for form and content and recommend that it be accepted in partial fulfillment of the requirements for the degree Master of Science, with a major in Civil Engineering.

Eric C. Drumm

Dr. Eric C. Drumm, Major Professor

We have read this thesis and
recommend its acceptance:

Alex B. Moore
Matthe Mould

Accepted for the Council:

Lew Minkel

Associate Vice Chancellor
and Dean of The Graduate School

STATEMENT OF PERMISSION TO USE

In presenting this thesis in partial fulfillment of the requirements for a Master's degree at The University of Tennessee, Knoxville, I agree that the Library shall make it available to borrowers under rules of the Library. Brief quotations from this thesis are allowable without special permission, provided that accurate acknowledgment of the source is made.

Permission for extensive quotation from or reproduction of this thesis may be granted by my major professor, or in his absence, by the Head of Interlibrary Services when, in the opinion of either, the proposed use of the material is for scholarly purposes. Any copying or use of the material in this thesis for financial gain shall not be allowed without my written permission.

Signature Jamie Hudson

Date December 3, 1992

THE RESILIENT RESPONSE OF FINE-GRAINED
TENNESSEE SUBGRADE SOILS

A Thesis

Presented for the

Master of Science

Degree

The University of Tennessee, Knoxville

Jamie Manis Hudson

December 1992

to my husband, Frank

ACKNOWLEDGEMENTS

The author wishes to thank Dr. Eric C. Drumm for providing the opportunity to work on this project and for his invaluable guidance and support throughout its duration. This volume would be sorely lacking without his input during its creation, and Dr. Drumm has made the graduate school experience an enjoyable one. The author also wishes to thank the Tennessee Department of Transportation for the financial support of this undertaking and also the project review committee for their valuable comments and suggestions. Special acknowledgement is also given to Professor A. B. Moore and Dr. Matthew Mauldon for their assistance by serving on the author's committee.

The magnitude of laboratory work performed here would have been impossible without the dedication of student assistants Mark Madgett, Derek Baker, Julia Ketron, and Craig Smith. Their various contributions to this project are enormous, and the author wishes to thank them for their hard work and their ability to maintain a sense of humor when the magnitude of tasks at hand seemed insurmountable. Also gratefully acknowledge is Mr. Curtis Allin, Civil Engineering Lab Technician, who readily shared not only his lab facilities but also his extensive knowledge of laboratory protocol. Sincere appreciation is also given to Dr. William F. Kane who provided the author an opportunity to gain valuable research experience as an undergraduate, and who kindled the interest

in soil mechanics that has ultimately led to the completion of this undertaking.

Finally, the author wishes to thank her husband Frank for his patience and understanding throughout her academic career. His support and encouragement have enhanced the learning experience, and have enabled the author to reach goals that at times seemed unattainable.

ABSTRACT

The resilient modulus is a relatively new material property that characterizes subgrade soil performance in a pavement system. The resilient modulus test procedure allows the measurement of resilient subgrade deflection by simulating in-situ traffic loadings. The magnitude of resilient subgrade deflection has been found to be a good indicator of pavement performance and inclusion of the resilient modulus in pavement design procedures should contribute to extended pavement life and decrease instances of mandatory pavement rehabilitation.

An investigation of the resilient modulus of seven fine-grained subgrade soils from across the state of Tennessee was conducted. Standard laboratory tests were performed to determine the index properties of each soil. Cyclic load triaxial tests were conducted at various water contents and dry densities in order to determine the effects of these parameters on the resilient response. The magnitude of applied confining pressure and deviator stress was also varied during testing to simulate variations in depth and lateral location from the applied wheel load. The specimen water content and the magnitude of applied deviator stress were found to significantly affect the resilient response of most of the soils tested. The effect of variations in the applied confining pressure on the resilient modulus was minimal. Variations in the specimen dry density affected only a few of the test specimens.

The data collected from all the laboratory tests for each soil were compiled in the form of a "Design Handbook" to be used by the Tennessee Department of Transportation for estimation of the resilient characteristics of future highway project subgrade soils.

TABLE OF CONTENTS

CHAPTER 1	
THE RESILIENT MODULUS AND ITS EFFECT ON	
PAVEMENT PERFORMANCE	1
1.1 Definition on the Resilient Modulus, M_r	1
1.2 The Effect of the Resilient Modulus on	
Pavement Performance	4
CHAPTER 2	
COMPARISON OF TEST PROCEDURES AND	
REVIEW OF RESILIENT MODULUS INVESTIGATIONS	7
2.1 Comparison of Test Procedures	7
2.2 Review of Resilient Modulus Testing	8
2.2.1 Variations in Equipment	8
2.2.1.1 Loading Systems	8
2.2.1.2 Deformation Measurement	
Devices	14
2.2.1.3 Load Cells	19
2.2.2 Specimen Preparation Considerations	20
2.2.2.1 Grouting	20
2.2.2.2 Thixotropy	21
2.2.3 Resilient Modulus Testing	23
2.2.3.1 Specimen Conditioning	23
2.2.3.2 Confining Pressure	25
2.2.3.3 Deviator Stress	28
2.2.4 Prediction of the Resilient Modulus	31
2.2.4.1 Predictions using CBR	31
2.2.4.2 Mathematical Models	33
2.2.4.2.1 Bilinear Model	33
2.2.4.2.2 Log-Log Model	34
2.2.4.2.3 Hyperbolic Model	35
2.2.4.2.4 Modified Hyperbolic	
Model	35
2.3 Effect of Compaction, Density and Water	
Content on the Resilient Modulus	36
2.3.1 Compaction	36
2.3.2 Density	40
2.3.3 Water Content	41
CHAPTER 3	
LABORATORY TESTING OF FINE-GRAINED TENNESSEE SUBGRADE	
SOILS	46
3.1 Selection of Representative Soils and Field	
Sampling	46
3.2 Properties of Representative Soils	49
3.2.1 Index Testing	49
3.2.2 Moisture-Density Relationships	50
3.2.3 California Bearing Ratio (CBR)	51

3.3	Resilient Modulus Testing of Fine-Grained Tennessee Subgrade Soils	52
3.3.1	Target Water Contents and Densities of Laboratory Test Specimens	52
3.3.2	Compaction of Test Specimens	53
3.4	Resilience Testing of Representative Soils	56
3.4.1	Test Apparatus	56
3.4.2	Test Procedure	57
3.4.3	Data Acquisition and Reduction	60
CHAPTER 4		
	RESILIENT RESPONSE OF FINE-GRAINED TENNESSEE SUBGRADE SOILS	62
4.1	Results of Laboratory Resilient Modulus Testing	62
4.2	Analysis of Results	65
4.2.1	Effect of Confining Pressure	66
4.2.2	Effect of Water Content	69
4.2.3	Effect of Dry Density	71
4.3	Design Handbook of Resilient Response	75
4.4	Mathematical Models	76
4.4.1	Bilinear Model	76
4.4.2	Log-Log Model	77
4.4.3	Hyperbolic Model	78
4.4.4	Modified Hyperbolic Model	79
CHAPTER 5		
	SUMMARY, CONCLUSIONS AND RECOMMENDATIONS FOR ADDITIONAL WORK	82
5.1	Summary and Conclusions	82
5.2	Recommendations For Additional Work	85
	LIST OF REFERENCES	87
	APPENDICES.	94
APPENDIX A		
	MODEL PARAMETERS AND RESILIENT MODULUS PLOTS	95
	Rutledge Pike	96
	Pellissippi Parkway Station 400	103
	Pellissippi Parkway Station 500	110
	Airport Connector Station 47	117
	Airport Connector Station 85	126
	State Route 20 Station 781+75	133
	State Route 20 Station 1081+50	140
APPENDIX B		
	DESIGN HANDBOOK OF RESILIENT RESPONSE	146
	Rutledge Pike	147
	Pellissippi Parkway Station 400	152
	Pellissippi Parkway Station 500	157
	Airport Connector Station 47	162

Airport Connector Station 85	167
State Route 20 Station 781+75	172
State Route 20 Station 1081+50	177
Examples of How Handbook May be Used to Estimate M _r	182
VITA	186

LIST OF TABLES

Table 2-1. Comparison of Suggested Testing Equipment For Four Resilient Modulus Test Procedures	9
Table 2-2. Comparison of Test Specimen Compaction Specifications For Four Resilient Modulus Test Procedures	10
Table 2-3. Comparison of Four Resilient Modulus Test Procedures for Cohesive Materials	11
Table 2-4. Comparison of Four Resilient Modulus Test Procedures For Granular Materials	12
Table 3-1. Classifications and Index Properties of Candidate Soil Samples	48
Table 3-2. CBR Data for Selected Soil Samples	52
Table 3-3. Calibration Constants	61
Table 4-1. Effect of Variations in Dry Density on the Resilient Modulus for A.C. Station 47 Tests	73
Table 4-2. Effect of Variations in Dry Density on the Resilient Modulus for P.P. Station 400 Soil	74
Table 4-3. Effect of Variations in Dry Density on the Resilient Modulus for P.P. Station 500 Soil	74
Table 4-4. Effect of Variations in Dry Density on the Resilient Modulus for Rutledge Pike Soil	75
Table A-1. Hyperbolic and Log-Log Model Parameters For Rutledge Pike Resilient Modulus Tests	97
Table A-2. Hyperbolic and Log-Log Model Parameters For Pellissippi Parkway Station 400 Resilient Modulus Tests	104
Table A-3. Hyperbolic and Log-Log Model Parameters For Pellissippi Parkway Station 500 Resilient Modulus Tests	111
Table A-4. Hyperbolic and Log-Log Model Parameters For Airport Connector Station 47 Resilient Modulus Tests	118
Table A-5. Hyperbolic and Log-Log Model Parameters For Airport Connector Station 85 Resilient Modulus Tests	127
Table A-6. Hyperbolic and Log-Log Model Parameters For State Route 20 Station 781+75 Resilient Modulus Tests	134
Table A-7. Hyperbolic and Log-Log Model Parameters For State Route 20 Station 1081+50 Resilient Modulus Tests	141

LIST OF FIGURES

Figure 1-1. Effect of Subgrade Resilient Modulus on Predicted Relative Traffic Life (after Elliott and Thornton 1986)	6
Figure 3-1. Sampling Locations of Candidate Soils	47
Figure 3-2. Standard Proctor Density-Moisture Curves of Selected Soils	51
Figure 3-3. Targeting Scheme for Test Specimen Compaction	53
Figure 3-4. Modified Triaxial Cell Used During Resilient Modulus Determinations	58
Figure 4-1. Typical Resilient Response	62
Figure 4-2. Results of Test No. 5, S.R. 20 Station 1081+50, Illustration Stress Hardening Response at a Water Content 4.3 Percent Less Than Optimum . .	64
Figure 4-3. Results of Test No. 2, S.R. 20 Station 1081+50, Illustrating Stress Hardening Response at a Water Content 0.9 Percent Less Than Optimum . .	64
Figure 4-4. Results of Test No. 3, S.R. 20 Station 1081+50, Illustrating Decrease in Stress Hardening Response as the Water Content Reaches Optimum . .	65
Figure 4-5. Resilient Modulus Curve Illustrating Typical Increase in Resilient Moduli For $\sigma_c = 4$ psi and 2 psi	67
Figure 4-6. Resilient Modulus Curve Illustrating Decrease in Moduli With Increasing σ_c For an A-4 Soil Specimen Prepared at a Water Content Greater Than Optimum	68
Figure 4-7. Results of Test for S.R. 20 Station 1081+50 Soil Prepared at a Water Content Dry Of Optimum .	69
Figure 4-8. Results of Test Conducted at Optimum Water Content for S.R. 20 Station 1081+50 Soil	70
Figure 4-9. Results of Test Conducted at Water Content Greater Than Optimum for S.R. 20 Station 1081+50 Soil	70
Figure 4-10. Results of Test No. 1, S.R. 20 Station 1081+50	71
Figure 4-11. Results of Test No. 2, S.R.20 Station 1081+50	72
Figure 4-12. Bilinear Model and Rutledge Pike Test No. 5 Resilient Modulus Data	77
Figure 4-13. Log-Log Model and Rutledge Pike Test No. 5 Resilient Modulus Data	78
Figure 4-14. Hyperbolic Model and Rutledge Pike Test No. 5 Resilient Modulus Data	79
Figure 4-15. Modified Hyperbolic Model and Rutledge Pike Test No. 5 Resilient Modulus Data	80
Figure A-1. Resilient Response For Rutledge Pike Test No. 1	98

Figure A-2.	Resilient Response For Rutledge Pike Test No. 2	98
Figure A-3.	Resilient Response For Rutledge Pike Test No. 3	99
Figure A-4.	Resilient Response For Rutledge Pike Test No. 4	99
Figure A-5.	Resilient Response For Rutledge Pike Test No. 5	100
Figure A-6.	Resilient Response For Rutledge Pike Test No. 6	100
Figure A-7.	Resilient Response For Rutledge Pike Test No. 7	101
Figure A-8.	Resilient Response For Rutledge Pike Test No. 8	101
Figure A-9.	Resilient Response For Rutledge Pike Test No. 9	102
Figure A-10.	Resilient Response For Rutledge Pike Test No. 10	102
Figure A-11.	Resilient Response For Pellissippi Parkway Station 400 Test No. 1	105
Figure A-12.	Resilient Response For Pellissippi Parkway Station 400 Test No. 2	105
Figure A-13.	Resilient Response For Pellissippi Parkway Station 400 Test No. 3	106
Figure A-14.	Resilient Response For Pellissippi Parkway Station 400 Test No. 4	106
Figure A-15.	Resilient Response For Pellissippi Parkway Station 400 Test No. 5	107
Figure A-16.	Resilient Response For Pellissippi Parkway Station 400 Test No. 6	107
Figure A-17.	Resilient Response For Pellissippi Parkway Station 400 Test No. 7	108
Figure A-18.	Resilient Response For Pellissippi Parkway Station 400 Test No. 8	108
Figure A-19.	Resilient Response For Pellissippi Parkway Station 400 Test No. 9	109
Figure A-20.	Resilient Response For Pellissippi Parkway Station 400 Test No. 10	109
Figure A-21.	Resilient Response For Pellissippi Parkway Station 500 Test No. 1	112
Figure A-22.	Resilient Response For Pellissippi Parkway Station 500 Test No. 2	112
Figure A-23.	Resilient Response For Pellissippi Parkway Station 500 Test No. 3	113
Figure A-24.	Resilient Response For Pellissippi Parkway Station 500 Test No. 4	113
Figure A-25.	Resilient Response For Pellissippi Parkway Station 500 Test No. 5	114
Figure A-26.	Resilient Response For Pellissippi Parkway Station 500 Test No. 7	114
Figure A-27.	Resilient Response For Pellissippi Parkway Station 500 Test No. 8	115

Figure A-28. Resilient Response For Pellissippi Parkway Station 500 Test No. 9	115
Figure A-29. Resilient Response For Pellissippi Parkway Station 500 Test No. 10	116
Figure A-30. Resilient Response For Pellissippi Parkway Station 500 Test No. 11	116
Figure A-31. Resilient Response For Airport Connector Station 47 Test No. 3	119
Figure A-32. Resilient Response For Airport Connector Station 47 Test No. 6	119
Figure A-33. Resilient Response For Airport Connector Station 47 Test No. 7	120
Figure A-34. Resilient Response For Airport Connector Station 47 Test No. 8	120
Figure A-35. Resilient Response For Airport Connector Station 47 Test No. 9	121
Figure A-36. Resilient Response For Airport Connector Station 47 Test No. 10	121
Figure A-37. Resilient Response For Airport Connector Station 47 Test No. 11	122
Figure A-38. Resilient Response For Airport Connector Station 47 Test No. 12	122
Figure A-39. Resilient Response For Airport Connector Station 47 Test No. 13	123
Figure A-40. Resilient Response For Airport Connector Station 47 Test No. 14	123
Figure A-41. Resilient Response For Airport Connector Station 47 Test No. 15	124
Figure A-42. Resilient Response For Airport Connector Station 47 Test No. 16	124
Figure A-43. Resilient Response For Airport Connector Station 47 Test No. 17	125
Figure A-44. Resilient Response For Airport Connector Station 47 Test No. 18	125
Figure A-45. Resilient Response For Airport Connector Station 85 Test No. 1	128
Figure A-46. Resilient Response For Airport Connector Station 85 Test No. 2	128
Figure A-47. Resilient Response For Airport Connector Station 85 Test No. 3	129
Figure A-48. Resilient Response For Airport Connector Station 85 Test No. 4	129
Figure A-49. Resilient Response For Airport Connector Station 85 Test No. 5	130
Figure A-50. Resilient Response For Airport Connector Station 85 Test No. 6	130
Figure A-51. Resilient Response For Airport Connector Station 85 Test No. 7	131
Figure A-52. Resilient Response For Airport Connector Station 85 Test No. 8	131
Figure A-53. Resilient Response For Airport Connector Station 85 Test No. 9	132

Figure A-54.	Resilient Response For State Route 20	
	Station 781+75 Test No. 1	135
Figure A-55.	Resilient Response For State Route 20	
	Station 781+75 Test No. 2	135
Figure A-56.	Resilient Response For State Route 20	
	Station 781+75 Test No. 3	136
Figure A-57.	Resilient Response For State Route 20	
	Station 781+75 Test No. 4	136
Figure A-58.	Resilient Response For State Route 20	
	Station 781+75 Test No. 5	137
Figure A-59.	Resilient Response For State Route 20	
	Station 781+75 Test No. 6	137
Figure A-60.	Resilient Response For State Route 20	
	Station 781+75 Test No. 7	138
Figure A-61.	Resilient Response For State Route 20	
	Station 781+75 Test No. 8	138
Figure A-62.	Resilient Response For State Route 20	
	Station 781+75 Test No. 9	139
Figure A-63.	Resilient Response For State Route 20	
	Station 1081+50 Test No. 1	142
Figure A-64.	Resilient Response For State Route 20	
	Station 1081+50 Test No. 2	142
Figure A-65.	Resilient Response For State Route 20	
	Station 1081+50 Test No. 3	143
Figure A-66.	Resilient Response For State Route 20	
	Station 1081+50 Test No. 4	143
Figure A-67.	Resilient Response For State Route 20	
	Station 1081+50 Test No. 5	144
Figure A-68.	Resilient Response For State Route 20	
	Station 1081+50 Test No. 6	144
Figure A-69.	Resilient Response For State Route 20	
	Station 1081+50 Test No. 7	145
Figure A-70.	Resilient Response For State Route 20	
	Station 1081+50 Test No. 8	145

LIST OF SYMBOLS AND ABBREVIATIONS

- AASHO -- American Association of State Highway Officials
- AASHTO -- American Association of State Highway and
Transportation Officials
- ASTM -- American Standards for Testing and Materials
- CBR -- California Bearing Ratio
- ESAL -- Equivalent Single Axle Load
- FWD -- Falling Weight Deflectometer
- K_1, K_2 -- Regression coefficients for resilient modulus log-log
model
- LL -- Liquid limit
- LVDT -- Linear variable differential transducer
- M_r -- Resilient modulus (psi or kPa)
- PI -- Plasticity index
- PL -- Plastic limit
- SHRP -- Strategic Highway Research Program
- TNDOT -- Tennessee Department of Transportation
- u_a -- pore air pressure
- u_w -- pore water pressure
- USCS -- Unified Soil Classification System
- ϵ_r -- resilient, or recoverable strain (in/in or mm/mm)
- σ_c -- confining pressure (psi or kPa)
- σ_d -- cyclic deviator stress (psi or kPa)
- σ_1 -- applied axial or major principal stress (psi or kPa)
- σ_3 -- applied radial or minor principal stress (psi or kPa)

CHAPTER 1
THE RESILIENT MODULUS AND ITS EFFECT ON PAVEMENT PERFORMANCE

1.1 Definition on the Resilient Modulus, M_r

The resilient modulus of subgrade soil is a material property that expresses the relationship between applied load and recoverable deformation in the form of a stress-strain ratio. The resilient modulus is defined by the equation (AASHTO: "Methods" 1986):

$$M_r = \frac{\sigma_d}{\epsilon_r}$$

where

M_r = resilient modulus (psi or kPa)

σ_d = $\sigma_1 - \sigma_3$, the cyclic deviator stress (psi or kPa)

σ_1 = applied axial or major principal stress (psi or kPa)

σ_3 = applied radial or minor principal stress (psi or kPa)

ϵ_r = resilient, or recoverable, axial strain (in/in or mm/mm)

While similar in concept to the more commonly known "Young's Modulus" or the "modulus of elasticity," the resilient modulus differs in the method by which it is determined due to differences in strain which occur under different loading conditions. Young's Modulus is determined by measuring the strain which occurs due to the application of a monotonic load

that is gradually increased until failure occurs. For nonlinear materials such as subgrade soils, Young's modulus is then usually taken as the initial tangent modulus of the stress-strain curve. Studies (Seed et al. 1962) have shown the resilient moduli to be as much as 500 percent higher than the initial tangent moduli for a given soil.

The test method for determination of the resilient modulus, AASHTO T274-82 (AASHTO: "Methods" 1986), consists of a cyclic-load triaxial-compression test. The application of a cyclic, rather than a monotonic load better simulates the in-service conditions of soil or granular base material in a pavement system since traffic loadings occur cyclically, rather than monotonically. When a load is applied to the pavement system (and the laboratory test specimen), the strain increases along with the applied stress, but the strains which occur under the cyclic loading are much less than those that would occur under a monotonic load. As the load is removed, the stress and strain decrease, but some of the strain is unrecoverable. This plastic, or permanent, portion of the total strain is not considered in the determination of the resilient modulus. Only the recoverable, or resilient portion of the strain is of interest (Elliott and Thornton 1988; Yoder and Witczak 1975).

The resilient modulus was first included in pavement design in the 1986 AASHTO Design Guide (AASHTO *Guide* 1986). The pavement design procedures in the 1986 Guide and its

predecessor, AASHTO *Interim Guide for Design of Pavement Structures* (1972), are based on empirical "best fit" relationships developed from the 1958 - 1960 AASHTO Road Test (AASHTO *Guide* 1986). The AASHTO Road Test, conducted using only one type of subgrade soil and one set of materials for each type of pavement, did not consider the variability of subgrade soil strength. When the Road Test was conducted, it was found that 60 to 80 percent of the measured surface deflection was developed in the subgrade (Highway Research Board 1962). It was also found that the magnitude of surface deflection under applied load could be used as an indicator of pavement performance. Although this information was quite valuable, it was impossible to correlate soil type with measurable surface deflection, and the design equations which resulted from the test were only applicable to the subgrade soil at the Ottawa, Illinois test site (AASHTO *Guide* 1986). When the 1972 *Interim Guide* was developed, a soil support scale was established and incorporated into the design to account for variability of subgrade soil. A testing procedure was not established for the determination of the support scale, and each transportation agency had to adopt their own test procedure and determine a relationship between the test results and the support scale (Elliott and Thornton 1988). When the soil support scale was replaced with the resilient modulus in the 1986 *Guide*, a much needed standard test method for the estimation of subgrade soil behavior, namely AASHTO T274, was

established.

1.2 The Effect of the Resilient Modulus on Pavement Performance

The resilience, or lack thereof, of the subgrade material has a significant effect on the structural performance of the pavement system. Pavement performance, which pertains to the physical condition of the pavement system, has been reported to increase as the resilient modulus of the subgrade soil increases (Elliott and Thornton 1988). This increase in the modulus value is indicative of an increase in the stiffness of the subgrade material and therefore a decrease in the resilient strain under application of a cyclic load. Also, the increased modulus value indicates a decrease in surface deflection of the pavement system, which leads to longer pavement service. Other studies (Seed et al. 1962) have shown a close correlation between the magnitude of surface deflection that occurs and the extent to which cracks in the asphaltic cement layer develop (or serviceability declines).

Typical resilient modulus test results for fine-grained subgrade soils show an increase in the resilient modulus as the applied deviator stress is decreased. The nonlinear relationship which exists between the resilient response and the applied deviator stress is important in pavement design and repair, since an increase in the pavement design thickness will result in a decrease in the magnitude of deviator stress transferred through the pavement system to the subgrade. This

decrease in deviator stress will result in an increase in the subgrade resilient modulus and therefore an improvement in pavement performance. This relationship indicates the economic significance of an accurate measurement of the subgrade resilient modulus at the expected in-situ deviator stress levels. Elliott and Thornton (1988) estimated that an error of 30 percent in the resilient modulus would result in a 1 - 1.5 inch (25.4 - 38.1 mm) error in total design pavement thickness, thus yielding an uneconomical design.

Thornton and Elliott (1986) prepared a plot of resilient modulus versus predicted relative traffic life, as shown in Figure 1-1. Relative traffic life is defined as the number of 18-kip equivalent single axle loads (ESAL) sustainable for a given resilient modulus value divided by the number of 18-kip (124.2 MPa) ESAL's for an arbitrarily assumed base resilient modulus value of 5 ksi (34.5 MPa). As can be seen in Figure 1-1, a pavement system with a subgrade resilient modulus of 10 ksi (69 MPa) has been estimated to carry almost 5 times as much traffic as an identical pavement constructed on a 5 ksi (34.5 MPa) subgrade.

In addition to the subgrade resilient modulus, Seed et al. (1962) pointed out that knowledge of the expected loading and the resilient characteristics of the base course and the asphaltic cement layer are also necessary to evaluate pavement performance. Surface cracking, an indicator of pavement failure, is dependent not only on the subgrade resilient

modulus, but also on the magnitude and distribution of surface loading and on the resilient characteristics of the asphaltic cement and base course layers within the pavement system. Without the evaluation of all factors involved, only a partial representation of the expected field performance of a pavement system can be derived.

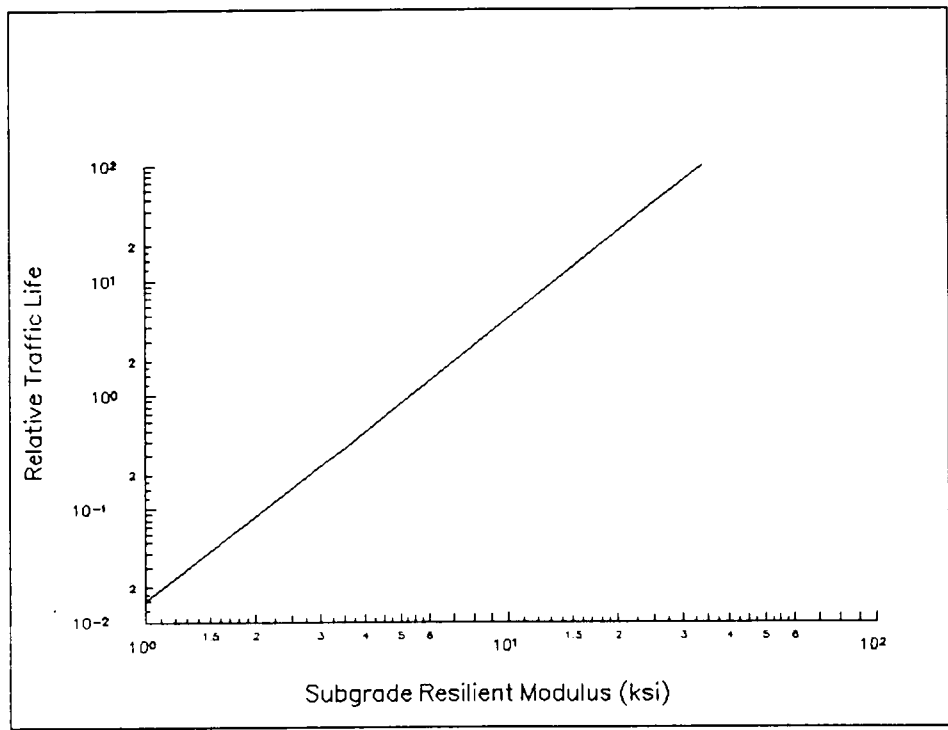


Figure 1-1. Effect of Subgrade Resilient Modulus on Predicted Relative Traffic Life (after Elliott and Thornton 1986) (Note: See page 5 for definition of relative traffic life)

CHAPTER 2
COMPARISON OF TEST PROCEDURES AND
REVIEW OF RESILIENT MODULUS INVESTIGATIONS

2.1 Comparison of Test Procedures

The test method for determination of the subgrade resilient response is basically a triaxial compression test in which a cyclic axial load is applied to a cylindrical test specimen. The magnitude of the applied load is measured by the use of a load cell, while the resilient, or recoverable, deformation is typically measured by use of an LVDT, or linear variable differential transducer. The test is usually conducted by applying a number of stress repetitions over a range of deviator stress and confining stress levels representing variations in depth or location from the applied load. Typical results for fine-grained soils show a decrease in the resilient modulus with increasing deviator stress, indicating what is commonly referred to as "stress-softening" behavior. The effect of the confining pressure on the resilient modulus typically varies according to the material gradation.

Four methods of resilient modulus testing have been compared with regard to suggested testing equipment, compaction specifications and testing procedures for both cohesive and granular materials. The four methods of test considered are the AASHTO T274-82 Method (AASHTO: "Methods" 1986), SHRP PROTOCOL P46 (SHRP 1989), AASHTO T294-92I Method (AASHTO: "Methods" 1992), and the simplified procedure

suggested by Robnett and Thompson (Transportation Research Board 1975).

The results of the test method comparison are shown in Tables 2-1 to 2-4. These tables summarize the diversity in proposed testing methods, and reinforce the need for continuing research in resilient modulus testing.

2.2 Review of Resilient Modulus Testing

A literature review of previous resilient modulus investigations has been conducted and will be presented in the following sections. Noteworthy variations in the equipment used and the test procedure followed will be included, along with a discussion of specimen preparation considerations. An examination of the effects of the method of compaction, test specimen density and specimen water content will also be included.

2.2.1 Variations in Equipment

Variations in test equipment are frequently found in the literature, and some of the most noteworthy with respect to loading systems and load and deformation measurement devices will be discussed in the following sections.

2.2.1.1 Loading Systems

Commonly used loading systems for cyclic triaxial resilient modulus testing include both pneumatic piston and electrohydraulic closed-loop systems (Chan and Mulilis 1976). Pneumatic loading systems such as the one used by Robnett and

Table 2-1. Comparison of Suggested Testing Equipment For Four Resilient Modulus Test Procedures

APPARATUS	AASHTO T274-82	SHRP PROTOCOL P46	AASHTO T294-92I	SIMPLIFIED
LVDTs	INTERNAL, 2 LVDTs wired together and clamped to specimen EXTERNAL may be used if $M_r < 15000$ psi	2 EXTERNAL LVDTs	2 EXTERNAL LVDTs	EXTERNAL, mounted in line with longitudinal axis of specimen
CHAMBER FLUID	air, water or water/alcohol mix			
LOADING DEVICE	any device capable of providing varying repeated loads in fixed cycles of load and pulse	closed-loop electro-hydraulic system required	closed-loop electro-hydraulic system required	
LOAD DURATION	0.1 sec	0.1 sec	0.1 sec	0.06 sec
CYCLE DURATION	1-3 sec	1 sec	1 sec	3 sec
STRESS PULSE	sine, haversine, rectangular or triangular	haversine	haversine	
LOAD CELL	internal	internal	internal	
MEMBRANE THICKNESS	.01 - .025 in.	.01 - .031 in.	.01 - .031 in.	

Table 2-2. Comparison of Test Specimen Compaction Specifications For Four Resilient Modulus Test Procedures

COMPACTION SPECIFICATION	AASHTO T274-82	SHRP PROTOCOL P46	AASHTO T294-92I	SIMPLIFIED
SPECIMEN SIZE	minimum diameter = 2.8" or 6 x largest particle size minimum length = 2 x diameter	minimum diameter = 2.8" or 5 x nominal particle size minimum length = 2 x diameter 4" and 6" diameter also used, depending on nominal particle size	same as SHRP PROTOCOL P46	2" diameter 4" length
COHESIVE	gyratory, kneading or static, depending on anticipated field condition	AASHTO T99-86	static	kneading
GRANULAR	kneading, static or vibratory	AASHTO T180-85	vibratory	the SIMPLIFIED procedure is for cohesive soils only
SPECIMEN CURING	24 hours	none	none	

Table 2-3. Comparison of Four Resilient Modulus Test Procedures for Cohesive Materials

TEST PROCEDURE	AASHTO T274-82			SHRP PROTOCOL P46			AASHTO T294-92I			SIMPLIFIED		
	σ_c	σ_d	REP	σ_c	σ_d	REP	σ_c	σ_d	REP	σ_c	σ_d	REP
COHESIVE CONDITIONING	6	1	200	6	4	200	6	4	1000	0	7	1000
		2	200							0	3	20
		4	200							0	5	20
		8	200							0	7.5	20
		10	200							0	10	20
										0	15	20
COHESIVE TESTING	6	1	200	6	2	100	6	2	100	0	3*	10-20
	3	1	200	6	4	100	6	4	100			
	0	1	200	6	6	100	6	6	100			
	6	2	200	6	8	100	6	8	100			
	3	2	200	6	10	100	6	10	100			
	0	2	200	4	2	100	3	2	100			
	6	4	200	4	4	100	3	4	100			
	3	4	200	4	6	100	3	6	100			
	0	4	200	4	8	100	3	8	100			
	6	8	200	4	10	100	3	10	100			
	3	8	200	2	2	100	0	2	100			
	0	8	200	2	4	100	0	4	100			
	6	10	200	2	6	100	0	6	100			
	3	10	200	2	8	100	0	8	100			
	0	10	200	2	10	100	0	10	100			
COMMENTS	<p>ALL PRESSURES LISTED ABOVE ARE IN UNITS OF PSI</p> <p>* The deviator stress should be increased by approximately 3 psi increments until an upper value of 20-25 psi is reached.</p>											

Table 2-4. Comparison of Four Resilient Modulus Test Procedures For Granular Materials

TEST PROCEDURE	AASHTO T274-82			SHRP PROTOCOL P46			AASHTO T294-92I			SIMPLIFIED
GRANULAR CONDITIONING	σ_c	σ_d	REP	σ_c	σ_d	REP	σ_c	σ_d	REP	NOT APPLICABLE FOR GRANULAR MATERIALS
	5	5	200	15	15	200	15	15	1000	
	5	10	200							
	10	10	200							
	10	15	200							
	15	15	200							
	15	20	200							
GRANULAR TESTING	20	1	200	3	3	100	3	3	100	
		2	200		6	100		6	100	
		5	200		9	100		9	100	
		10	200	5	5	100	5	5	100	
		15	200		10	100		10	100	
		20	200		15	100		15	100	
	15	1	200	10	10	100	10	10	100	
		2	200		20	100		20	100	
		5	200		30	100		30	100	
		10	200	15	10	100	15	10	100	
		15	200		15	100		15	100	
		20	200		30	100		30	100	
	10	1	200	20	15	100	20	15	100	
		2	200		20	100		20	100	
		5	200		40	100		40	100	
		10	200							
		15	200							
	5	1	200							
		2	200							
		5	200							
		10	200							
		15	200							
	1	1	200							
		2	200							
		5	200							
		7.5	200							
		10	200							
COMMENTS	ALL PRESSURES LISTED ABOVE ARE IN UNITS OF PSI									

Thompson (1973) use a system of valves and programmable regulators to apply a cyclic load. Although the AASHTO T274-82 test procedure permits the use of any device capable of producing varying repeated loads in fixed cycles of load and pulse, the electrohydraulic systems required in both SHRP Protocol P46 and AASHTO T294-92I test procedures (see Table 2-1) have become more common in recent years, and have the advantage of feedback control. These closed-loop systems continuously monitor the actual applied load and/or displacement, and correct the output to assure that the desired loading is applied. These systems result in precise control of the loading history.

Another loading system that may prove useful in resilient modulus determinations is the U.S. Army Corps of Engineers Gyrotory Testing Machine (GTM). The GTM has been experimented with by George (1992) as an alternative to the customary triaxial cyclic load resilient modulus testing system. The GTM has been used previously by the Corps of Engineers for bituminous mix design and base/subgrade density control (Corps of Engineers 1962; 1962). The GTM, described as a combination shear testing, kneading compaction, and "dynamic consolidation" apparatus, has the ability to simulate the insitu "kneading action" produced during compaction and traffic application. The apparatus could therefore be used for both compaction and testing, although modifications to the GTM were necessary for both cyclic testing and data

acquisition. Furthermore, an assumed value of Poisson's ratio was required for calculation of the resilient modulus. The resulting "kneading resilient modulus" for coarse-grained soils was shown to be 69 percent to 92 percent less than the resilient modulus found using the triaxial testing system. For fine-grained soils there was no relation shown between results for the two test systems, but the author noted that further development of the GTM could result in realistic measurement of the subgrade resilient response.

2.2.1.2 Deformation Measurement Devices

A variety of deformation measurement devices have been evaluated by researchers to assess their usefulness in reliable resilient modulus determinations. The accurate measurement of deformation is important since typical resilient displacements are very small. One of the most common deformation measurement devices used is the LVDT (linear variable differential transducer). Linton et al. (1988) noted several characteristics that make LVDTs useful for deformation measurement, including near frictionless measurement, a long mechanical life and high resolution.

A variety of LVDTs are available, including both AC and DC (alternating and direct current, respectively) devices. Linton et al. (1988) evaluated both types of LVDTs and found that AC LVDTs (which were generally smaller than the available DC devices) may yield erratic readings due to interference by external power sources. Also reported was the necessity for

repeated calibration due to drift of the AC devices.

Of major concern in resilient modulus testing is the placement of deformation measurement devices, which varies according to the test procedure followed. These variations in placement are due to differing opinions on what factors most significantly affect the accuracy of deformation measurement. The AASHTO T274-82 test procedure summarized in Table 2-1 specifies the use of either internally or externally mounted LVDTs, depending on the anticipated magnitude of the resilient response. Internally-mounted LVDTs refer to those located inside the triaxial chamber. Internally-mounted LVDTs may be attached directly on the test specimen, or may be fastened to the top platen and referenced to some point within the triaxial chamber. Other procedures (SHRP Protocol P-46, AASHTO T294-92I, Robnett and Thompson's simplified procedure (Transportation Research Board 1975)) call for the use of externally mounted deformation measurement devices which refer to those placed outside the triaxial chamber. Externally-mounted LVDTs are typically bracketed to the loading piston and referenced to the top of the triaxial cell. The use of externally-mounted LVDTs in resilient modulus testing has been widespread in the past. More recently, however, researchers have begun to utilize internally-mounted devices, but not without some reservations.

Jardine et al. (1984) noted that possible errors caused by deflections in the loading and measurement systems could

result in a poor determination of the stress-strain properties of a material at small strains such as those typically encountered in resilient modulus testing. Further noted was the fact that triaxial testing tends to disclose lower soil stiffness than that actually observed in the field. The use of external deflection measurement devices routinely results in low measurements of soil stiffness, due mainly to specimen end effects (blemishes and faults), specimen tilting, unsymmetrical test specimens, undesirable movement between the loading piston and the top of the triaxial cell where the LVDT is referenced, and compressibility of the test equipment (Jardine et al. 1984; Nataatmadja and Parkin 1990; Brown and Snaith 1974).

Another problem associated with the use of externally-mounted LVDTs is that it must be assumed that the distribution of strain is uniform throughout the test specimen length. This assumption has been found to be incorrect (Claros et al. 1990). A possible solution to this problem is the use of a non-contact LVDT, such as the electro-optical biaxial tracking system investigated by Claros et al. (1990). It is suggested that this type of device could allow the determination of correction factors that could be applied to the external LVDT readings to determine the true resilient deformation.

Other researchers (Nataatmadja and Parkin 1990) reported that specimen-mounted LVDTs should be used to measure deflection, since externally-mounted measurement devices are

susceptible to several sources of error as previously discussed. However, several problems were noted with the use of specimen-mounted LVDTs. These problems included restrictions on the type of confining medium that can be used in order to avoid damage to the LVDTs, and also error that may be large due to membrane slippage at large strains (greater than 15 percent). However, since large magnitude strains are rarely achieved during resilient modulus testing, membrane slippage may not be a critical factor (Nataatmadja and Parkin 1990; Jardin et al. 1984).

Claros et al. (1990), during resilient modulus testing for SHRP, used an externally-mounted LVDT bracketed to the loading piston. This was due to the observation that specimen-mounted LVDTs are difficult to adequately secure to the test specimen to ensure that no movement of the LVDT occurs during testing. Claros et al. (1990) noted that slippage of specimen-mounted LVDTs may result in a 50 percent change in the resilient modulus of a 40,000 psi (275.8 MPa) modulus sample tested at a deviator stress of 2 psi (13.8 kPa). Also, when fine plastic soils are tested, the permanent sample deformation may cause the internally-mounted LVDT to slip out of range, resulting in a halt in the test procedure while LVDTs are readjusted.

In order to avoid errors typically encountered when externally-mounted devices are used, Jardine et al. (1984) conducted undrained triaxial tests using a specimen-mounted

deflection measurement device that employs an electrolytic liquid enclosed in a glass capsule. The impedance between a central and two outer partially-submerged electrodes vary as the capsule is tilted, due to a change in the liquid level inside the capsule. These devices, which are sensitive to vibrations and temperature changes, are capable of detecting both deformation and tilt of the specimen during testing. The tests conducted by Jardine et al. reported a resolution of about 0.001 percent using these electrolyte devices.

Brown and Snaith (1974) also used a specimen mounted device. Their axial deflection measurement instrumentation consisted of two averaged LVDTs that were held in contact with pre-secured targets on opposite sides of the specimen by split collars. The splits allowed for the occurrence of lateral deformation during testing. The two collar halves were held together by a hinge on one side and a spring on the other. The spring functioned to keep two pointers, one per collar half, located on the targets. Specimen tilting was prevented by the placement of foam rubber between the specimen and collars. The devices were wired in such a manner as to allow separation of permanent and elastic deformations. This system allowed for the resolution of recoverable strains down to around 1.5×10^{-4} percent.

Pezo et al. (1991) conducted experiments to determine the best location within a triaxial setup to monitor deformation. They monitored four locations and compared the relative

movement that occurred between these locations during resilient modulus testing. Results showed the best location to be the inside base of the triaxial cell, since relative movement here was the least. They also noted that the top of the specimen was a better location to measure deformation than the external LVDT bracket. Based on these results, Pezo et al. used two diametrically-opposed internal LVDTs that were attached to the top cap of the test specimen. The LVDTs were supported by steel bars attached to the chamber base. This arrangement eliminated possible errors due to slippage of specimen-mounted LVDTs and those caused by equipment compressibility and undesirable loading piston movement when external deformation measurement devices are used. They noted that axial strains smaller than approximately 10^{-2} percent could not be measured accurately, due to transducer resolution and test system limitations.

Edris and Lytton (1977) reported the use of two induction coils for the measurement of axial displacement. The induction coils, which measured changes in the magnetic field due to relative movement of the coils, were reportedly capable of measuring deflections of plus or minus 0.0005 inches (0.0127 mm) accurately.

2.2.1.3 Load Cells

Load cells are used during resilient modulus testing to measure the magnitude of axial load applied to the test specimen. As shown in Table 2-1, load cells are generally

specified as internally-located (inside the triaxial chamber) devices for resilient modulus testing, although external devices have been commonly used in the past. The use of internal devices eliminates the effects of loading piston friction (Pezo et al. 1991), and gives a more accurate measurement of actual applied load, especially at lower levels of deviator stress.

Various arrangements of internal load cells have been described in the literature, including placement directly above the top porous stone (Claros et al. 1990) and also directly above the top platen, where load is applied and measured via a ball bearing centered in the top platen (Pezo et al. 1991).

2.2.2 Specimen Preparation Considerations

2.2.2.1 Grouting

Recent experiments using hydrostone grout to eliminate errors due to flawed specimen ends hold much promise. Pezo et al. (1991) grouted the specimen to both the top and bottom platens when conducting calibration tests for their resilient modulus testing system. In order to evaluate its effectiveness, tests were conducted using both grouted and ungrouted synthetic specimens. Results showed resilient modulus deviations greater than 20,000 psi (138 MPa) for some materials, with the ungrouted specimens reporting the lower resilient modulus values.

Pezo et al. (1992) further recommend the use of grouted

specimen ends in order to eliminate the need for sample conditioning. One of the functions of conditioning is to improve contact between the specimen ends and the loading platens to assure full contact before data collection begins. It was suggested that by grouting specimen ends, applied stresses and the resulting axial strains are more uniform and specimen conditioning is no longer required for contact surface improvement.

2.2.2.2 Thixotropy

A major concern to researchers is the effects of thixotropic strength gains on the resilient response. These strength gains occur in remolded specimens during the storage period between sample preparation and testing. The gains occur mainly due to capillary tensions that develop within the soil pores due to menisci that form along the specimen perimeter (Lambe and Whitman 1969). These capillary tensions result in increases in negative pore water pressures and thus increase the effective stress within the soil specimen. As a result of the effective stress increase, the strength of the soil specimen increases. This strength increase, known as "apparent cohesion," is generally more significant at low strains and within remolded specimens that possess a high liquidity index (Lambe and Whitman 1969). Because the apparent cohesion changes with time, most resilient modulus test procedures specify a sample curing time to eliminate variations in results caused by thixotropy (see Table 2-1).

Early research on thixotropic strength gains conducted by Seed et al. (1962) compared several test specimens compacted and tested in the same manner, with the only variable, specimen age, ranging from 15 minutes to 50 days. Initial results of these tests showed a large range of resilient modulus values for the specimens tested. However, as the number of stress repetitions increased, the range in resilient modulus values became smaller. Seed et al. concluded that thixotropic strength gains reduced the resilient deflection for tests conducted below approximately 40,000 stress repetitions. Above that number, the specimen aging period showed little effect on the resilient modulus.

Beaton et al. (1967) noted that previous resilient modulus research comparing tests on undisturbed samples and those obtained from newly compacted embankments of the same clay soil reported significant differences in the resilient response. Tests conducted at identical water contents and dry densities reported resilience values for the newly compacted material as high as three times those of the undisturbed material. Beaton et al. felt that an evaluation was necessary in order to determine a specimen storage period for their test soils that would allow the remolded soil to gain a magnitude of strength that would be similar to that gained over time in-situ. Tests were conducted on remolded specimens of sixteen soils ranging in age from immediately after compaction to 76 days. Only three of the sixteen soils tested showed a

significant strength increase due to thixotropy. Results of tests conducted on the "most sensitive material" showed a strength regain of 50 percent after 7 days, 60 percent after 14 days, and 64 percent after 21 days. Beaton et al. noted the behavior of this material was extreme, and probably not characteristic of most clay soils.

In 1991, Pezo et al. conducted resilient modulus tests on specimens of an AASHTO classification A-7-6 soil that were aged for two days. The specimens then remained in the triaxial cell for the next four days (with reportedly no reduction in moisture content), then tested again. Tests were compared on the basis of the coefficients K_1 and K_2 in the equation:

$$M_r = K_1 (\sigma_d)^{K_2}$$

where K_1 and K_2 are coefficients determined by regression analyses and σ_d is the applied axial deviator stress. The comparisons showed a significant change in the coefficients between the tests conducted at 2 and 6 days, prompting Pezo et al. to note that sample aging should be addressed to obtain consistency and repeatability in resilient modulus determinations.

2.2.3 Resilient Modulus Testing

2.2.3.1 Specimen Conditioning

Specimen conditioning is that portion of resilient

modulus testing which serves to eliminate the effects of initial permanent deformation and specimen loading imperfections. It may also reduce any effects due to property changes that may occur between loading and compaction (deMedina and Preussler 1982; AASHTO T274-82). Significant differences exist between the various testing procedures with respect to the magnitude and quantity of conditioning load cycles as shown in Tables 2-3 and 2-4 for cohesive and granular materials, respectively. The AASHTO T274-82 test procedure specifies the application of 200 cycles each of deviator stress values of 1, 2, 4, 8 and 10 psi (6.9, 13.8, 27.6, 55.2 and 69 kPa), while holding the confining pressure constant at 6 psi (41.4 kPa). SHRP Protocol P-46 specifies 200 repetitions of deviator stress of 4 psi (27.6 kPa) and confining pressure of 6 psi (41.4 kPa), while AASHTO T294-92I specifies 1000 repetitions at these same stress levels. Finally, the simplified procedure suggested by Robnett and Thompson (Transportation Research Board 1975) specifies conditioning with deviator stress values of 7, 3, 5, 7.5, 10 and 15 psi (48.3, 20.7, 34.5, 51.8, 69 and 103.5 kPa). The 7 psi (48.3 kPa) conditioning stress is applied for 1000 repetitions while 20 repetitions are applied for all other stress levels with no confining pressure.

Several researchers (Jin et al. 1992; deMedina and Preussler 1982; Fredlund et al. 1977) have adopted their own criteria for sample conditioning, some of which are based on

estimates of in-situ behavior.

Pezo et al. (1991, 1992) experimented with the use of grouted specimen ends, which seemed to eliminate the errors due to specimen loading imperfections. The use of grout to improve contact between the loading device and the specimen has been discussed previously.

2.2.3.2 Confining Pressure

Specimen confining pressure is applied in the laboratory triaxial chamber in order to simulate the stress condition that exists in-situ due to overburden (Jin et al. 1992). Although the lateral and axial stresses experienced in the field occur cyclically, a constant confining stress is applied in the laboratory to simplify the test procedure since the resilient response is not significantly affected when a cyclic lateral stress is applied (Matthews and Pandey 1991).

Researchers and standard test methods alike seem to disagree on the exact values of confining pressure to use when testing cohesive materials, but most recommend confining stress levels less than or equal to 6 psi (41.4 kPa). In three of the test methods summarized in Table 2-3 specimens are subjected to a confining pressure of 6 psi (41.4 kPa) (AASHTO T274-82, SHRP Protocol P46, AASHTO T294-92I) for sample conditioning, then various combinations of confining and deviator stresses during testing. Thompson and Robnett (1979) utilized zero confining stress for both conditioning and testing. This decision was based on the following

factors: (1) testing ease and simplicity; (2) finite element and elastic layer theory analysis showed that very low confining pressures, usually less than 5 psi (34.5 kPa), exist in the upper regions of typical flexible highway pavements; (3) a literature review resulted in numerous examples of resilient modulus testing of fine-grained soils using zero confining pressure; (4) previous studies conducted by Robnett and Thompson (1973) revealed small confining pressures (up to 5 psi (34.5 kPa)) showed no significant effect on the resilient properties of fine-grained soils; and (5) studies by Fredlund et al. (1977) showed that the resilient modulus is not significantly influenced by confining pressures if fine-grained soils are compacted wet of optimum. On the other hand, Claros et al. (1990) eliminated the zero confining stress state from the AASHTO T274 test sequence because it was not considered to be a realistic stress state for a pavement subgrade.

Several researchers have examined the level of confining stress that should be applied during resilience testing of cohesive soil. While performing resilient modulus tests on a compacted glacial till, Fredlund et al. (1977) noted the range of in-situ confining pressure that could normally be expected is from 3 to 6 psi (20.7 to 41.4 kPa). Later, Thompson and Robnett (1979) reported that confining pressure values determined by finite element and elastic layer theory analyses were normally less than 5 psi (34.5 kPa). Elliott and

Thornton (1988) recommended that AASHTO T274-86 should be modified to include only one value of confining stress, 3 psi (20.7 kPa), because this value "...is more consistent with the confining stress expected in the field and more in keeping with the design reliability concept used in the AASHTO Guide."

Other researchers have reported the effects of confining pressure on the resilience of fine-grained materials. Brodsky (1989) found that for the zero confining stress state, the resilient modulus decreased as the deviator stress increased, suggesting the traditional "stress-softening" response. However, when 3 psi (20.7 kPa) and 6 psi (41.4 kPa) confining stresses were applied, the modulus first increased then decreased with increasing deviator stress. A comparison of results for a deviator stress of 1 psi (6.9 kPa) showed that the resilient modulus decreased as the confining pressure increased. With a high deviator stress of 10 psi (69 kPa), the resilient modulus increased as the confining pressure increased for all samples except three, all of which came from the same county.

Other researchers have examined the effect of confining stress on the resilient response when the specimen water content is varied. Fredlund et al. (1977) found the confining stress to have little effect on the resilient modulus for specimens tested near optimum water content, but the effect was greater for water contents below optimum. This is probably due to the fact that above optimum water content,

the large amount of water in void spaces is at low matrix suction, and increasing the confining stress does not greatly affect the resilient modulus. Matrix suction is defined as

$$\text{Suction} = u_a - u_w$$

where

u_a = pore air pressure (approximately equal to atmospheric pressure)

u_w = pore water pressure

When matrix suction is high (or the water content is low), an increase in the confining stress may result in an increase in the resilient modulus (Fredlund et al. 1977).

2.2.3.3 Deviator Stress

The deviator stress is defined as

$$\sigma_d = \sigma_1 - \sigma_3$$

where

σ_1 = applied axial, or major principal stress (psi or kPa)

σ_3 = applied confining, or minor principal stress (psi or kPa)

The deviator stress is applied cyclically to the laboratory test specimen and is intended to simulate the stress state caused by a vehicle moving across the pavement structure (Jin et al. 1992). Seed et al. (1962) stated that the deviator stress experienced in the subgrade varies with respect to depth and lateral location from the applied load.

For cohesive materials, the values of deviator stress

used during laboratory testing vary with the test method used, but most are less than or equal to 10 psi (69 kPa) as shown in Table 2-3.

Wilson et al. (1990) conducted multiaxial resilient modulus tests on several fine-grained Ohio subgrade soils. In multiaxial testing, load is applied independently to the six faces of a cube-shaped test specimen by pressurized flexible membranes. This loading arrangement allows the simulation of complex stress states since variation of any of the principal stresses can be achieved. For their tests, Wilson et al. applied a steady confining stress of 5 psi (34.5 kPa) along two coordinate axes, while dynamic deviator stress loads were applied along the third axis. These tests showed a rapid decrease in the resilient modulus with increasing deviator stress at levels of 0 to 2 psi (13.8 kPa). The resilient modulus usually leveled off or increased slightly for higher deviator stresses in the range of 2 to 8 psi (13.8 to 55.2 kPa). These results indicate an increase in the resilient modulus with depth, and are analogous to the results typically found during triaxial resilient modulus testing.

Claros et al. (1990) found the resilient deformation at 1 psi (6.9 kPa) deviator stress impossible to measure accurately. It was believed that the magnitude of resilient deformation was no larger than the noise of the transducer signal, and therefore it could not be accurately determined.

Fredlund et al. (1977) conducted investigations on the

effect of deviator stress on the resilient modulus with varying water content. They found the deviator stress to be much more significant than confining pressure for test specimens prepared at optimum water content. Above optimum water content, deviator stresses larger than 12 psi (88 kPa) resulted in some strain-hardening behavior. Fredlund et al. further noted that below optimum water content, the resilient modulus is typically affected less by variations in the deviator stress than those specimens tested above optimum water content.

Several researchers have examined the effect of the number of load repetitions on strain in silty clay. Pell and Brown (1972) presented data showing an increase in permanent axial strain with increasing number of deviator stress repetitions. The rate of increase in permanent strain became larger as the applied deviator stress drew nearer the undrained shear strength of the cohesive soil tested. Seed et al. (1962) reported a significant decrease in resilient axial strain with increasing number of stress applications. The AASHO subgrade silty soil examined tended to exhibit peak resilient deformation somewhere between 1-5000 repetitions of 10 psi deviator stress, with a substantial decrease in resilient deformation occurring after about 10,000 repetitions. The permanent axial strain was shown to increase with increasing number of stress applications, exhibiting behavior similar to that of the soil investigated by Pell and

Brown.

2.2.4 Prediction of the Resilient Modulus

2.2.4.1 Predictions using CBR

Researchers have also investigated the possibility of a correlation between the resilient modulus and the CBR (California Bearing Ratio), a commonly used criteria for pavement design. Brodsky (1989) compared the resilient modulus values for typical South Dakota subgrade soils determined via the AASHTO T274-82 method of test with those computed by the equation $M_r = 1500 \times \text{CBR}$ as suggested in the 1986 AASHTO Design Guide (AASHTO Guide 1986). It was found that for CBR values of 3.1 to 7.0, the slope of the 1500 x CBR line was a reasonable fit when plotted along with resilient modulus values for 4 levels of deviator stress, but the Y-intercept was consistently low. The 1500 x CBR line fell below all compared plots of the laboratory-measured resilient modulus. This would result in a low estimation of the resilient modulus, and thus a conservative (and uneconomical) pavement design.

Thompson and Robnett (1973) also investigated the possibility of a relationship between the resilient modulus and the CBR. A plot of soaked CBR versus resilient modulus values for tests conducted at 2 percent above optimum water content showed no relation between CBR and resilient modulus. The resilient modulus values used in the plot were found at a stress level estimated to be the vertical compressive subgrade

stress. Further noted was the fact that soils with similar soaked CBR values exhibited significantly different resilient behavior.

Barksdale and Leonards (1967) noted that soils with similar behavior under monotonic loading may exhibit significant differences in permanent and resilient deformation under cyclic loading. They concluded that static tests such as the CBR cannot be expected to characterize soil behavior under cyclic loading conditions.

deMedina and Preussler (1982) noted that the resilient modulus may be difficult to predict from CBR values because no lateral pressure control is maintained during CBR testing, and high shear stresses are produced due to piston penetration. The techniques of resilient modulus testing provide a constant lateral pressure, and much more uniform shear stresses throughout the specimen. deMedina and Preussler (1982) found discrepancies between resilient modulus and CBR values for sandy Brazilian soils. These discrepancies were attributed to the fact that grain size and characteristics of the fines greatly influence the resilient response of sandy soils, but have less effect on the CBR. For clayey Brazilian soils they found the CBR-resilient modulus correlation to be M_r (psi) = $4657 + 957*(CBR)$, with a correlation coefficient r of 0.82. This correlation was performed using soaked CBR values and resilient modulus values at a relatively high deviator stress of 14 psi (96.6 MPa).

2.2.4.2 Mathematical Models

Mathematical models are typically used to describe the relationship between resilient modulus and deviator stress as determined in the laboratory. These models are used later in finite element procedures to back-calculate moduli from field-measured FWD (falling weight deflectometer) deflections (Drumm et al. 1992). Four such models will be described in the following sections. The models are: a bilinear model; a log-log or exponential function; a hyperbolic model; and a modified hyperbolic function.

2.2.4.2.1 Bilinear Model

A bilinear model described by Terrel and Award (1972) has been used by several researchers (Thompson and Robnett 1976; 1979; Drumm and Moore 1988) to represent the nonlinear resilient response of fine-grained soils. The bilinear model defines the nonlinear resilient response in terms of two straight lines and a "breakpoint" resilient modulus. The breakpoint resilient modulus has been defined as the resilient modulus corresponding to the point of intersection of the two straight line segments that have been fitted to the resilient modulus curve. The breakpoint resilient modulus has been observed to occur at approximately 6 psi (41.4 kPa) deviator stress (Thompson and Robnett 1976).

The bilinear model has the form:

$$\begin{aligned} M_r &= c_1 && \text{for} && 0 \leq \sigma_d \leq \sigma_{\min} \\ M_r &= a_1 + k_1 \sigma_d && \text{for} && \sigma_{\min} \leq \sigma_d \leq \sigma_i \end{aligned}$$

$$M_r = a_2 + k_2 \sigma_d \quad \text{for} \quad \sigma_i \leq \sigma_d \leq \sigma_{\max}$$

$$M_r = c_2 \quad \text{for} \quad \sigma_{\max} \leq \sigma_d$$

where

$$\sigma_{\min} = 2 \text{ psi}$$

c_1 = upper limit resilient modulus

c_2 = lower limit resilient modulus

k_1 = slope of first straight line segment = -1.11 ksi/psi

k_2 = slope of second straight line segment = -.178
ksi/psi

σ_i = breakpoint deviator stress ≈ 6 psi

a_1 = Y-intercept of first straight line segment

a_2 = Y-intercept of second straight line segment

The parameters σ_{\min} , σ_i , k_1 and k_2 are assumed to be the constants given above for all resilient responses. The parameter σ_{\max} is dependent on the soil response, and has differing values for very soft, soft, medium, and stiff material behavior (see Thompson and Robnett 1976).

2.2.4.2.2 Log-Log Model

The log-log model (Moossazadeh and Witczak 1981) is specified for the presentation of resilient modulus lab data in SHRP Protocol P46 and AASHTO T294-92I methods of test. The exponential relationship is given by:

$$M_r = K_1 (\sigma_d)^{K_2}$$

where K_1 and K_2 are obtained from regression analysis as the Y-intercept and the slope of the line, respectively.

Use of this model will result in excessively high

resilient modulus values at low deviator stresses since no upper limit or lower limit is imposed. These limits must therefore be arbitrarily chosen in order to avoid excessively high resilient modulus values.

2.2.4.2.3 Hyperbolic Model

The hyperbolic model (Kondner 1963) has been used to describe stress softening response (Boateng-Poku and Drumm 1989) as:

$$M_r = [a + b(\sigma_d)]/\sigma_d$$

where

a = the slope of the relationship at low deviator stresses

b = minimum value of M_r at large deviator stresses

As for the log-log model, an upper limit must be specified. Advantages of this model are that the parameters a and b have physical significance and are easy to determine. The lower limit is also defined.

2.2.4.2.4 Modified Hyperbolic Model

The modified hyperbolic model suggested by Drumm et al. (1992) has both upper and lower limits, an improvement over the previously discussed models. The modified hyperbolic model has the form:

$$M_r = [(E_{\max} - E_{\min}) / (1 + a(\sigma_d)^b)] + E_{\min}$$

where

E_{\max} = upper limit resilient modulus

E_{\min} = lower limit resilient modulus

a and b are material parameters

A disadvantage of this model is the fact that the parameters a and b have no physical significance and must therefore be determined by trial-and error.

2.3 Effect of Compaction, Density and Water Content on the Resilient Modulus

Several researchers have investigated the effects of compaction method, specimen density, and specimen water content on the resilient response of fine-grained soils. Some of the more significant observations with regard to these factors will be discussed in the following sections.

2.3.1 Compaction

The method of compaction has been reported to have a significant effect on the soil structure and thus the resilient behavior of laboratory compacted test specimens. For cohesive materials, impact, static or kneading compaction techniques are usually specified for resilient modulus determinations as shown in Table 2-2. The AASHTO T274-82 test procedure recommends the method of compaction should be based on anticipated conditions in-situ.

Monismith (1992) pointed out that the dry density, water content, soil structure and method of specimen compaction all affect the resilient response of fine-grained soils. Seed et al. (1962) noted that variations in soil structure are dependent on both the water content and the method of compaction, and appear to be caused mainly by variations in

the degree of shear strain occurring during compaction. When soils are compacted dry of optimum water content, no method of compaction will result in appreciable shear strains, and a flocculated or random soil particle structure results (Seed et al. 1962). When wet of optimum fine-grained soils are compacted, a dispersed, or parallel particle array will result as long as the compaction technique allows the occurrence of shear deformations. Wahls and Langfelder (1967) noted that a higher degree of particle dispersion occurs with larger shearing strains. When impact or kneading compaction techniques are used, large shear deformations are induced as a result of lateral soil movement caused by penetration of the compaction foot or hammer into a portion of the soil surface (Seed et al. 1962). The shearing strains which occur are larger for kneading than for impact techniques. When static compaction is used, the soil is placed in a mold, and static pressure is applied uniformly to the entire soil surface. Lateral soil movement is not possible, and thus no appreciable shear strains occur. This results in a flocculated soil structure, regardless of the soil water content (Seed et al. 1962). Thus, for soils compacted wet of optimum, the degree of soil particle dispersion obtainable decreases from kneading to dynamic to static compaction techniques (Wahls and Langfelder 1967). These differences in soil particle arrangement due to varying compaction techniques result in variations in the resilient response, even though the same

specimen water content and dry density may be assumed.

Monismith (1992), examining the interdependence of compaction technique and water content, noted that two test specimens, the first prepared dry of optimum using kneading compaction techniques then soaked to the desired water content, and the second also prepared using kneading compaction but compacted at the desired water content, would exhibit different resilient responses. However, if a third test specimen were prepared at the desired water content using static compaction techniques, the same resilient response would occur as for the soaked specimen prepared by kneading compaction. For fine-grained soils, Monismith summarized by stating that static compaction results in approximately the same soil structure (flocculated, or random) as kneading compaction at water contents dry of optimum.

Seed et al. (1962) presented a plot of resilient modulus tests conducted on specimens of the AASHO Road Test subgrade. Specimens were prepared at 95 percent saturation and compacted by both static and kneading techniques. The specimens prepared by static compaction showed resilient modulus values as much as 400 percent higher than the kneaded specimens for deviator stresses less than 32 psi (220.8 kPa). At a deviator stress of 32 psi (220.8 kPa), the resilient response of both specimens was approximately the same.

Seed et al. (1962) also conducted resilient modulus tests on undisturbed specimens taken from untrafficked loops of the

AASHO test road that were compacted with rubber-tired rollers. They found the resilient strains for these specimens to be comparable to those found for specimens prepared by kneading compaction, but were much higher than the resilient strains produced in the statically-prepared specimen. Seed et al. concluded that kneading compaction produced a similar soil structure to that obtainable with rubber-tired rollers in the field. Their conclusion is in close agreement with Wahls and Langfelder (1967), who noted that sheepsfoot and rubber-tired rollers induce large shearing strains in the field, and kneading compaction techniques more closely approximate these conditions than impact compaction techniques.

Prapaharan et al. (1991) conducted research on the fabric of a medium plastic clay under field and laboratory compaction conditions. In the field, compaction was achieved by a 63,000 lb (28.6 MPa) static segmented-pad roller and a 25,000 lb (11.3 MPa) vibratory segmented-pad roller and the applied compaction energies were calculated. A 6 percent range of field water contents was unavoidable for any one section, although considerable effort was made to control the water content to preselected values.

In the laboratory, three energy levels of impact compaction and also kneading compaction techniques were applied to test specimens. It was concluded that soil compacted in the field and the laboratory, although compacted to "comparable specifications," should be considered

different, and thus will exhibit different engineering behavior. Also, for a given type of compaction and water content, a difference in the level of applied energy results in a difference in soil fabric. When specimens were compacted wet of optimum using the standard Proctor compactive effort, both impact and kneading compaction techniques resulted in the same fabric as was observed in the field. This was not found to be true for soils compacted on the dry side of optimum. It was further concluded that no current laboratory compaction procedure is consistently able to reproduce the fabric of field-compacted soil, and laboratory testing should be conducted on field-compacted specimens when the resulting material behavior data is critical for design.

2.3.2 Density

Variations in the density of laboratory test specimens with the same water content have been found to produce variable effects on the resilient response of fine-grained soils.

Thompson and Robnett (1973; 1979) reported on the influence of varying compactive effort from 95 percent to 100 percent of AASHTO T-99 density for specimens prepared at optimum water content plus 2 percent. Examination of the effects of compactive effort on resilient modulus values showed the maximum increase in resilient modulus due to increased compactive effort was approximately 1.6 ksi (11 MPa), while the minimum increase was approximately 1.2 ksi

(8.3 MPa). These same effects were shown to occur with a 4 percent or 5 percent change in the degree of saturation (or approximately 1 percent change in the water content).

Seed et al. (1962) also investigated the effect of variations in dry density on the resilient response. They prepared plots of resilient axial strain at 60,000 load applications versus dry density for numerous resilient modulus tests performed on the AASHO Road Test subgrade soil. For all the tests conducted at water contents below optimum and densities below maximum, only slight decreases in the resilient axial strain occurred with increasing dry density. Below optimum water content but above maximum dry density, significant increases in resilient axial strain occurred as the dry density increased. Above optimum water content, the resilient axial strain quickly increased with increasing dry density.

2.3.3 Water Content

Several researchers have commented on the effect of variations in water content on the resilient response of fine-grained soils. Seed et al. (1962) noted a rapid increase in resilient deformations for specimens of the AASHO Road Test subgrade soil compacted at increasing water contents above optimum. For specimens compacted below optimum water content, resilient deformations were characteristically low. Seed et al. noted that at high degrees of saturation (approximately 85 percent), small changes in density and water content can

significantly affect the resilient response due to changes in soil structure that occur during compaction, as previously discussed.

Seed et al. also showed evidence of an increase in resilient axial strain for resilient modulus test specimens compacted at a high degree of saturation over those initially compacted at a low water content and then allowed to reach the same degree of saturation by absorption without volume change. Specimens used during this analysis were prepared at 96 percent standard AASHO density by kneading techniques. Test results showed as the degree of saturation reached 85 percent, resilient axial strains for the specimens compacted at high saturation were as much as three times those of the specimens allowed to reach the same degree of saturation by absorption. Seed et al. pointed out the difficulty in obtaining a uniform degree of saturation throughout the test specimen at any value other than essentially 100 percent saturation when absorption techniques are used. Specimens that have nonuniform water contents due to soaking to intermediate degrees of saturation would exhibit different properties than those having a uniform water content throughout the specimen.

Thompson and Robnett (1979) also reported a decrease in the resilient modulus with increasing degree of saturation. They compared values of the "breakpoint" resilient modulus, which was defined in section 2.2.4.2.1. It was found that for soils compacted wet of optimum, higher degrees of saturation

and lower breakpoint resilient modulus values existed regardless of the level of compaction. It was further found that soils with a high percentage of clay and high plasticity tended to be less sensitive to changes in the degree of saturation.

Fredlund et al. (1977) examined the effect of variation in deviator stress on the resilient modulus for specimens prepared at both dry and wet of optimum water content. For wet of optimum specimens, the resilient modulus was effected more by variations in deviator stress than those tested dry of optimum. Typical behavior showed a significant decrease in the resilient modulus with increasing deviator stress for wet of optimum test specimens. For those tested dry of optimum, the resilient modulus also decreased with increasing deviator stress, but to a much lesser extent than those tested wet of optimum.

Seed et al. (1962) presented data from tests investigating the effect of an increase in water content after compaction for the AASHO road test subgrade soil. Specimens were prepared at 96 percent and 100 percent standard AASHO compaction densities at approximately 80 percent saturation by static compaction techniques. Some samples were tested at compaction conditions while others were allowed to absorb moisture without volume change until reaching varying degrees of saturation up to approximately 90 percent. Resilient modulus tests conducted on the specimens at

progressively higher degrees of saturation indicated a substantial increase in the resilient axial strain (decrease in modulus) at a degree of saturation of 90 percent for the specimens prepared at 96 percent standard AASHO density. For the specimens prepared at 100 percent standard AASHO density, the resilient axial strain did increase from 80 percent saturation to 90 percent saturation, but the resilient axial strain at 90 percent saturation was only about one fifth of that measured for the 96 percent standard AASHO density specimen. These results indicated the benefits of increased density with regard to the minimization of resilient strain for this soil.

Ruiz (1967) commented on the difference in magnitude of the elastic compressibility of subgrade soils with differing water content. When a load is applied to soil, the compressibility of the solid phase (soil particles) is dependent on both particle arrangement and the quantity of water present. The quantity of water present controls the degree to which cohesive forces exist among soil particles and an increase in water content tends to lubricate particles. This reduces the effective stress and allows greater compressibility of the solid phase. The compressibility of the fluid phase (air and water) is dictated by the opportunity for drainage of free air upon application of load and reaches a maximum when free drainage is possible. When a load is applied, hydrostatic pressure over the fluid phase is

developed, but will dissipate if fluid flow is possible, as is the case in dry of optimum soils. Therefore, for soils compacted on the dry side of optimum, total elastic compressibility is limited due to higher effective stress and the speedy dissipation of hydrostatic pressure over the fluid phase caused by the drainage of free air. On the wet side of optimum, elastic compressibility is larger, due to decreased effective stress and increased fluid phase hydrostatic pressure.

CHAPTER 3
LABORATORY TESTING OF FINE-GRAINED TENNESSEE SUBGRADE SOILS

3.1 Selection of Representative Soils and Field Sampling

The project goal was to investigate the resilient response of a number of subgrade soils from across the state of Tennessee covering a range of AASHTO classifications, Atterburg limits, and Proctor densities. Several on-going highway projects were identified as potential sampling locations with the help of TNDOT personnel (Trollinger 1991). The counties where several bulk samples were obtained are shown in Figure 3-1. The locations and AASHTO classifications of the candidate soils are summarized in Table 3-1. All of the candidate soils except the one identified as Rutledge Pike were collected from on-going highway projects. The Rutledge Pike soil, collected from an embankment along US11W in Knox County, was selected because previous resilient modulus research has been performed on soil taken from this location (Johnson 1986). The samples identified as Airport Connector Station 47, Station 85, Ramp A, and Orchard Pine Road were collected at the I-40 and Airport Road Connector project on the Roane/Cumberland county line. These sampling sites were identified with the help of TNDOT personnel present on the job site. The Station 47 soil was obtained from an area at the south end of SR 299 that was being used for subgrade fill soil. The remaining three soils obtained from the project were sampled from cut embankments at their respective

Table 3-1. Classifications and Index Properties of Candidate Soil Samples

LOCATION	SOIL CLASSIFICATION			ATTERBERG LIMITS			PASSING #200 SIEVE (%)	SPECIFIC GRAVITY	USE FOR Mr TESTS?
	AASHTO	GROUP INDEX	USCS	LL	PL	PI			
Rutledge Pike	A-7-6	50	CH	71	28	43	97.8	2.60	✓
Pellissippi Pky STA 400	A-7-5	36	MH	70	41	29	94.2	2.61	✓
Pellissippi Pky STA 500	A-7-6	15	CL	45	22	23	70.4	2.70	✓
Pellissippi Pky STA 600	A-7-5	44	CH-MH	69	33	36	98.4	2.71	
Airport-Ramp A	A-4	3	CL	26	17	9	64.9	---	
Airport-STA 47	A-6	8	CL	34	21	13	72.3	2.65	✓
Airport-STA 85	A-4	0	CL-ML	21	16	5	56.1	2.60	✓
Airport-Orchard Pine Road	A-4	7	CL	30	20	10	84.5	---	
S.R. 20 STA 171+85	A-6	14	CL	35	22	13	98.6	---	
S.R. 20 STA 781+75	A-4	1	ML	24	22	2	97.2	2.59	✓
S.R. 20 866+00	A-4	7	CL-ML	31	24	7	97.8	---	
S.R. 20 STA 925+20	A-6	11	CL	33	22	11	99.1	---	
S.R. 20 STA 1081+50	A-6	15	CL	36	22	14	98.9	2.62	✓
I-840 STA 28+26	A-7-6	36	CH	55	19	36	92.7	2.84	

locations. The Pellissippi Parkway Station 400, Station 500, and Station 600 soils were sampled from the Pellissippi Parkway Connector project in Knox County. All three samples were located with the help of TNDOT personnel and a set of construction plans showing Proctor test data. The soils were sampled at approximately the centerline of the finished roadway subgrade. The 5 soils identified as S.R. 20 were obtained from the State Route 20, US 421 project in Crockett and Dyer Counties. The sample identified as Station 171+85 was obtained from a cut embankment in Dyer County. The remaining 4 S.R. 20 soils were sampled in Crockett County, and all were obtained from the centerline of the finished roadway subgrade except for Station 1081+50, which came from the outside shoulder of Westbound S.R. 20. The final soil, identified as I-840 Station 28+26 was taken from a bridge abutment on the I-840 Bypass project in Wilson County. All station numbers used in identifying the soils were taken from grade stakes at each location. Care was taken during collection to ensure that representative samples were obtained from each site. Approximately 200 pounds (90.7 kg) of each candidate soil were obtained so that enough material would be available to perform all required testing.

3.2 Properties of Representative Soils

3.2.1 Index Testing

Index tests were performed on the candidate soils in

order to obtain their AASHTO and USCS classifications. The required testing included a determination of the Atterberg limits and the specific gravity of solids, according to ASTM test procedures D4318-84 and D854-83, respectively. The grain size distribution was determined by performing washed sieve and hydrometer analyses according to ASTM test procedure D 422-63. Several determinations were made using each of these test procedures, the averages of which are shown in Table 3-1 along with the corresponding sample locations and classifications. The last column in Table 3-1 indicates which soils were finally selected for resilient modulus testing. The soil properties listed in Table 3-1 indicate a good range of soil types and thus variations in the resilient behavior are to be expected.

3.2.2 Moisture-Density Relationships

The moisture-density relationships of each soil were determined in accordance with the AASHTO T-99 test procedure. A minimum of three determinations were performed for each soil. Once these tests were performed, the final selection of soils as indicated in Table 3-1 was made based on this data and the results of the index tests and classifications. The Proctor curves for the samples selected for resilient modulus testing are shown collectively in Figure 3-2. The Proctor curves shown in Figure 3-2 were obtained by a "best-fit" procedure utilizing the test data from all three determinations. Figure 3-2 illustrates the range of optimum

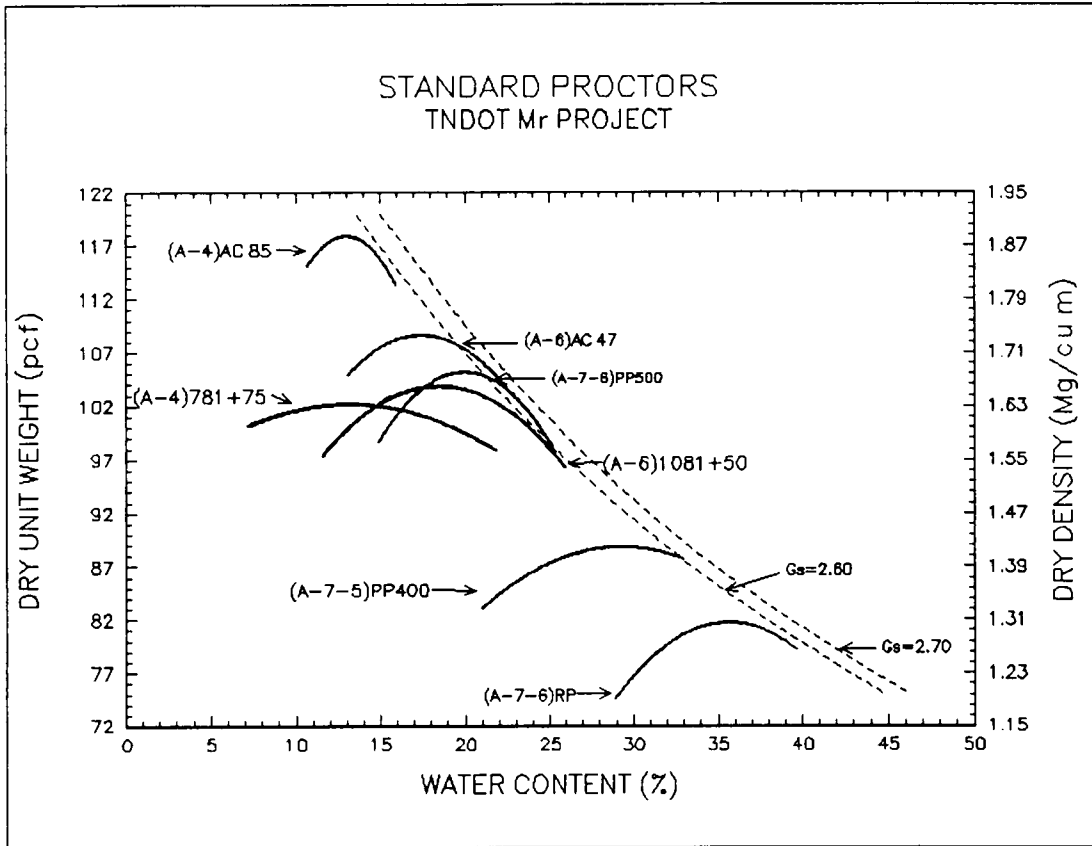


Figure 3-2. Standard Proctor Density-Moisture Curves of Selected Soils

moisture content and maximum dry density combinations present in the selected soils and also indicates the wide variation in these properties for subgrade soils across the state of Tennessee.

3.2.3 California Bearing Ratio (CBR)

Soaked California Bearing Ratio tests were performed for each selected soil in accordance with ASTM D 1883-87. The results of these tests are summarized in Table 3-2.

Table 3-2. CBR Data for Selected Soil Samples

SAMPLE LOCATION	CALIFORNIA BEARING RATIO	
	0.1"	0.2"
Rutledge Pike	3.3	3.0
Pellissippi Parkway Station 400	6.19	5.25
Pellissippi Parkway Station 500	4.52	3.13
Airport Connector Station 47	3.85	3.30
Airport Connector Station 85	5.02	4.58
S.R.20 Station 781+75	11.22	13.62
S.R.20 Station 1081+50	3.35	3.01

3.3 Resilient Modulus Testing of Fine-Grained Tennessee Subgrade Soils

3.3.1 Target Water Contents and Densities of Laboratory Test Specimens

The "best-fit" Proctor curves shown in Figure 3-2 were used to determine the target water contents and densities for the resilient modulus test specimens. A targeting scheme similar to that used by Montalvo et al. (1984) during their investigations of Oregon soils was utilized, and is illustrated in Figure 3-3. Five test specimens, two at 100

percent standard Proctor dry density and three at 95 percent standard Proctor dry density, were to be compacted as shown by the darkened circles in Figure 3-3. This targeting scheme would allow the investigation of changes in the resilient behavior of each soil with variations in the "as-compacted" water content and/or the dry density.

3.3.2 Compaction of Test Specimens

The test specimens used for resilient modulus testing were prepared using kneading compaction techniques. The decision to use kneaded specimens for resilient modulus testing was based on the fact that this technique is specified in several resilient modulus test procedures, and has also been shown by Seed et al. (1962) and Wahls and Langfelder (1967) to produce a soil fabric similar to that obtained by field compaction equipment as discussed in Section 2.3.1.

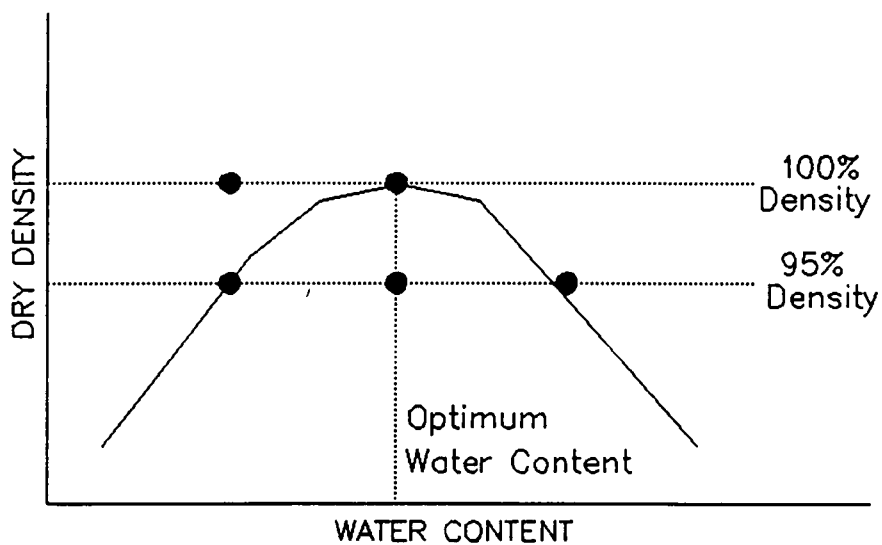


Figure 3-3. Targeting Scheme for Test Specimen Compaction

The cylindrical test specimens, which were approximately 2.8 inches (71.1 mm) in diameter and 5.6 inches (142.2 mm) tall, were compacted inside a rubber membrane using a Soiltest Model No. CN-425-A kneading compactor. The compactor, which was originally designed to produce 4 inch (101.6 mm) and 6 inch (152.4 mm) diameter bituminous samples, was modified to accommodate the 2.8 inch (71.1 mm) diameter specimen mold. The required modifications consisted of the fabrication of a wedge-shaped compaction foot that would fit just inside the cylindrical specimen mold without tearing the rubber membrane. The compaction foot used here was similar to one used by Johnson (1986), who modified the compactor to fit a 2 inch (50.8 mm) diameter specimen mold.

Once the compaction foot was fabricated and put in place, the specimen mold was attached to the compactor turntable. The turntable was then adjusted until the specimen mold and compaction foot were within the allowable tolerances for membrane clearance. The degree to which the turntable rotated after each stroke was adjustable, and was set at 30 degrees per stroke of the compaction foot. The dwell time corresponding to the duration the compaction foot was in contact with the soil was also variable, and was set at 0.3 seconds.

During specimen compaction, a trial-and-error process was necessary to obtain a consistent variation in the density of the prepared test specimens. The magnitude of pressure

applied per stroke of the compaction foot was adjustable, and was varied according to the desired density. The number of layers and the number of blows per layer necessary to obtain each target specimen density also varied.

The resulting specimen densities and water contents are summarized in Appendix A for each of the representative soils. The compaction trial-and-error process necessary for density variation along with the variability of the representative soils made it difficult to pinpoint the exact target densities of 100 percent and 95 percent standard Proctor density. As a result of these difficulties, a 1.5 pcf (24 kg/m³) tolerance was specified for each target density. This procedure resulted in most of the "low" density test specimens being at a density slightly less than the target 95 percent standard Proctor, but this was considered acceptable, since a greater range in specimen density would accentuate any possible effects of density on the resilient response. This procedure also resulted in testing more than five samples for each soil.

The greatest compaction difficulties were experienced with the two A-4 soils, Airport Connector Station 85 and State Route 20, Station 781+75. Adequate bonding between compacted layers of these test specimens was difficult to maintain and specimens frequently separated at layer divisions. These difficulties were due to the silty nature of the A-4 soils.

Most of the target water contents were acceptable, with the exception of the Airport Connector Station 85 soil. The

highest water content, originally targeted at 16.5 percent, produced samples that were unsuitable for resilient modulus testing. This water content, which was slightly greater than the soil's plastic limit, resulted in significant sample deformation under the slightest application of deviator stress. The target water content was subsequently readjusted to 15 percent, 1 percent below the soil's plastic limit of 16 percent.

After compaction, the test specimens were sealed in airtight containers and placed in a high humidity atmosphere for 6 to 8 days prior to resilient modulus testing. The maximum 2-day age difference was not considered to significantly affect the consistency of the test results, since previous research by Beaton et al. (1967) using a soil that was considered to be highly sensitive showed only a 10 percent increase in strength between specimens aged for 7 days and those aged for 14 days as discussed in Chapter 2.

3.4 Resilience Testing of Representative Soils

3.4.1 Test Apparatus

A Research Engineering Model RE-SS-2400 load frame was used to apply the repeated loads to the prepared test specimens. Cyclic air pressure was supplied to a pneumatic actuator located on top of the load frame by an electropneumatic cyclic loader. The magnitude, shape, and frequency of the applied load pulse was controlled by an Exact

Electronics Model # 506 waveform generator. This equipment was used by Johnson (1986) and Boateng-Poku (1988) in earlier resilient modulus testing. The Research Engineering Model RE-STC-150P triaxial cell used during resilient modulus testing was returned to the factory for modification in order to obtain measurements of deformation and applied load inside the cell. As discussed in Chapter 2, the measurement of these variables inside the triaxial cell eliminates possible errors due to friction along the loading piston and/or compressibility of the test equipment. A section through the modified cell is shown in Figure 3-4. A 333 pound (15.1 kg) load cell was attached to the loading piston, and the applied cyclic load was transferred to the top platen and measured via a ball bearing between the load cell and platen. Resilient deformation was measured by averaging two Schlumberger SM3 LVDTs that were diametrically opposed and attached firmly to the top platen. The LVDTs were held close to their zero point by externally-adjustable LVDT contacts.

A Schaevitz DTR-451 digital transducer readout was used to display voltage signals from the two averaged LVDTs. Voltage signals from the load cell were boosted by a DC bridge amplifier before being digitally displayed. The analog signals were then recorded on an X-Y-Y recorder.

3.4.2 Test Procedure

The resilient modulus test procedure adopted for this project was SHRP Protocol: P46, "Resilient Modulus of Unbound

of a pneumatic loading system.

Prior to testing, the compacted test specimens were removed from high-humidity storage and measured for height and diameter. The specimen ends were then capped with Hydrocal gypsum cement. The cement, which sets in approximately 10 minutes, readily fills all imperfections in the specimen ends and provides a smooth surface for specimen loading. After capping, the specimen height was measured again to determine the Hydrocal thickness, and the specimen was placed inside the triaxial cell. The top platen was fitted in place, and the specimen membrane ends were folded over the platens and secured with an O-ring. The ball bearing was put in place in the center of the top platen, and assembly of the triaxial cell was completed. The averaged LVDTs were then placed at their zero point by the use of a circuit designed to permit each LVDT to be zeroed separately. The triaxial cell was put into place in the load frame, and 6 psi (41.1 kPa) confining pressure was applied inside the cell. The sample was then conditioned by applying 200 repetitions of a deviator stress of 4 psi (27.6 kPa). After conditioning, the loading sequence shown in column 2 of Table 2-3 was followed. The loading duration for all deviator stress applications was 0.1 seconds, with a total cycle duration of 1 second. The magnitude of applied deviator stress was adjusted using the "DC offset" control on the waveform generator.

After completion of the required loading sequence, the

specimen confining pressure was removed, the triaxial cell was disassembled, and the final height of the test specimen (including the Hydrocal thickness) was determined. The entire soil specimen was then used to determine the final water content.

The inclusion of the Hydrocal thickness in the final height measurement was necessary because attempted removal of the Hydrocal cap resulted in severe damage to the specimen ends. Therefore, the Hydrocal thickness was determined prior to testing so that the increase in specimen height due to the Hydrocal could be deducted prior to calculation of axial strain.

3.4.3 Data Acquisition and Reduction

After 100 repetitions of a selected deviator stress and confining pressure combination had been applied to the test specimen, the axial load and deformation data for the last 23 cycles was captured with a Yokogawa Model 3025 A4 X-Y-Y recorder with time sweep. The recorder pen speed was set at 1 cm/sec in order to verify the load application and cycle duration times of 0.1 second and 1 second, respectively. Both pens of the X-Y-Y recorder were utilized in order to capture pen traces of the load and deformation data separately. The input voltage sensitivity of each pen could be adjusted from 0.05 mV/cm to 5 V/cm in order to vary the amplitude of the pen's oscillation in response to the load cell and LVDT input signals. This feature allowed amplification (and thus greater

precision in computations) of the resilient deflection trace for low levels of applied deviator stress. Calibration procedures were performed several times over the course of resilient modulus testing to determine the magnitude of each pen's response to several voltage sensitivities. The calibration procedures resulted in conversion factors that could be easily applied to the recorded height of each pen's trace to obtain the magnitude of the applied load (lb) and the corresponding axial deflection (in). This calibration data is provided in Table 3-3.

The specimen area was calculated by averaging diameter measurements of the top, middle, and bottom of the test specimen, while the specimen height was determined as the average of the initial and final heights (not including Hydrocal thickness). The specimen area, specimen height, load and deflection trace heights, and the appropriate conversion factors were then put into a spreadsheet for calculation of the resilient modulus value for the last 5 cycles at each deviator stress level.

Table 3-3. Calibration Constants

Input Voltage Sensitivity	Load Conversion Factor (cm/lb)	Deflection Conversion Factor (cm/in)
10 mV/cm	----	2000
25 mV/cm	0.4	800
50 mV/cm	0.1	400
0.1 V/cm	0.04	200

CHAPTER 4
RESILIENT RESPONSE OF FINE-GRAINED TENNESSEE SUBGRADE SOILS

4.1 Results of Laboratory Resilient Modulus Testing

Cyclic load triaxial tests were performed on laboratory-compacted specimens of the candidate soils. The resulting resilient response is presented in terms of resilient modulus versus deviator stress. A typical resilient response is shown in Figure 4-1, and the complete data is presented in Appendix A. Each graph contains information on the density and water content of the test specimen. The legend at the bottom of each graph shows the plotting symbol used for resilient modulus values found at confining pressures of 6, 4 and 2 psi (41.4, 27.6 and 13.8 kPa).

A concern during resilient modulus testing was the effect

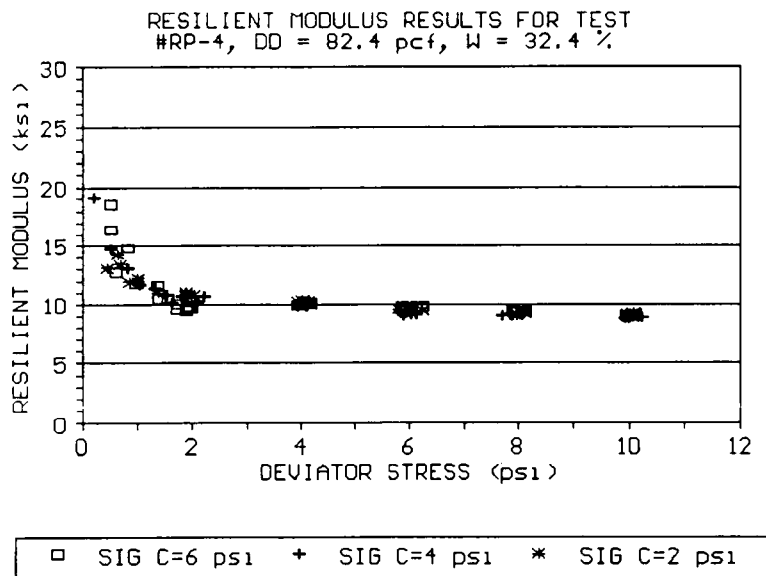


Figure 4-1. Typical Resilient Response

of confining pressure on the output of the internal load cell. Observations during testing showed an increase in load on the digital load readout when the confining pressure was increased. However, the confining pressure was found to have a negligible effect on the deviator stress. Therefore no correction was necessary for effects of confining pressure on the collected load data.

Most of the tests show the typical "stress-softening" response denoted by a decrease in the resilient modulus as the deviator stress increases. However, several of the graphs show a noticeable increase in the resilient modulus as the deviator stress increases to 8 and 10 psi (55.2 and 69 kPa), denoting "stress-hardening" behavior. Most of the tests showing the stress-hardening behavior were performed at a water content less than optimum, although all the tests conducted on S.R. 20, Station 781+75 show this behavior. An example of the stress-hardening response is shown in Figures 4-2, 4-3, and 4-4 for the S.R. 20, Station 1081+50 soil. Figure 4-2 shows a significant increase in the resilient response at the higher deviator stresses for a test conducted at a dry density of 105.2 pcf (1685.1 kg/m³) and a water content of 14.0 percent, 4.3 percent less than optimum water content. Figure 4-3, conducted at a dry density of 105.6 pcf (1691.5 kg/m³) and a water content of 17.4 percent (0.9 percent less than optimum), shows only a slight stress-hardening effect, while the test shown in Figure 4-4,

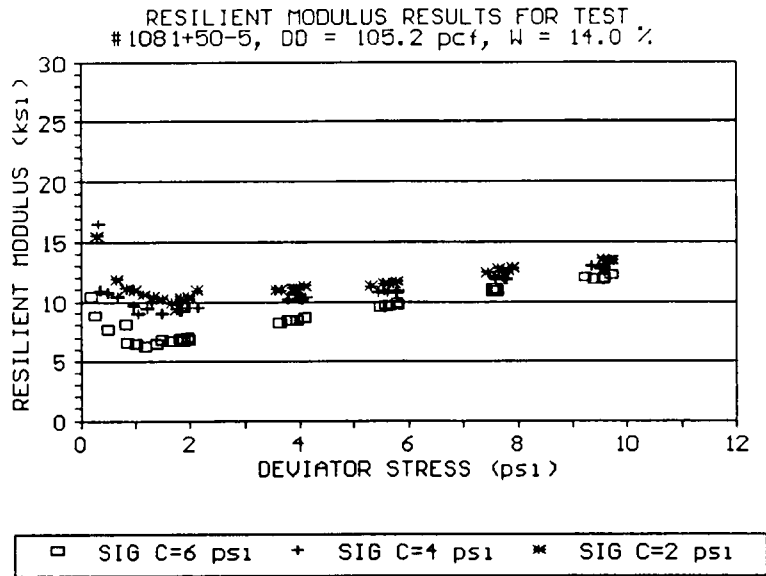


Figure 4-2. Results of Test No. 5, S.R. 20 Station 1081+50, Illustration Stress Hardening Response at a Water Content 4.3 Percent Less Than Optimum

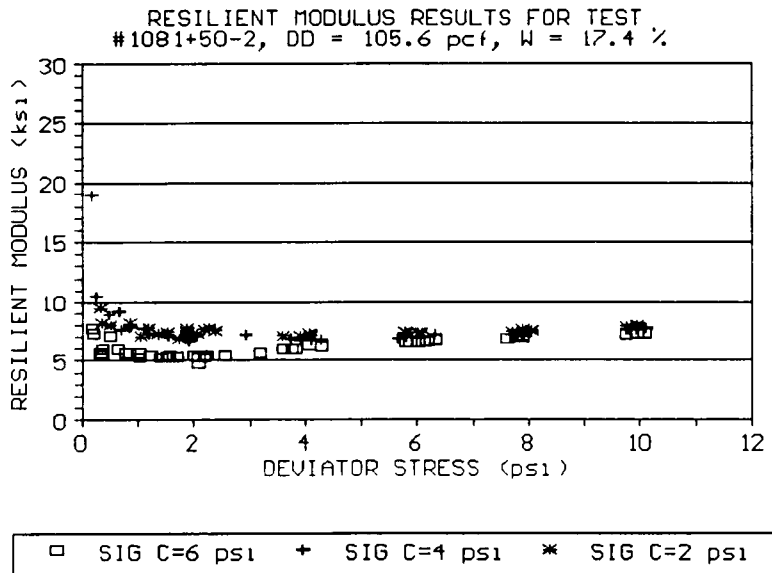


Figure 4-3. Results of Test No. 2, S.R. 20 Station 1081+50, Illustrating Stress Hardening Response at a Water Content 0.9 Percent Less Than Optimum

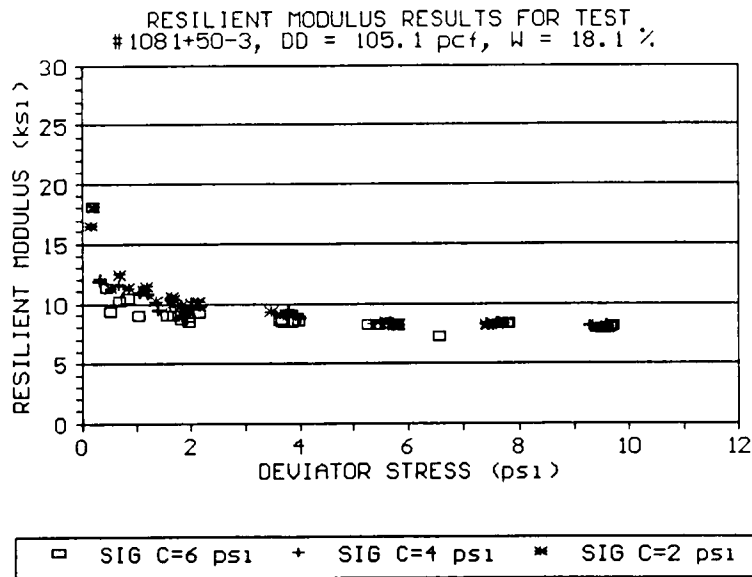


Figure 4-4. Results of Test No. 3, S.R. 20 Station 1081+50, Illustrating Decrease in Stress Hardening Response as the Water Content Reaches Optimum

conducted at a dry density of 105.1 pcf (1683.5 kg/m³) and a water content of 18.1 percent (0.2 percent less than optimum), shows a slight decrease in resilient modulus for increasing deviator stress, indicating the typical stress-softening response as the water content reaches optimum.

4.2 Analysis of Results

The resilient modulus test results were analyzed in order to determine the effects of variation in confining pressure, dry density and water content on the resilient response. The results of these analyses will be discussed in the following sections.

4.2.1 Effect of Confining Pressure

The graphs of resilient modulus versus deviator stress were examined in order to determine the effect of variation in confining pressure on the resilient response of the fine-grained soils tested. Typical test results show an increase in the resilient modulus after the first sequence of deviator stresses had been applied at a confining pressure of 6 psi (41.4 kPa). For the second and third stress sequences, which utilized confining pressures of 4 and 2 psi (27.6 and 13.8 kPa) respectively, there was no significant effect of confining stress on the resilient modulus values for any particular deviator stress. The resilient modulus curve shown in Figure 4-5 illustrates the typical increase in resilient modulus from a confining pressure of 6 psi (41.4 kPa) to the confining pressures of 4 psi (27.5 kPa) and 2 psi (13.8 kPa).

This behavior is believed to be due not to the change in confining pressure, but is a result of the relatively low deviator stress applied during the initial specimen conditioning phase as shown in Table 2-3. During specimen conditioning, a confining pressure of 6 psi (41.4 kPa) and a deviator stress of 4 psi (27.6 kPa) is maintained for 200 loading cycles. Resilient modulus testing and data collection is then begun by applying deviator stresses of 2, 4, 6, 8, and 10 psi (13.8, 27.6, 41.4, 55.2 and 69 kPa) while maintaining a confining pressure of 6 psi (41.4 kPa). The increase in deviator stress used during actual resilient modulus testing

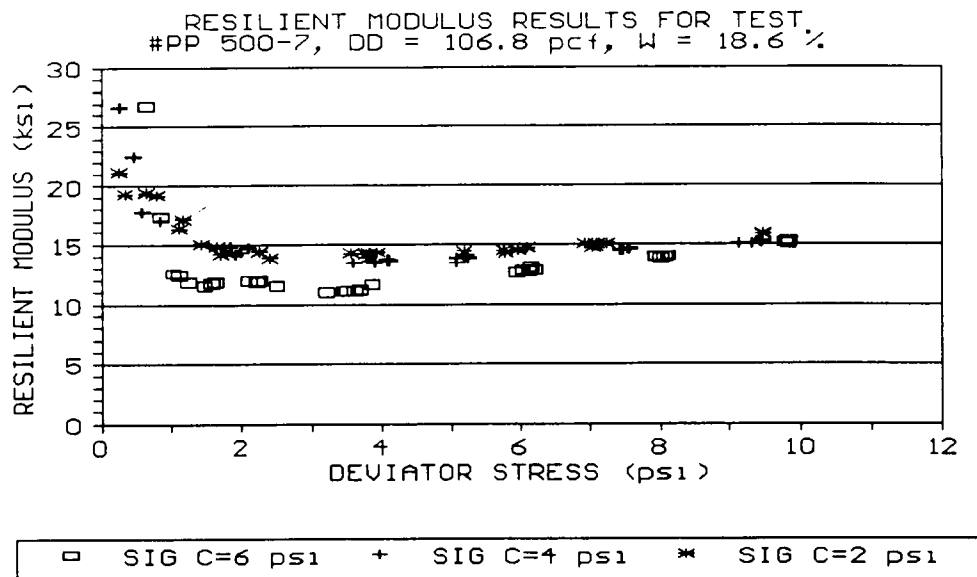


Figure 4-5. Resilient Modulus Curve Illustrating Typical Increase in Resilient Moduli For $\sigma_c = 4$ psi and 2 psi

over that used during conditioning results in greater densification of the laboratory test specimen during the first stress sequence. By the time the second stress sequence is applied, the laboratory test specimen has reached a greater density than when the test was first begun, and subsequently the material is stiffer. This increase in density and stiffness causes a reduction in the resilient strain, and thus an increase in the resilient modulus for the second and third stress sequences. This effect might be eliminated by conditioning the test specimen at the largest deviator stress to be used during the resilient modulus test sequence, as suggested by the AASHTO T274-82 method of test. Thus it is suggested here that the effect of confining stress is small, but conditioning effects may be significant. The effect of

conditioning could be verified by testing identical samples under different conditioning histories.

Except for the above noted trend, the magnitude of applied confining stress had no significant effect on the resilient response of most of the fine-grained soils tested, regardless of dry density and water content. However, for the two A-4 soils, S.R. 20 Station 781+75 and Airport Connector (A.C.) Station 85, the resilient modulus decreased slightly with decreasing confining pressure for all tests conducted on specimens at water contents greater than optimum. Figure 4-6 shows this behavior for the A.C. Station 85 soil. The results shown in Figure 4-6 were obtained from a test conducted at a water content of 13.8 percent, only slightly higher than this soil's optimum water content of 13.3 percent.

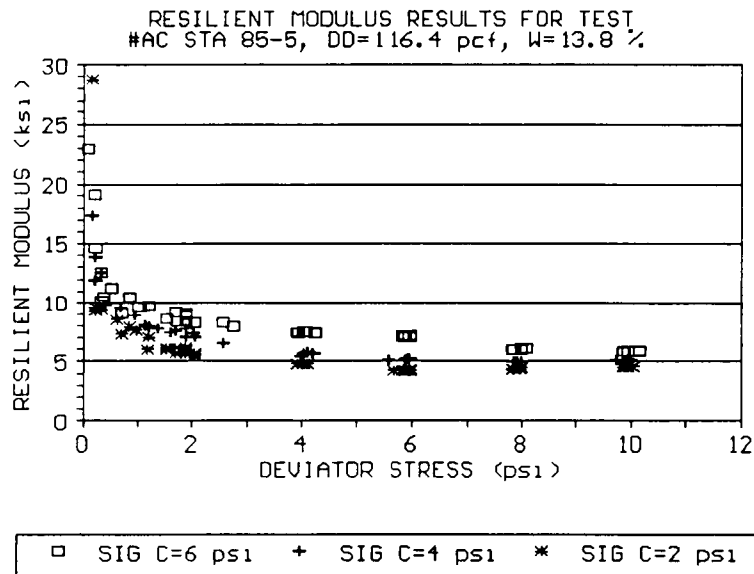


Figure 4-6. Resilient Modulus Curve Illustrating Decrease in Moduli With Increasing σ_c For an A-4 Soil Specimen Prepared at a Water Content Greater Than Optimum

4.2.2 Effect of Water Content

For most of the soils tested the resilient modulus decreased with increasing water content. This trend can be seen by examination of Figures 4-7, 4-8 and 4-9, which show the results of tests conducted on the station 1081+50 soil at water contents of 13.7 percent, 18.3 percent (optimum), and 22.2 percent, respectively. All of these tests were conducted at a dry density of about 100 pcf. This observation is consistent with that reported by Seed et al. (1962) and Thompson and Robnett (1979) as discussed in Chapter 2. The only variation in this trend was found for the two A-4 soils, S.R. 20 Station 781+75 and A. C. Station 85. For these two soils there was no significant effect by increasing the water

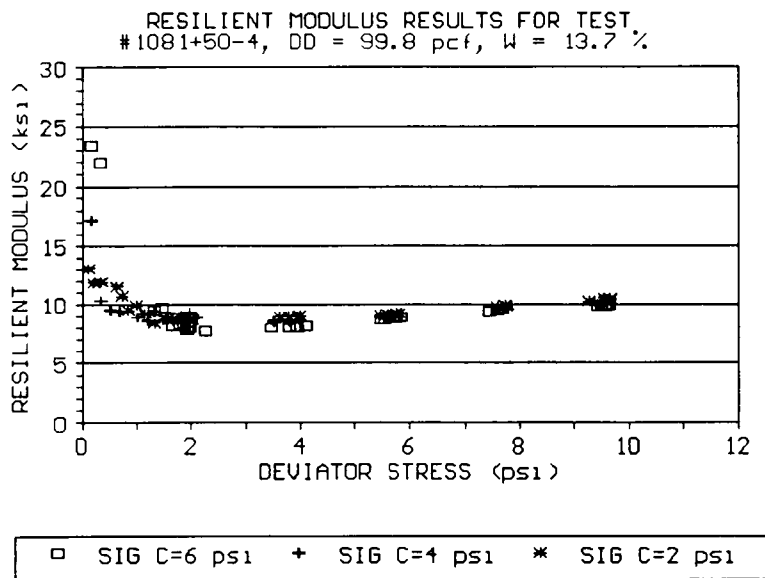


Figure 4-7. Results of Test for S.R. 20 Station 1081+50 Soil Prepared at a Water Content Dry Of Optimum

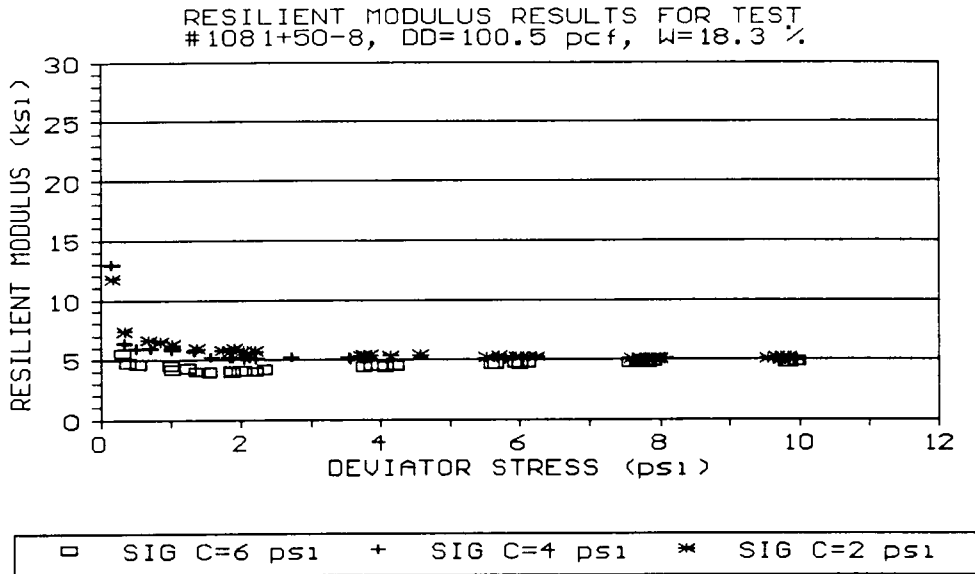


Figure 4-8. Results of Test Conducted at Optimum Water Content for S.R. 20 Station 1081+50 Soil

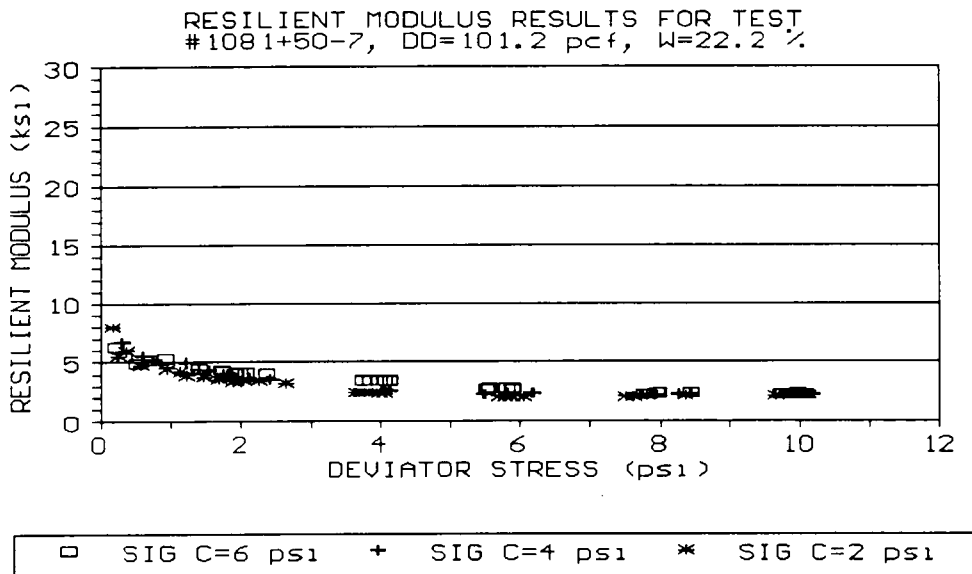


Figure 4-9. Results of Test Conducted at Water Content Greater Than Optimum for S.R. 20 Station 1081+50 Soil

content from less than optimum to optimum. The only noticeable change in the resilient modulus for the A-4 soils occurred when the water content was increased from optimum to greater than optimum.

4.2.3 Effect of Dry Density

For the two A-4 soils, S.R. 20 Station 781+75 and A.C. Station 85, there was no significant effect on the resilient response with variation in the dry density at any given water content. For the S.R. 20 Station 1081+50 soil (AASHTO classification A-6(15)), there were noticeable decreases in the resilient modulus for a small decrease in dry density as shown in Figures 4-10 and 4-11. Both of these tests were conducted at a water content of 17.4 percent, while the dry densities were 106.6 pcf (1707.5 kg/m³) and 105.6 pcf (1691.5

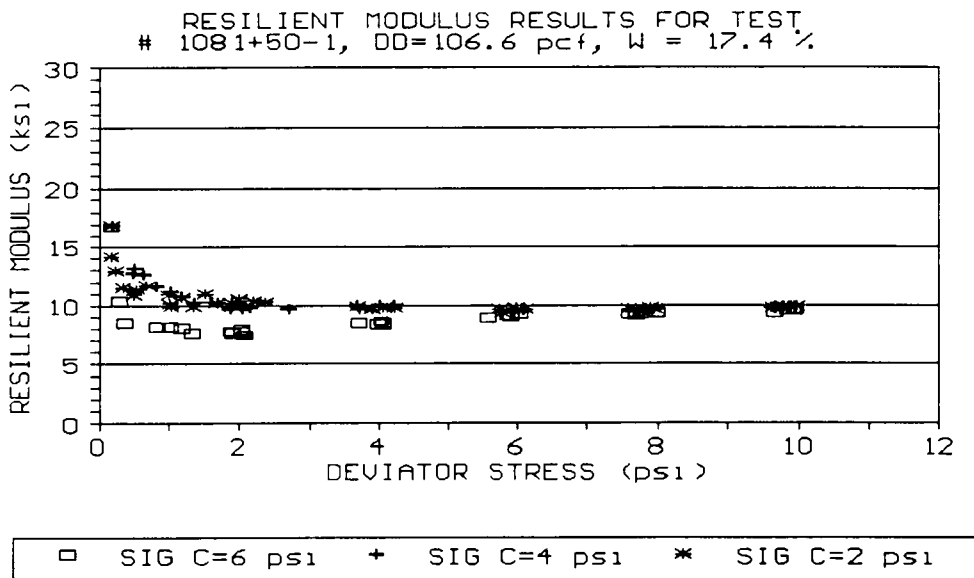


Figure 4-10. Results of Test No. 1, S.R. 20 Station 1081+50

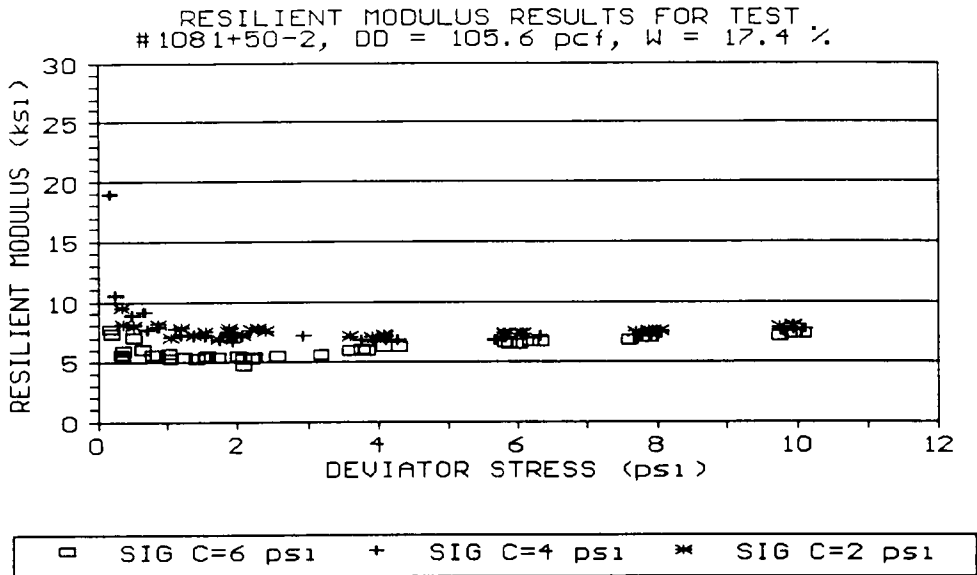


Figure 4-11. Results of Test No. 2, S.R.20 Station 1081+50

kg/m³). The difference in resilient modulus for these two tests was approximately 2.5 ksi (17.3 MPa) for a confining pressure of 6 psi (41.4 kPa) and deviator stress of 4 psi (27.6 kPa). This resilient modulus value was used for comparison because it is the representative resilient modulus value specified in SHRP Protocol P-46 for presentation of test data. Other test results for the S.R. 20 Station 1081+50 soil follow this trend, including tests no. 2 and no. 4, and tests no. 3 and no. 8, although these tests cannot be evaluated on the basis of dry density effects alone, since there were also small differences in the water contents of the test specimens.

For the A.C. Station 47 soil (AASHTO classification A-6(8)), there were six tests, two tests at each of three water contents at optimum or less than optimum, that indicated

significant increases in the resilient modulus with an increase in dry density. Above the optimum water content of 17.9 percent, there was only a slight decrease in the resilient modulus corresponding to a decrease in dry density. These tests are summarized in Table 4-1.

Similar effects of dry density on the resilient response for the three remaining soils, P.P. Station 400, P.P. Station 500 and Rutledge Pike, are summarized in Tables 4-2, 4-3 and 4-4. Although there is no observable relationship between changes in dry density and resilient modulus for these tests, a trend could possibly be established by testing numerous

Table 4-1. Effect of Variations in Dry Density on the Resilient Modulus for A.C. Station 47 Tests

Test No.	Water Content (%)	Dry Density (pcf)	M _r (ksi)	Difference in Dry Density (pcf)	Change in M _r (ksi)
15	13.1	101.5	6.17	+3.2	-1.03
16	13.1	104.7	5.14		
17	13.3	104.3	6.63	+5.9	+0.05
18	13.3	110.2	6.68		
13	13.8	97.1	5.41	+6.8	+3.82
14	13.8	103.9	9.23		
7	17.3	108.6	4.57	+2.6	+2.84
8	17.3	111.2	7.41		
9	17.9	103.1	4.22	+7.2	+4.60
10	17.9	110.3	8.82		
11	21.1	105.3	1.63	+2.5	+0.36
12	21.1	107.8	1.99		

Table 4-2. Effect of Variations in Dry Density on the Resilient Modulus for P.P. Station 400 Soil

Test No.	Water Content (%)	Dry Density (pcf)	M _r (ksi)	Difference in Dry Density (pcf)	Change in M _r (ksi)
10	25.6	87.0	9.63	+3.2	+6.41
9	25.6	90.2	16.04		
4	26.3	84.9	10.33	+3.6	+0.31
3	26.3	88.5	10.64		
7	29.6	91.0	8.05	+0.9	+3.20
8	29.6	91.9	11.25		
2	29.8	86.4	6.60	+0.7	+2.53
1	29.8	87.1	9.13		
5	33.6	86.0	4.31	+1.7	+1.72
6	33.6	87.7	6.03		

Table 4-3. Effect of Variations in Dry Density on the Resilient Modulus for P.P. Station 500 Soil

Test No.	Water Content (%)	Dry Density (pcf)	M _r (ksi)	Difference in Dry Density (pcf)	Change in M _r (ksi)
4	14.1	99.6	9.29	+0.9	-1.73
3	14.1	100.5	7.56		
10	14.2	99.7	7.06	+7.8	-0.96
11	14.2	107.5	6.10		
2	17.7	101.4	9.47	+4.5	+1.96
1	17.7	105.9	11.43		
5	18.6	101.3	11.90	+5.5	-0.51
7	18.6	106.8	11.39		
9	22.3	101.6	7.13	+1.1	+0.35
8	22.3	102.7	7.48		

Table 4-4. Effect of Variations in Dry Density on the Resilient Modulus for Rutledge Pike Soil

Test No.	Water Content (%)	Dry Density (pcf)	M _r (ksi)	Difference in Dry Density (pcf)	Change in M _r (ksi)
9	32.1	79.7	8.51	+5.3	+1.76
10	32.1	85.0	10.27		
4	32.4	82.4	10.24	+0.1	-2.12
3	32.4	82.5	8.12		
8	34.1	77.0	10.04	+0.2	-3.24
7	34.1	77.2	6.80		
6	35.7	79.4	6.00	+2.8	-0.04
5	35.7	82.2	5.96		
2	39.4	79.6	4.51	+2.9	-1.15
1	39.4	82.5	3.36		

specimens of each soil at various dry density and water content combinations as performed by Seed et al. (1962).

4.3 Design Handbook of Resilient Response

The resilient response at the five target water contents and dry densities, the log-log and hyperbolic model parameters, and the index properties of each candidate soil have been summarized in the form of a Design Handbook. The pavement designer will be able to select a soil (or soils) shown in the handbook with properties similar to the subgrade for which the new pavement is being designed, and estimate the resilient response. This will allow the design method given in the 1986 *AASHTO Guide for the Design of Pavement Structures*

(AASHTO Guide 1986) to be utilized without additional laboratory tests. The handbook pages for each of the candidate soils are shown in Appendix B, along with an example of how the handbook is used.

4.4 Mathematical Models

The four mathematical models described in Chapter 2 have been fitted to the resilient modulus curve for the Rutledge Pike test conducted at maximum dry density and optimum water content (test no. RP-5) in order to evaluate the effectiveness of each model in predicting the resilient response. Evaluations of these models will be discussed in the following sections.

4.4.1 Bilinear Model

Figure 4-12 shows the bilinear model along with test data for the Rutledge Pike soil. The following values were used in the model shown in Figure 4-12:

for $\sigma_{\min} = 2$ psi, the upper limit $M_r = c_1 = 11.0$ ksi

for $\sigma_{\max} = 13$ psi, the lower limit $M_r = c_2 = 5.3$ ksi

the first slope $k_1 = -1.11$ ksi/psi, $a_1 = 13.2$ ksi

the second slope $k_2 = -.178$ ksi/psi, $a_2 = 7.6$ ksi

and the breakpoint $\sigma_d, \sigma_i = 6.2$ psi.

As discussed in Chapter 2, the parameters σ_{\min} , σ_i , k_1 , and k_2 are assumed to be constants for all resilient responses. However, determination of the five other parameters necessary for this model make its development time consuming. The

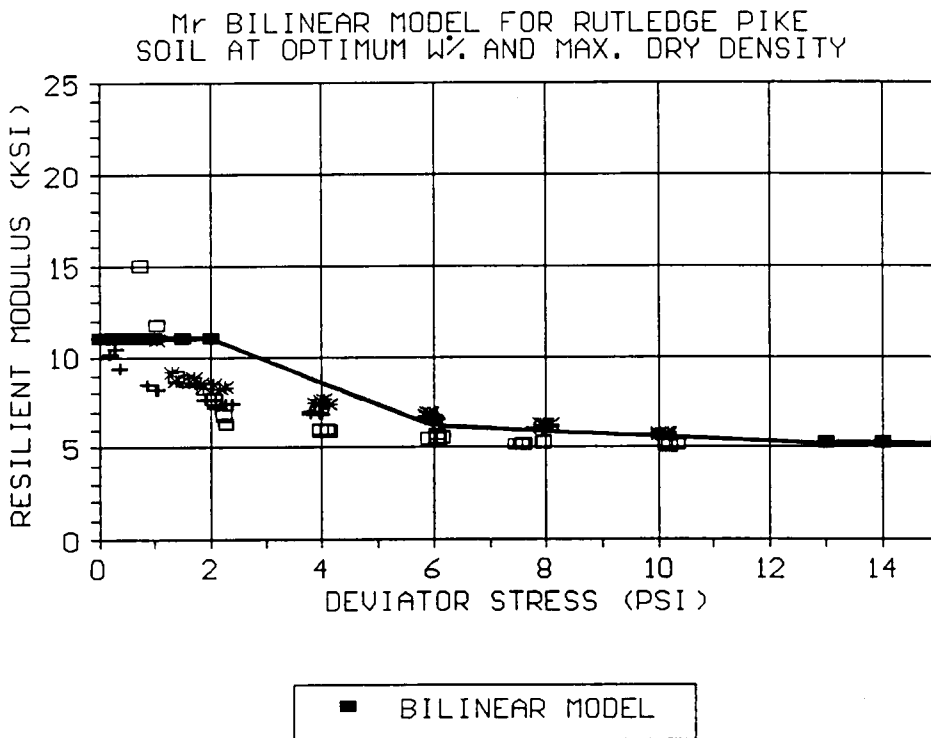


Figure 4-12. Bilinear Model and Rutledge Pike Test No. 5 Resilient Modulus Data

bilinear model also doesn't predict the values of resilient modulus at lower deviator stresses for the Rutledge Pike soil shown in Figure 4-12.

4.4.2 Log-Log Model

The log-log model shown in Figure 4-13 for the Rutledge Pike soil has the values of $K_1 = 9.09$ and $K_2 = -0.40$. The log-log model is an excellent fit to the actual Rutledge Pike test data shown in Figure 4-13.

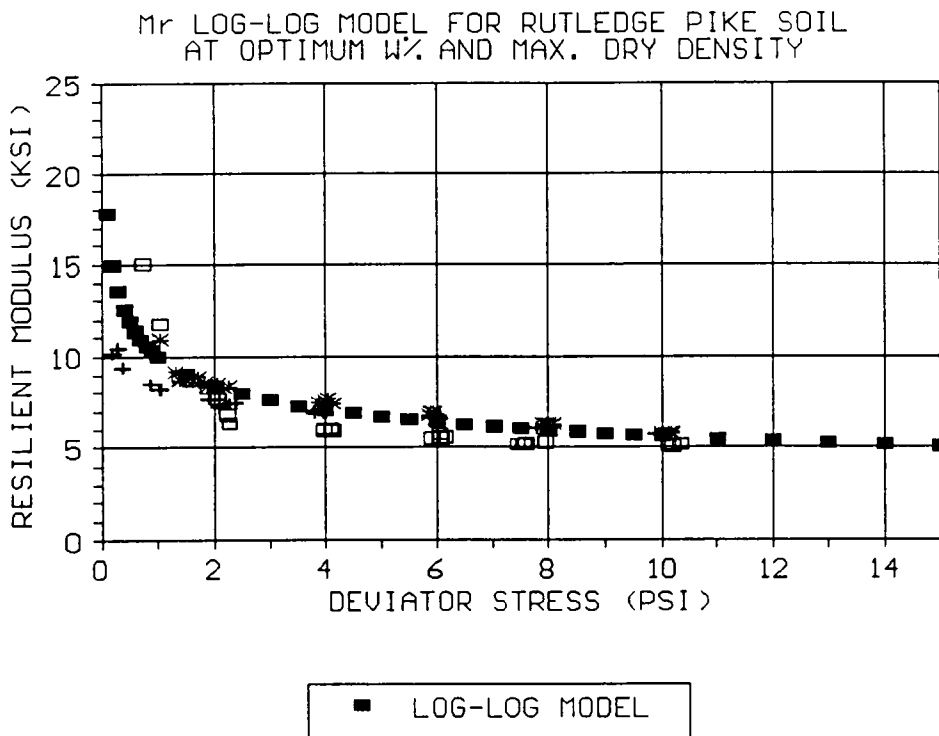


Figure 4-13. Log-Log Model and Rutledge Pike Test No. 5 Resilient Modulus Data

4.4.3 Hyperbolic Model

The hyperbolic model shown in Figure 4-14 has the values of $a = 5.72$ and $b = 5.13$. Like the log-log model, the hyperbolic model is also an excellent fit to the actual Rutledge Pike resilient modulus test data shown in Figure 4-14. The most significant difference between the hyperbolic and log-log models is the estimation of the resilient modulus at deviator stresses less than 1 psi (6.9 kPa). The hyperbolic model consistently predicts higher resilient modulus values than the log-log model at these low deviator stresses.

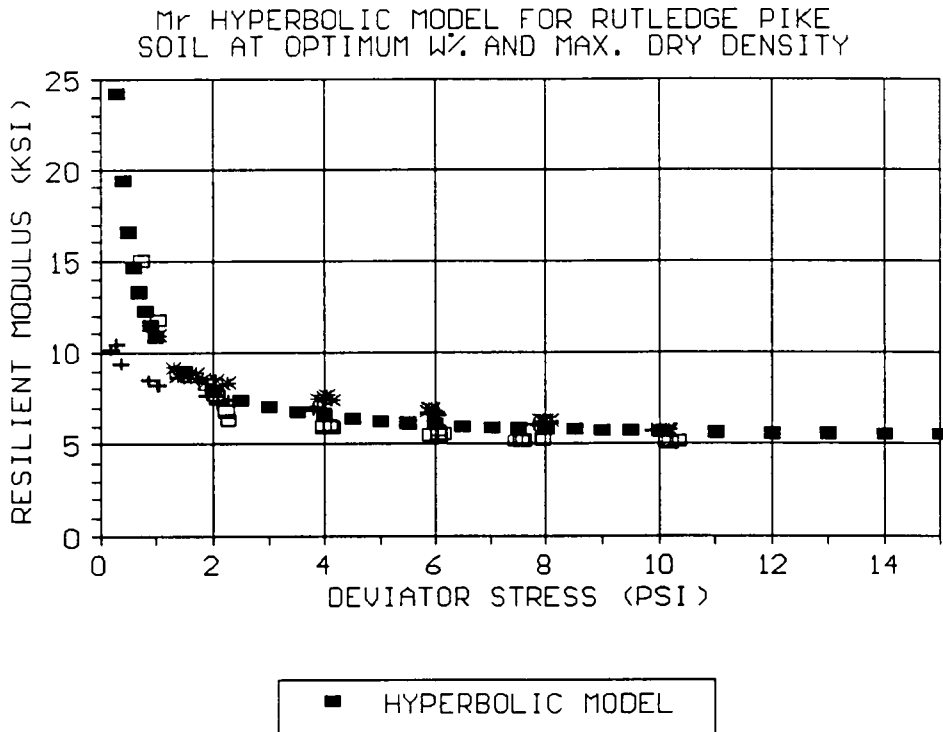


Figure 4-14. Hyperbolic Model and Rutledge Pike Test No. 5 Resilient Modulus Data

4.4.4 Modified Hyperbolic Model

The following values were used in the modified hyperbolic model shown in Figure 4-15:

$$E_{\max} = 14.98 \text{ ksi}$$

$$E_{\min} = 5.05 \text{ ksi}$$

$$a = 0.9$$

$$b = 1.25$$

As stated in Chapter 2, a disadvantage of this model is the fact that the parameters a and b have no physical significance, although this model represents the Rutledge Pike

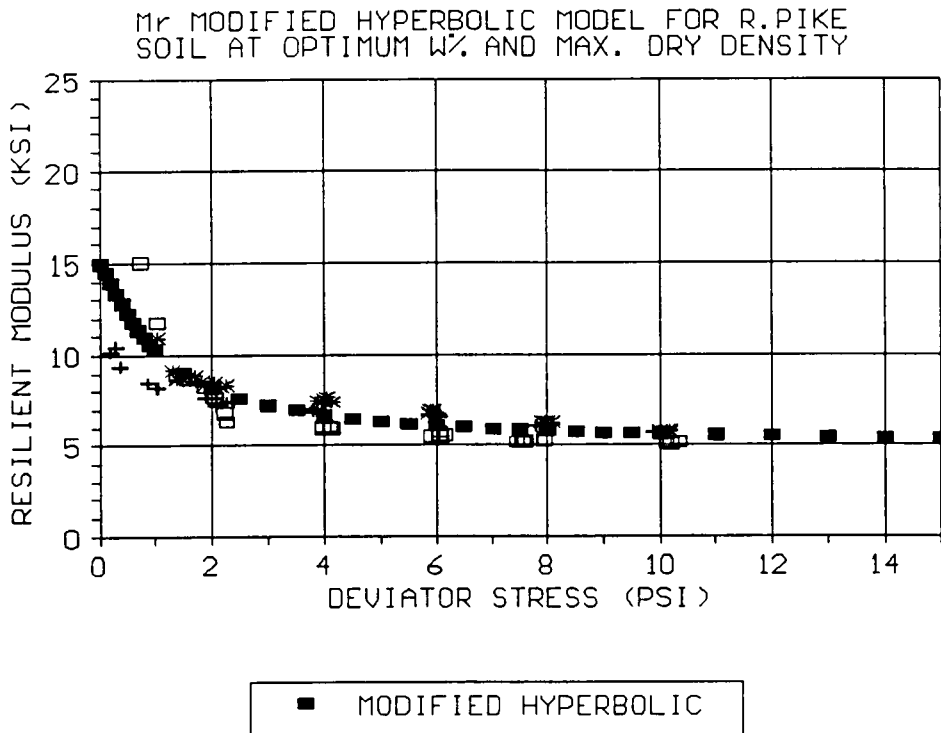


Figure 4-15. Modified Hyperbolic Model and Rutledge Pike Test No. 5 Resilient Modulus Data

data more accurately at lower deviator stresses than the other three models that were evaluated.

Parameters for the hyperbolic model and the log-log model have been found for all the resilient modulus tests conducted here, and are shown in Appendix A for each soil. The log-log model was chosen because it is specified for data presentation in both SHRP Protocol P-46 and AASHTO T294-92I methods of test. The hyperbolic model was chosen for evaluation because of the physical significance of its parameters a and b and the ease of parameter determination. The parameters for the hyperbolic and log-log model for tests conducted at the target

water contents and densities are contained in the Design Handbook shown in Appendix B.

CHAPTER 5 SUMMARY, CONCLUSIONS AND RECOMMENDATIONS FOR ADDITIONAL WORK

5.1 Summary and Conclusions

An investigation of the resilient modulus of seven fine-grained Tennessee subgrade soils was conducted. Previous resilient modulus research was reviewed. Laboratory equipment was modified and a standard method of test was adopted.

Fourteen subgrade soil samples were collected from across the state of Tennessee. Standard laboratory tests were performed to determine the index properties and classifications of the soils. Results of these tests were used to select seven soils for resilient modulus testing that covered a range of AASHTO classifications, Atterberg limits, and Proctor densities. Laboratory test specimens were prepared by kneading compaction techniques at various water content and dry density combinations. Cyclic load triaxial tests were conducted on the test specimens using confining pressures of 6, 4 and 2 psi (41.4, 27.6 and 13.8 kPa) at deviator stresses ranging from 2 to 10 psi (13.8 to 69 kPa).

Graphs of resilient modulus versus deviator stress were prepared for each test. Examination of these graphs indicated that all of the tests exhibited the typical "stress-softening" response denoted by a decrease in resilient modulus with increasing deviator stress. However, all of the tests for one of the A-4 soils and several of those performed for the other soils at water contents less than optimum exhibited a slight

"stress-hardening" behavior, denoted by an increase in the resilient modulus at higher deviator stress levels, after the initial decrease.

The resilient modulus versus deviator stress graphs were examined in order to determine the effects of confining pressure, water content and dry density on the resilient response of the test soils. The level of confining pressure was found to slightly affect the resilient response of only the tests conducted on the two A-4 soils at water contents greater than optimum. Typical test results of the other soils indicated an increase in the resilient modulus from the first stress sequence conducted at a confining pressure of 6 psi (41.4 kPa) to the second and third sequences conducted at confining pressures of 4 and 2 psi (27.6 and 13.8 kPa), respectively. This increase was believed to be due not to the confining pressure but rather was a result of increased density and stiffness of the test specimen after the first stress sequence had been completed. This trend may be eliminated by conditioning the test specimen at the highest level of deviator stress to be applied during the test sequence, as suggested by some test procedures.

The resilient modulus was found to decrease with increasing water content for all of the soils except those classified as A-4. For these two soils there was no significant effect due to increasing the water content from less than optimum to optimum. The only noticeable change in

the resilient response of the A-4 soils occurred when the water content was increased from optimum to greater than optimum.

For most of the tests, a change in dry density between two laboratory test specimens prepared at the same water content had no significant effect on the resilient response. However, there were a few test specimens that exhibited a change in the resilient modulus corresponding to a change in the dry density. Several tests for both of the A-6 soils and the A-7-5 soil showed increases in the resilient modulus with an increase in the dry density at a given water content. The effects of dry density varied for some of the tests performed on the two A-7-6 soils, with an increase in dry density causing either an increase or a decrease in the resilient modulus, with no particular observable pattern.

Four mathematical models were fitted to the results of the resilient modulus test conducted at optimum water content and maximum dry density for the Rutledge Pike soil in order to evaluate the effectiveness of each model in predicting the resilient response. The four models evaluated were: a bilinear model; a log-log model; a hyperbolic model; and a modified hyperbolic function. The modified hyperbolic model represented the modeled data more accurately than the others, particularly at low deviator stresses. Because two parameters in the modified hyperbolic model have no physical significance and would therefore make predictions of the resilient modulus

difficult, a decision was made to evaluate the parameters for the log-log and hyperbolic model for each resilient modulus test.

Finally, the index properties, log-log and hyperbolic model parameters, and the resilient response at five target water contents and dry densities of each soil were summarized in the form of a Design Handbook for use in pavement design. The handbook will allow the estimation of a resilient modulus value for new pavement subgrades based on index properties and the results of standard laboratory tests of the new soils. An example of how the handbook is used is also included.

5.2 Recommendations For Additional Work

Recommendations for additional resilient modulus testing are as follows:

1. A closed-loop electrohydraulic testing system should be used during resilient modulus testing. These systems allow precise control of the loading history and also permit computerized data collection and reduction. A closed-loop system would eliminate the timely processes of manual load adjustment and manual data reduction.
2. The effect of specimen conditioning should be further investigated by testing identical samples under different conditioning histories.
3. The effect of variations in dry density on the resilient response should be investigated further by testing numerous

specimens prepared over a range of dry density and water content combinations as performed by previous researchers.

4. Resilient modulus tests for fine-grained materials should be conducted using only one level of confining stress, since only minimal variations in the resilient response were found due to changes in the confining stress. This practice would reduce the time required for testing to approximately one-third of the time required by present testing procedures which utilize three levels of confining stress.

LIST OF REFERENCES

American Association of State Highway and Transportation Officials (1972). *AASHTO Interim Guide for the Design of Pavement Structures*, AASHTO, Washington, D.C.

American Association of State Highway and Transportation Officials, (1986). *AASHTO Guide for the Design of Pavement Structures* AASHTO, Washington, D.C.

American Association of State Highway and Transportation Officials (1986). *AASHTO Standard Method of Test for Resilient Modulus of Subgrade Soils, AASHTO Designation T274-82*, AASHTO, Washington, D.C.

American Association of State Highway and Transportation Officials (1992). *AASHTO Interim Method of Test for Resilient Modulus of Unbound Granular Base/Subbase Materials and Subgrade Soils - SHRP Protocol P46, AASHTO Designation T 294-92I*, AASHTO, Washington, D.C.

Barksdale, R.D. and Leonards, G.A. (1967). "Predicting Performance of Bituminous Surfaced Pavements," *The University of Michigan Second International Conference on the Structural Design of Asphalt Pavements Proceedings*, University of Michigan, Ann Arbor Michigan, August 7-11.

Beaton, J.L., Zube, E. and Forsyth, R. (1967). "Field Application of the Resilience Design Procedure for Flexible Pavements," *The University of Michigan Second International Conference on the Structural Design of Asphalt Pavements Proceedings*, University of Michigan, Ann Arbor, Michigan, August 7-11.

Boateng-Poku, Y. (1988). "Testing and Modeling of Subgrade Resilient Moduli for Tennessee Soils," Thesis presented for the Master of Science Degree, Department of Civil Engineering, The University of Tennessee, Knoxville.

Boateng-Poku, Y. and Drumm, E.C. (1989). "Hyperbolic Model for the Resilient Modulus Response of Fine-Grained Subgrade Soil," *Resilient Moduli of Soils: Laboratory Conditions*, Geotechnical Special Publication No. 24, American Society of Civil Engineers, New York, N.Y.

Brodsky, N.S. (1989). "Resilient Modulus Measurements on Cohesive Soils," *Resilient Moduli of Soils: Laboratory Conditions*, Geotechnical Special Publication No. 24, American Society of Civil Engineers, New York, N.Y.

Brown, S.F. and Snaith, M.S. (1974). "The Measurement of Recoverable and Irrecoverable Deformations in the Repeated Load Triaxial Test," *Geotechnique*, Vol. 24, No. 2, June.

Chan, C.K. and Mulilis, J. P. (1976). "Pneumatic Sinusoidal Loading System," *Proceedings of the American Society of Civil Engineers, Geotechnical Engineering Division*, Vol. 102, No. GT3, March.

Claros, G., Hudson, W.R. and Stokoe, K.H. II (1990). "Modifications to Resilient Modulus Testing Procedure and Use of Synthetic Samples for Equipment Calibration," *Transportation Research Record* No. 1278, Transportation Research Board, Washington, D.C..

Corps of Engineers (1962). "Development of the Gyrotory Testing Machine and Procedures for Testing Bituminous Paving Mixtures," Technical Report No. 3-595, U.S. Army Engineering Waterways Experiment Station, Vicksburg, MS.

Corps of Engineers (1962). "Gyrotory Compaction Method for Determining Density Requirements for Subgrade and Base of Flexible Pavements," Misc. Paper No. 4-494, U.S. Army Engineering Waterways Experiment Station, Vicksburg, MS.

de Medina, J. and Preussler, E.S. (1982). "Resilient Characteristics of Brazilian Soils," *Journal of the Geotechnical Engineering Division, American Society of Civil Engineers*, Vol. 108, No. GT5, May.

Drumm, E.C., Boateng-Poku, Y., and Johnson Pierce, T. (1990). "Estimation of Subgrade Resilient Modulus from Standard Tests," *Journal of the Geotechnical Engineering Division, American Society of Civil Engineers*, Vol. 116, No. 5.

Drumm, E.C., Hudson, J.M., Li, Z., Madgett, M., and Baker, D. (1992). "Resilient Response of Tennessee Subgrades," Interim Report submitted to Materials and Test Division, Tennessee Department of Transportation, Project #RES1009, February, 70 pp.

Drumm, E.C. and Moore, A.B. (1988). "Pavement Design Using Rapid Methods of Collecting and Analyzing Deflection Data, Phase II-Design Procedure Development," Report to Tennessee Department of Transportation, Project 83-25-2, August, 126 pp.

Edris, E.V. and Lytton, R.L. (1977). "Climatic Materials Characterization of Fine-Grained Soils," *Transportation Research Record* 642, Transportation Research Board, Washington, D.C.

Elfino, M.K. and Davidson, J.L. (1989). "Modeling Field Moisture in Resilient Modulus Testing," *Resilient Moduli of Soils: Laboratory Conditions*, Geotechnical Special Publication No. 24, American Society of Civil Engineers, New

York, N.Y.

Elliott, R.P. and Thornton, S.I. (1988). "Simplification of Subgrade Resilient Modulus Testing," *Transportation Research Record 1192*, Transportation Research Board, Washington, D.C.

Elliott, R.P. and Thornton, S.I. (1988). "Resilient Modulus and AASHTO Pavement Design," *Transportation Research Record 1196*, Transportation Research Board, Washington, D.C.

Fredlund, D.G., Bergan, A.T. and Wong, P.K. (1977). "Resilient Modulus Constitutive Relationship for Cohesive Soils," *Transportation Research Record 642*, Transportation Research Board, Washington, D.C.

George, K.P. (1992). "Resilient Testing of Soils Using Gyrotory Testing Machine," Transportation Research Board 71st Annual Meeting, Washington, D.C., January 12-16.

Highway Research Board (1962). *The AASHTO Road Test*, Special Report 73.

Jardine, R.J., Symes, M.J. and Burland, J.B. (1984). "The Measurement of Soil Stiffness in the Triaxial Apparatus," *Geotechnique*, Vol. 34, No. 3, September.

Jin, M., Lee, K.W. and Kovacs, W.D. (1992). "Field Instrumentation and Laboratory Study to Investigate Seasonal Variation of Resilient Modulus of Granular Soils," Transportation Research Board 71st Annual Meeting, Washington, D.C., January 12-16.

Johnson, T.D. (1986). *The Resilient Moduli of Subgrade Soil in the East Tennessee Area*, Thesis presented for the Master of Science Degree, Department of Civil Engineering, The University of Tennessee, Knoxville.

Kondner, R.L. (1963). "Hyperbolic Stress-Strain Response: Cohesive Soils," *Journal of the Soil Mechanics and Foundation Division*, American Society of Civil Engineers, Vol.89, No. SM1.

Lambe, T.W. and Whitman, R.V. (1969). *Soil Mechanics*, John Wiley and Sons, Inc..

Linton, P.F., McVay, M.C., and Bloomquist, D. (1988). "Measurement of Deformations in the Standard Triaxial Environment with a Comparison of Local Versus Global Measurements on a Fine, Fully Drained Sand," *Advanced Triaxial Testing of Soil and Rock*, ASTM STP 977, Robert T. Donaghe, C. Chaney, and Marshall L. Silver, Eds., American Society for Testing and Materials, Philadelphia, pp. 202-215.

Matthews, J.M. and Pandey, B.B. (1991). "Performance of Flexible Pavements," *Transportation Research Record 1307*, Transportation Research Board, Washington, D.C.

Monismith, C.L. (1992). "Analytically-Based Asphalt Pavement Design and Rehabilitation...Theory to Practice (1962-1992)," TRB Distinguished Lecture, Transportation Research Board 71st Annual Meeting, Washington, D.C., January 12-16.

Montalvo, J.R., Bell, C.A., and Wilson, J.E. (1984). "Comparison of Diametrial and Triaxial Repeated Load Testing Techniques for Untreated Soils," *Transportation Research Record 998*, Transportation Research Board, Washington, D.C.

Moossazadeh, J.M. and Witczak, W. (1981). "Prediction of Subgrade Moduli for Soil That Exhibits Nonlinear Behavior," *Transportation Research Record 810*.

Nataatmadja, A. and Parkin, A.K. (1990). "Axial Deformation Measurement in Repeated Load Triaxial Testing," *Geotechnical Testing Journal*, GTJODJ, Vol. 13, No. 1, March.

Pell, P.S. and Brown, S.F. (1972). "The Characteristics of Materials for the Design of Flexible Pavement Structures," *The University of Michigan Third International Conference on the Structural Design of Asphalt Pavements Proceedings*, Grosvenor House, Park Lane, London, England, September 11-15.

Pezo, R.F., Claros, G., and Hudson, W.R. (1992). "An Efficient Resilient Modulus Testing Procedure for Subgrade and Non-Granular Subbase Materials," Transportation Research Board 71st Annual Meeting, Washington, D.C., January 12-16.

Pezo, R.F., Kim, D., Stokoe II, K.H., and Hudson, W.R. (1991). "A Reliable Resilient Modulus Testing System," *Transportation Research Record 1307*, Transportation Research Board, Washington, D.C.

Prapaharan, S., White, D.M. and Altschaeffl, A.G. (1991). "Fabric of Field- and Laboratory-Compacted Clay," *Journal of Geotechnical Engineering*, American Society of Civil Engineers, Vol. 117, No. 12, December.

Robnett, Q.L. and Thompson, M.R. (1973). "Interim Report-Resilient Properties of Subgrade Soils-Phase I-Development of Testing Procedure," Transportation Engineering Series No. 5, Civil Engineering Series, Illinois Cooperative Highway Research Program, Series No. 139, University of Illinois at Urbana-Champaign, Urbana, Ill., May.

Ruiz, C. (1967). "Measurement and Interpretation of the Elastic Compressibility of Subgrades and Its Relations to the

Behavior of Asphalt Pavements," *The University of Michigan Second International Conference on the Structural Design of Asphalt Pavements Proceedings*, University of Michigan, Ann Arbor Michigan, August 7-11.

Seed, H.B., Chan, C.K., and Lee, C.E. (1962). "Resilience Characteristics of Subgrade Soils and Their Relation to Fatigue Failures in Asphalt Pavements," *International Conference on the Structural Design of Asphalt Pavements Proceedings*, University of Michigan, Ann Arbor, Michigan, August 20-24.

Strategic Highway Research Program (1989). "Resilient Modulus of Unbound Granular Base/Subbase Materials and Subgrade Soils," SHRP Protocol P-46, UG07, SS07.

Terrel, R.L. and Award, I.S. (1972). "Laboratory Considerations," *Proceedings Association of Asphalt Paving Technologists*, AAPT Symposium of Technology of Thick Lift Construction.

Thompson, M.R. and Robnett, Q.L. (1973). "Interim Report, Resilient Properties of Subgrade Soils, Phase 1 - Development of Testing Procedure," *Civil Engineering Series, Transportation Engineering Series No. 5*, Illinois Cooperative Highway Research Program, Series No. 139, May.

Thompson, M.R. and Robnett, Q.L. (1976). "Final Report, Resilient Properties of Subgrade Soils," *Civil Engineering Studies Transportation Engineering Series No. 14*, Illinois Cooperative Highway and Transportation Series No. 160.

Thompson, M.R. and Robnett, Q.L. (1979). "Resilient Properties of Subgrade Soils," *Transportation Engineering Journal*, American Society of Civil Engineers, Vol. 105, No. TE1, January.

Thornton, S.I. and Elliott, R.P. (1986). "Resilient Modulus-What Does It Mean?", *Proceedings of the 37th Annual Highway Geology Symposium*, Helena, Montana, August 20-22.

Transportation Research Board (1975). *Testing Procedures for Characterizing Dynamic Stress-Strain Properties of Pavement Materials*, Special Report 162, Washington, D.C.

Trollinger, B. (1991). Personal communication.

Wahls, H.E. and Langfelder, L.J. (1967). "The Influence of Compaction Methods and Conditions on the Structural Behavior of Compacted Subgrades," *The University of Michigan Second International Conference on the Structural Design of Asphalt Pavements Proceedings*, University of Michigan, Ann Arbor,

Michigan, August 7-11.

Wilson, B.E., Sargand, S.M., Hazen, G.A., and Green, R. (1990). "Multiaxial Testing of Subgrade," *Transportation Research Record 1278*, Transportation Research Board, Washington, D.C.

Yoder, E.J. and Witczak, M.W. (1975). *Principles of Pavement Design*, John Wiley and Sons, Inc..

APPENDICES

APPENDIX A
MODEL PARAMETERS AND RESILIENT MODULUS PLOTS

Rutledge Pike
Model Parameters
and
Resilient Modulus Plots

Table A-1. Hyperbolic and Log-Log Model Parameters For Rutledge Pike Resilient Modulus Tests

TEST NO.	DRY DENSITY (pcf)	WATER CONTENT (%)	HYPERBOLIC MODEL		LOG-LOG MODEL	
			a	b	K ₁	K ₂
1	82.5	39.4	5.0458	2.4625	6.0673	-.3692
2	79.6	39.4	5.5570	2.9230	6.7198	-.3839
3	82.5	32.4	0.6247	8.4260	8.6169	-.0251
4	82.4	32.4	3.7475	8.7295	12.2786	-.3909
5	82.2	35.7	5.7173	5.1267	9.0876	-.4016
6	79.4	35.7	5.4376	4.5213	8.3214	-.3859
7	77.2	34.1	0.3236	6.7880	7.7577	-.1178
8	77.0	34.1	6.4531	7.9846	11.9046	-.3883
9	79.7	32.1	0.2389	10.0799	10.6158	.0713
10	85.0	32.1	0.4320	11.3976	12.2780	-.0464

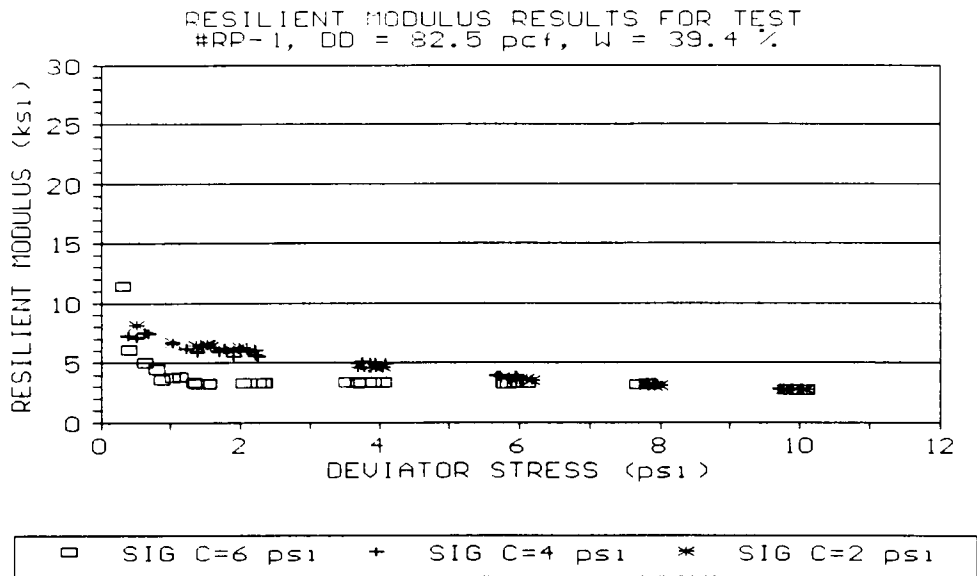


Figure A-1. Resilient Response For Rutledge Pike Test No. 1

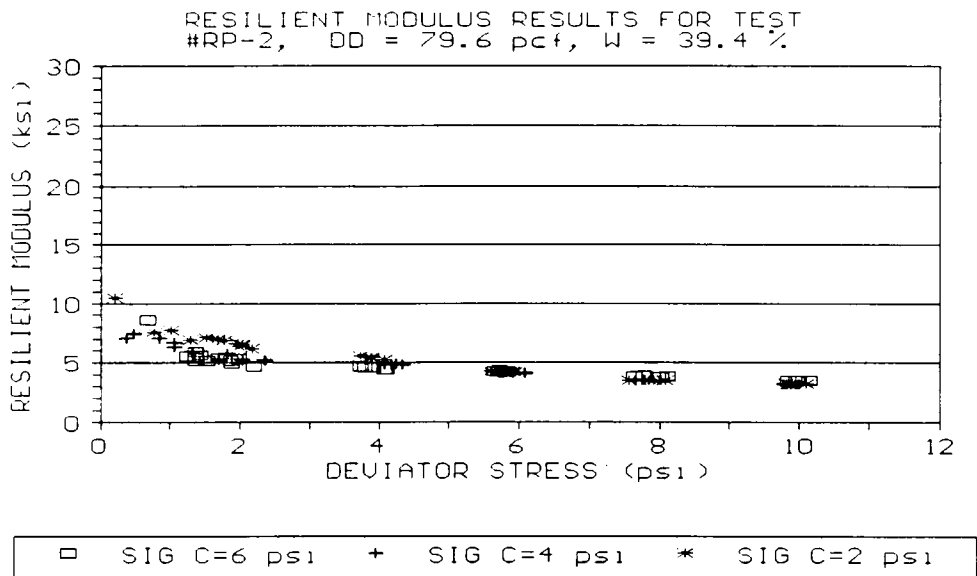


Figure A-2. Resilient Response For Rutledge Pike Test No. 2

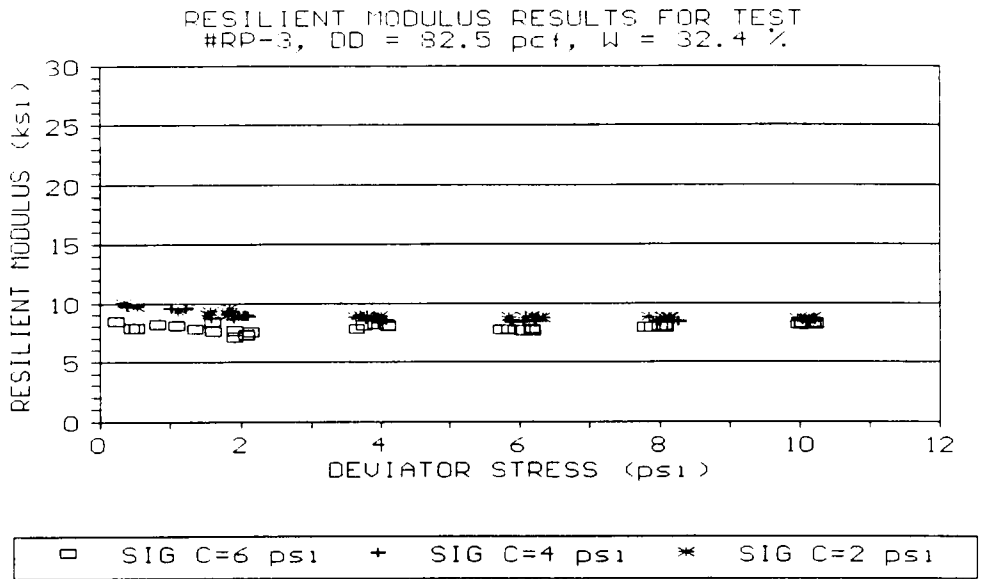


Figure A-3. Resilient Response For Rutledge Pike Test No. 3

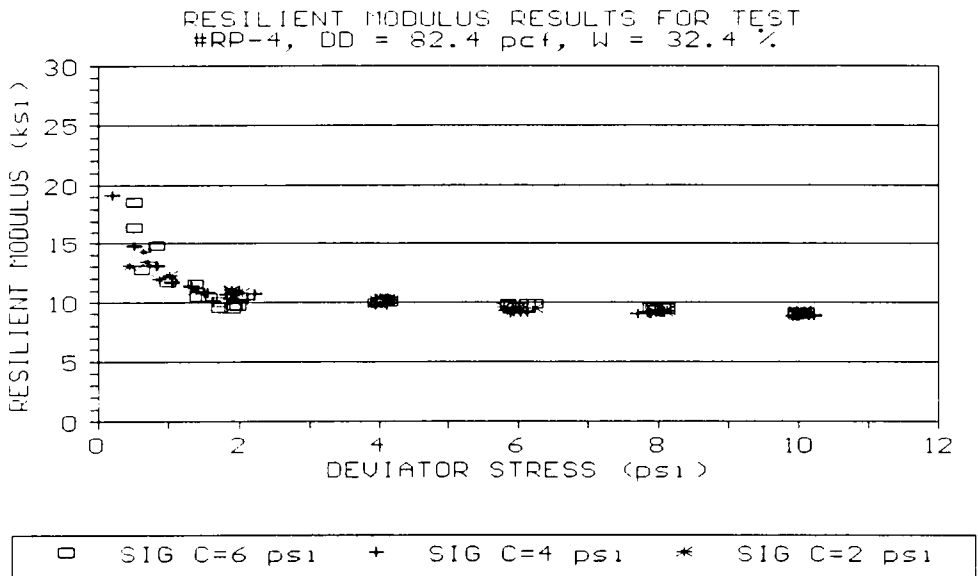


Figure A-4. Resilient Response For Rutledge Pike Test No. 4

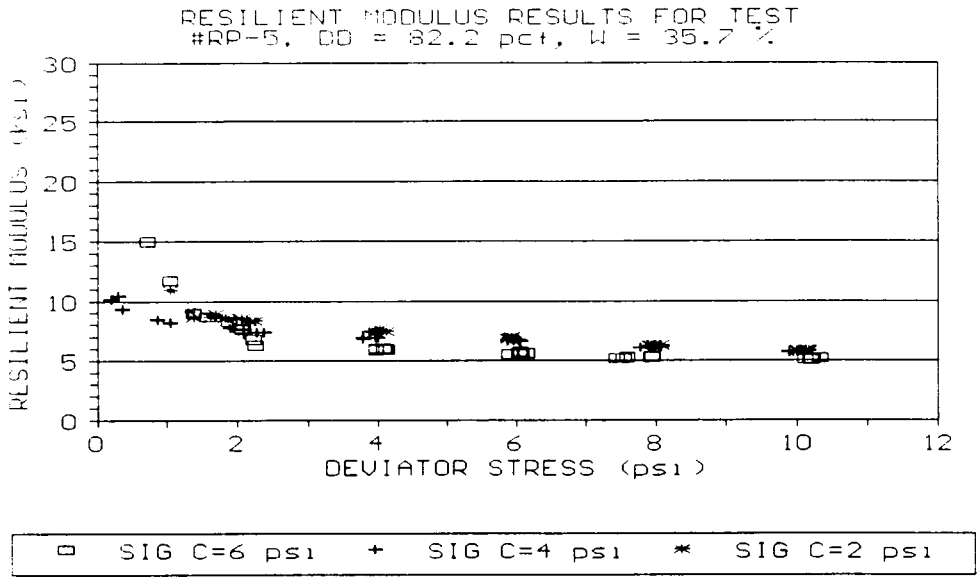


Figure A-5. Resilient Response For Rutledge Pike Test No. 5

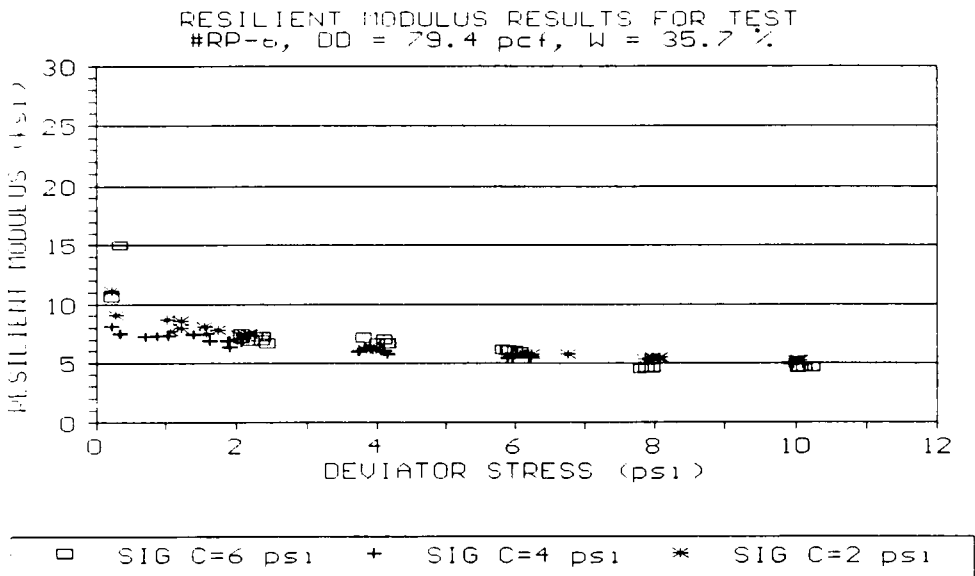


Figure A-6. Resilient Response For Rutledge Pike Test No. 6

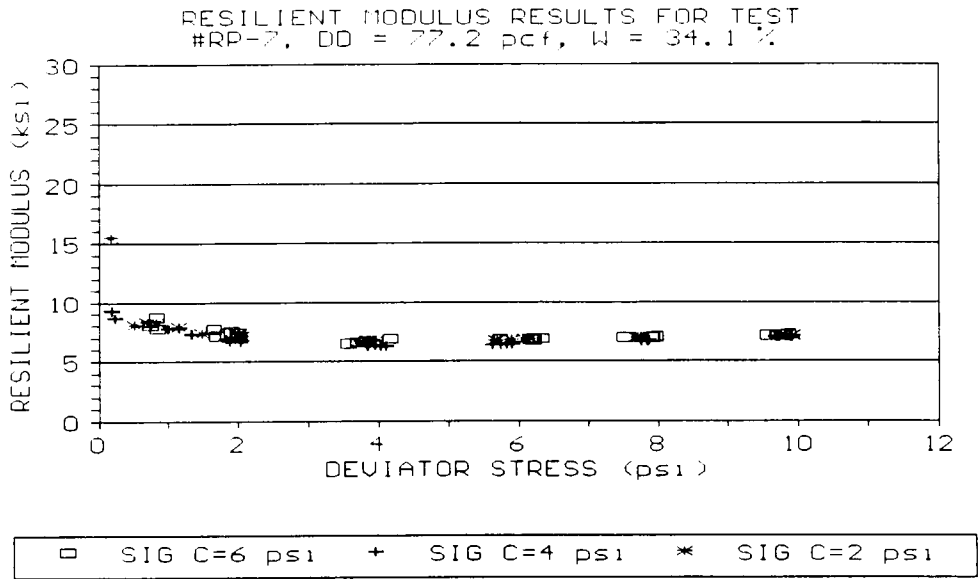


Figure A-7. Resilient Response For Rutledge Pike Test No. 7

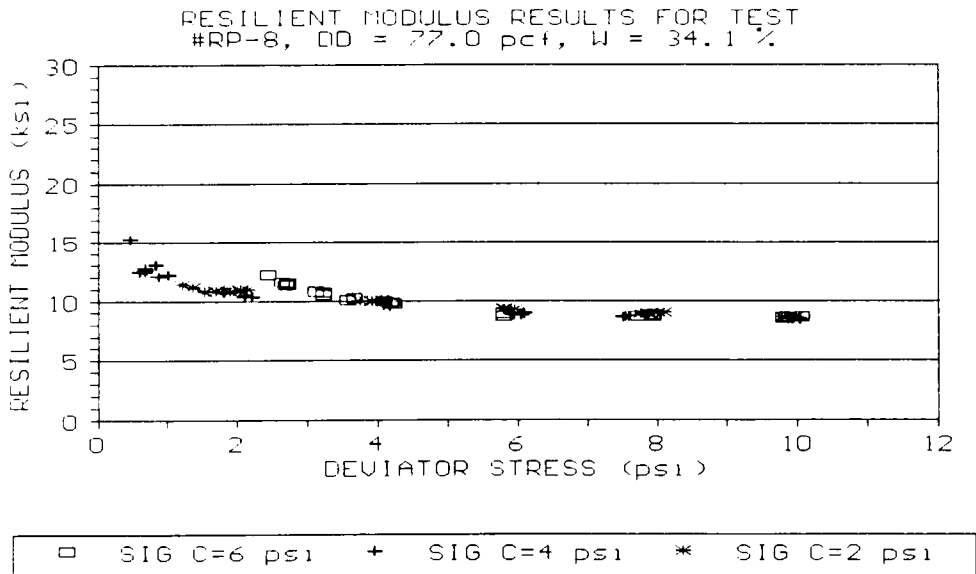


Figure A-8. Resilient Response For Rutledge Pike Test No. 8

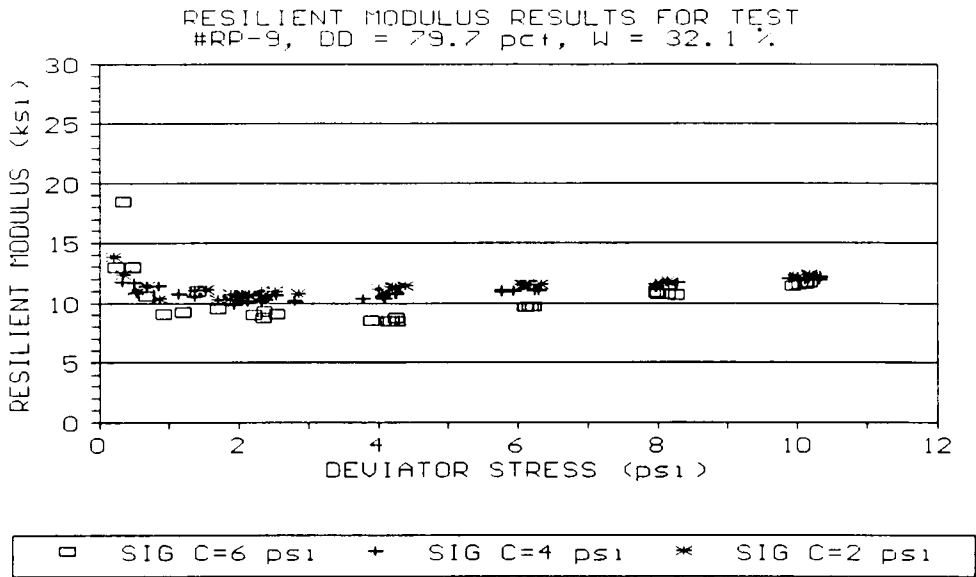


Figure A-9. Resilient Response For Rutledge Pike Test No. 9

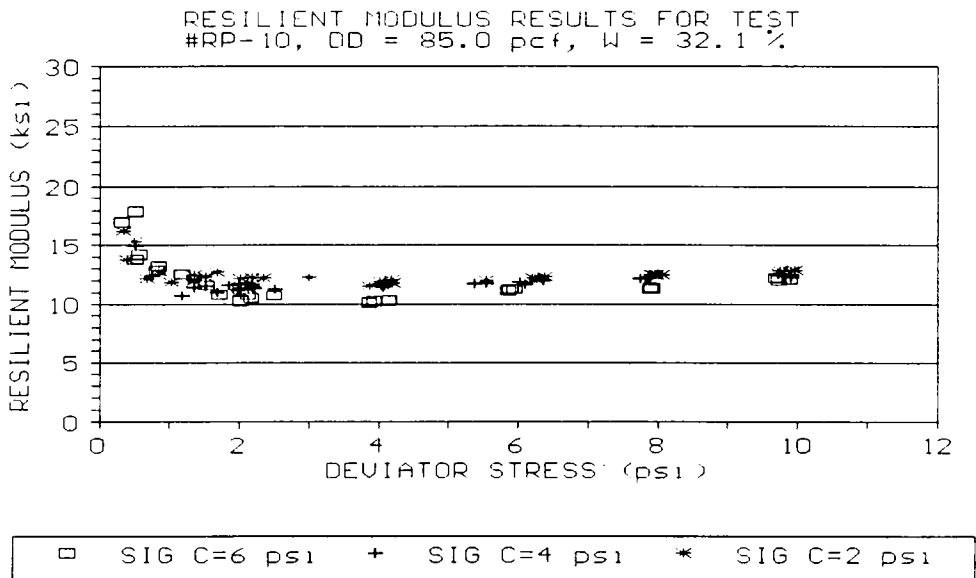


Figure A-10. Resilient Response For Rutledge Pike Test No. 10

Pellissippi Parkway Station 400

**Model Parameters
and
Resilient Modulus Plots**

Table A-2. Hyperbolic and Log-Log Model Parameters For Pellissippi Parkway Station 400 Resilient Modulus Tests

TEST NO.	DRY DENSITY (pcf)	WATER CONTENT (%)	HYPERBOLIC MODEL		LOG-LOG MODEL	
			a	b	K ₁	K ₂
1	87.1	29.8	4.9871	8.8064	11.6387	-.2692
2	86.4	29.8	2.7282	6.3962	8.7345	-.2545
3	88.5	26.3	4.0555	11.6273	14.2715	-.2937
4	84.9	26.3	1.3080	11.8837	12.2416	-.0718
5	86.0	33.6	1.3472	5.3055	5.8074	-.0804
6	87.7	33.6	3.3737	5.7069	8.5143	-.2962
7	91.0	29.6	1.4153	8.2548	9.8835	-.1710
8	91.9	29.6	0.8500	11.8918	12.0642	-.0728
9	90.2	25.6	0.8619	14.5811	15.6214	.0948
10	87.0	25.6	0.6270	10.5517	11.5623	-.1066

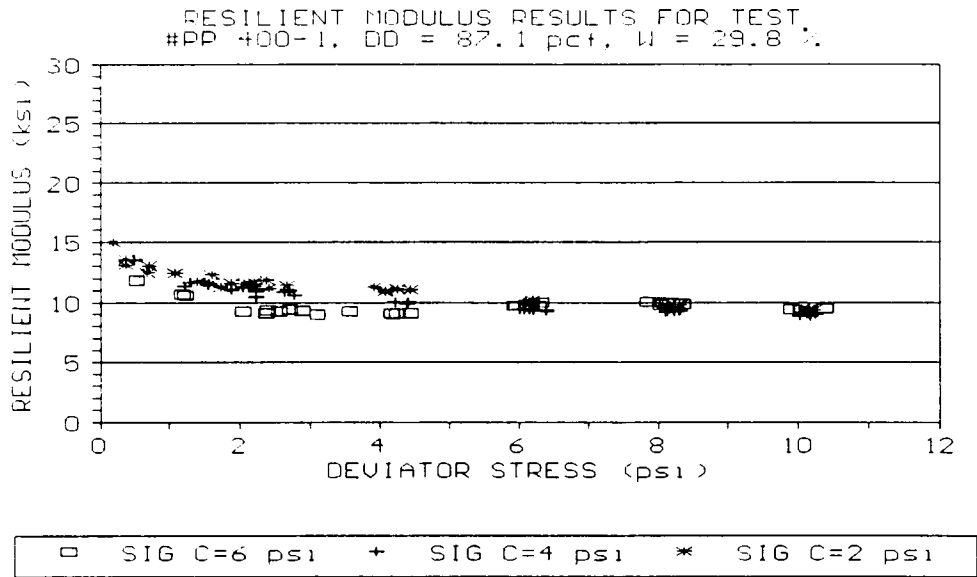
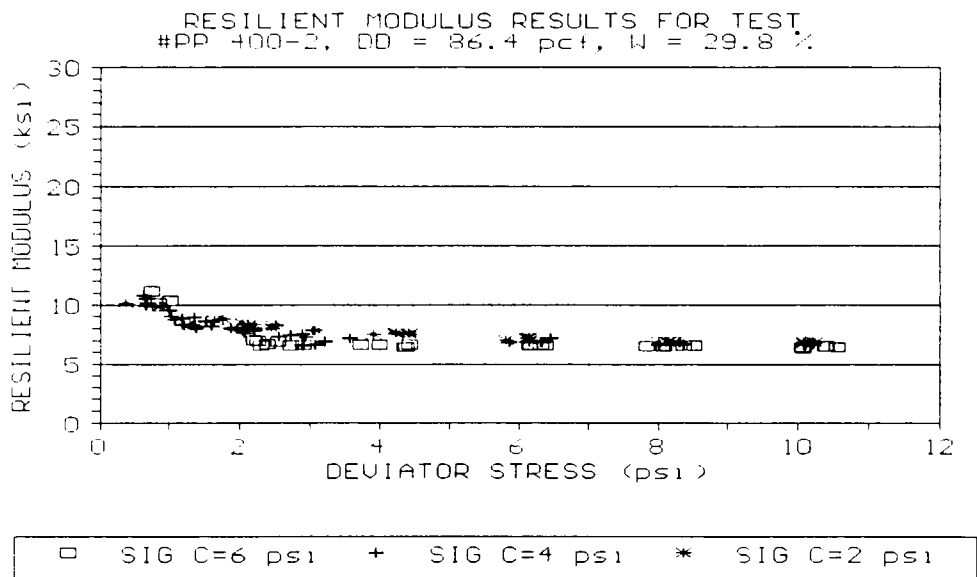


Figure A-11. Resilient Response For Pellissippi Parkway Station 400 Test No. 1



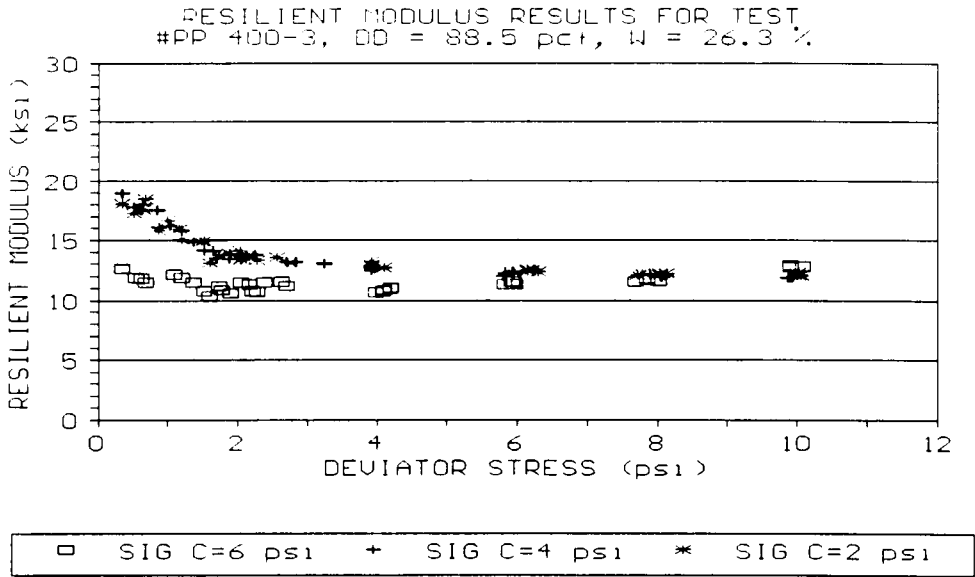


Figure A-13. Resilient Response For Pellissippi Parkway Station 400 Test No. 3

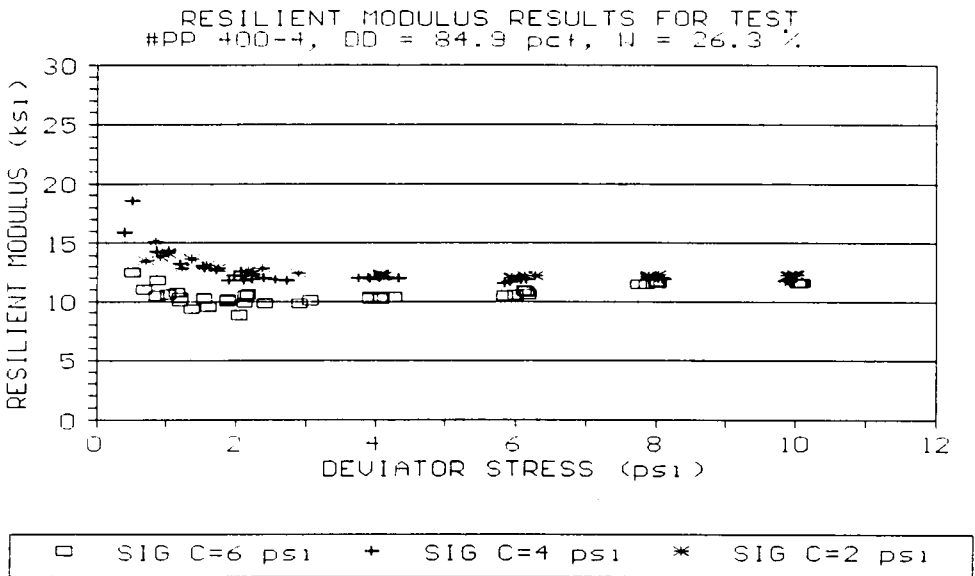


Figure A-14. Resilient Response For Pellissippi Parkway Station 400 Test No. 4

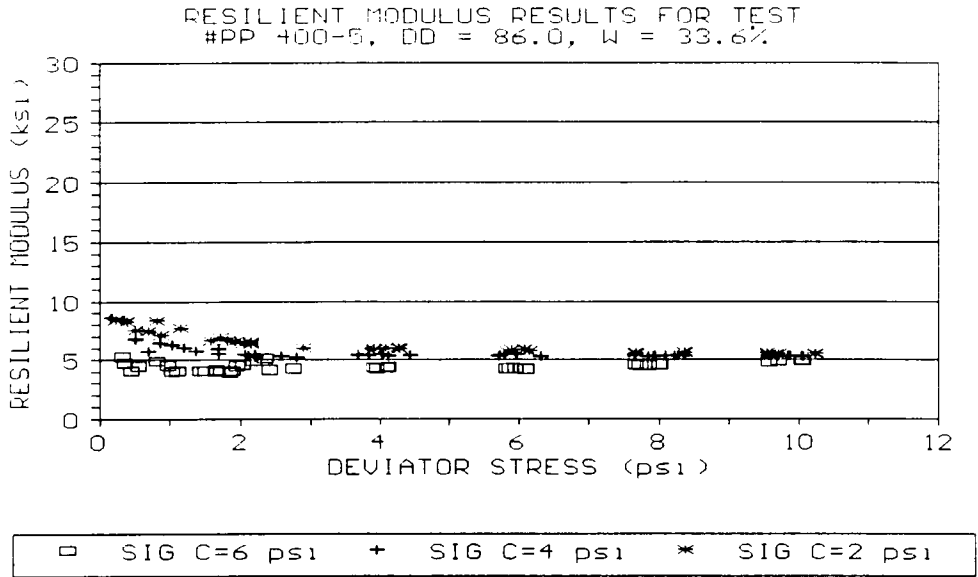


Figure A-15. Resilient Response For Pellissippi Parkway Station 400 Test No. 5

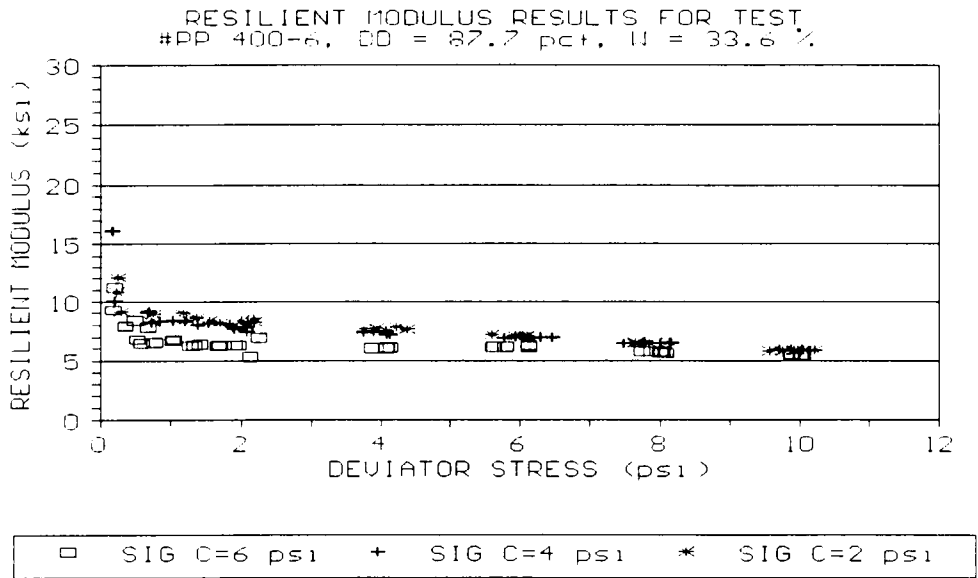


Figure A-16. Resilient Response For Pellissippi Parkway Station 400 Test No. 6

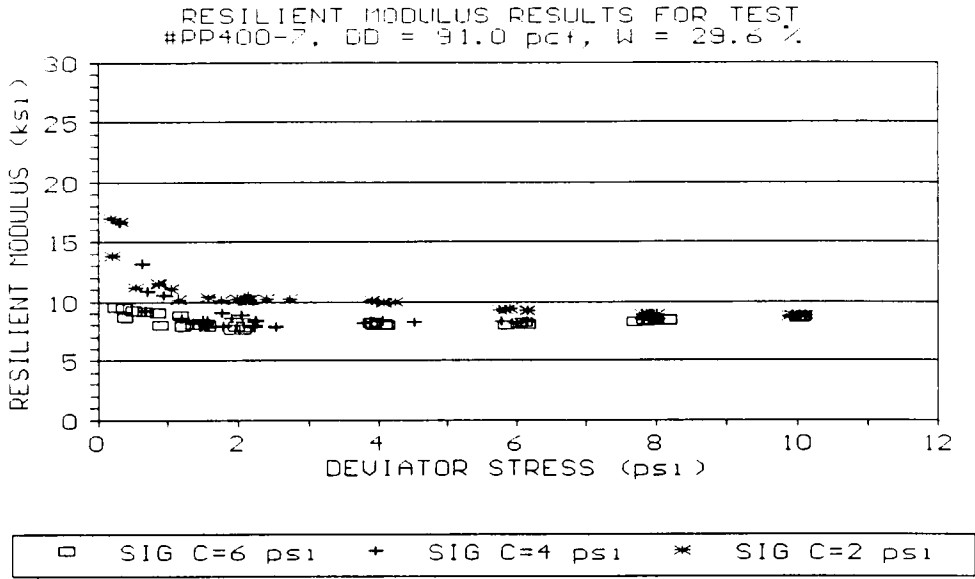


Figure A-17. Resilient Response For Pellissippi Parkway Station 400 Test No. 7

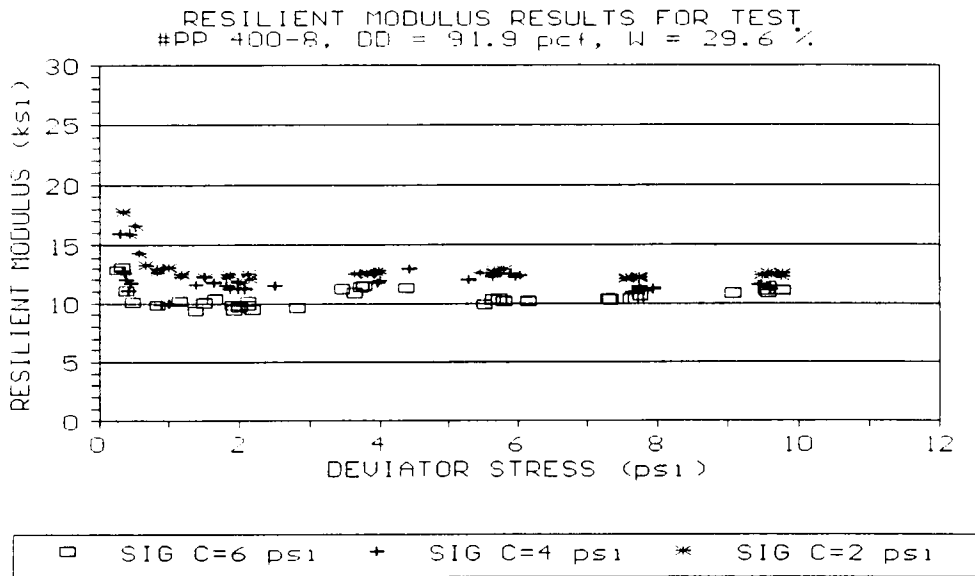


Figure A-18. Resilient Response For Pellissippi Parkway Station 400 Test No. 8

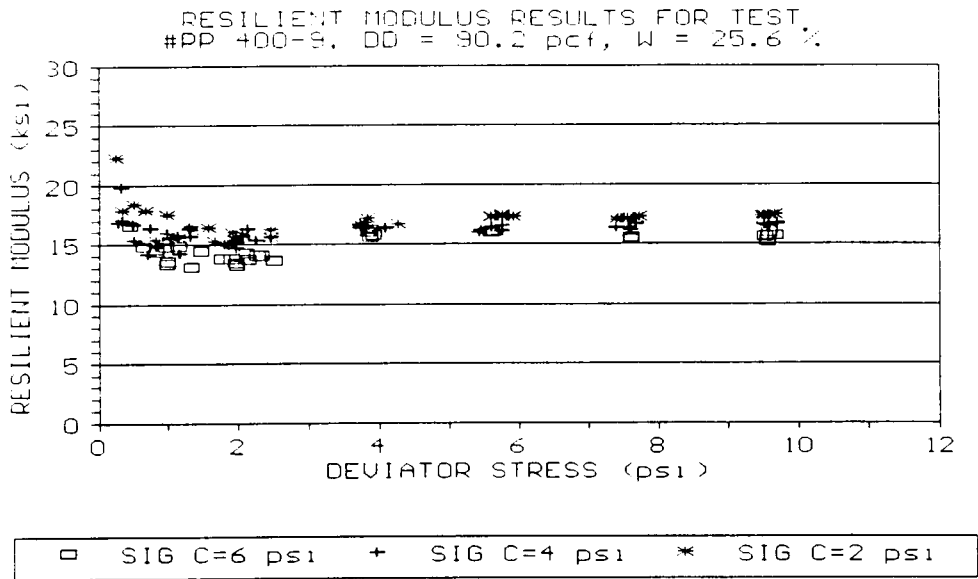


Figure A-19. Resilient Response For Pellissippi Parkway Station 400 Test No. 9

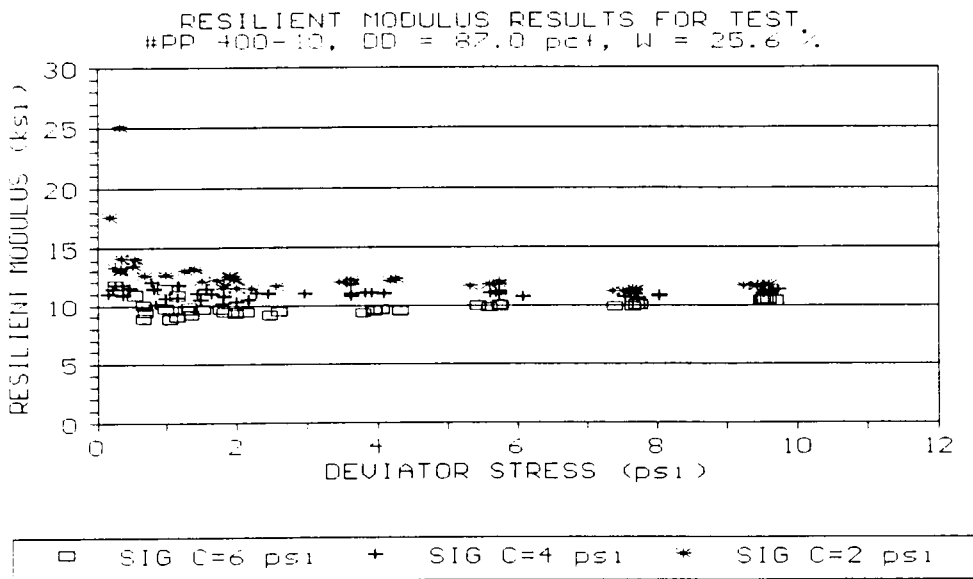


Figure A-20. Resilient Response For Pellissippi Parkway Station 400 Test No. 10

Pellissippi Parkway Station 500

**Model Parameters
and
Resilient Modulus Plots**

Table A-3. Hyperbolic and Log-Log Model Parameters For Pellissippi Parkway Station 500 Resilient Modulus Tests

TEST NO.	DRY DENSITY (pcf)	WATER CONTENT (%)	HYPERBOLIC MODEL		LOG-LOG MODEL	
			a	b	K ₁	K ₂
1	105.9	17.7	1.7189	13.4859	14.9126	-.2107
2	101.4	17.7	2.5630	10.4252	11.9616	-.1824
3	100.5	14.1	2.8599	7.0657	9.5198	-.2714
4	99.6	14.1	1.5434	9.4793	11.7531	-.2799
5	101.3	18.6	5.0636	11.2551	15.2328	-.4319
7	106.8	18.6	3.0519	12.3001	15.3235	-.1423
8	102.7	22.3	8.5969	4.3566	10.5641	-.6355
9	101.6	22.3	6.6993	5.5799	10.4411	-.4992
10	99.7	14.2	0.4881	7.3428	7.9052	.0503
11	107.5	14.2	.7695	7.6365	6.9751	.1664

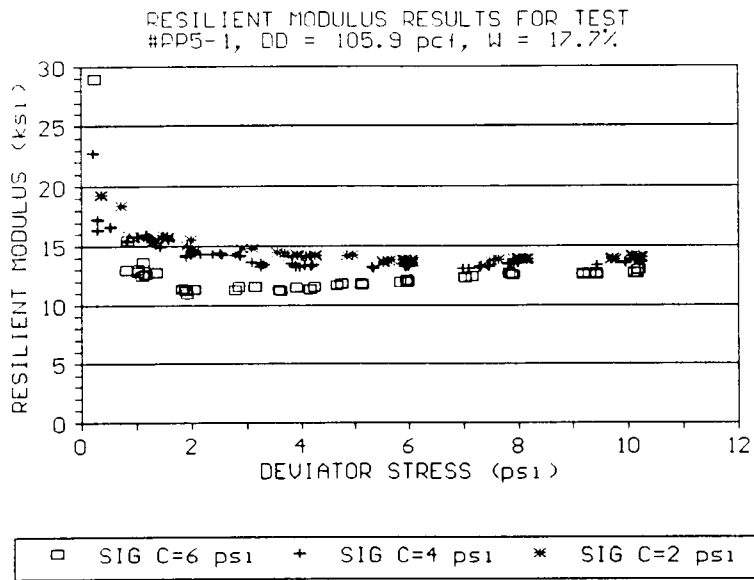


Figure A-21. Resilient Response For Pellissippi Parkway Station 500 Test No. 1

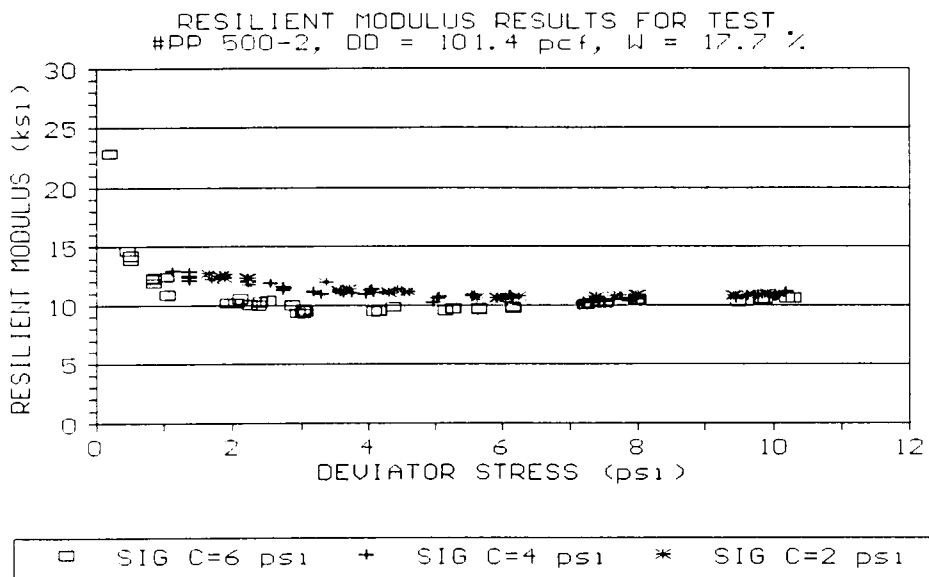


Figure A-22. Resilient Response For Pellissippi Parkway Station 500 Test No. 2

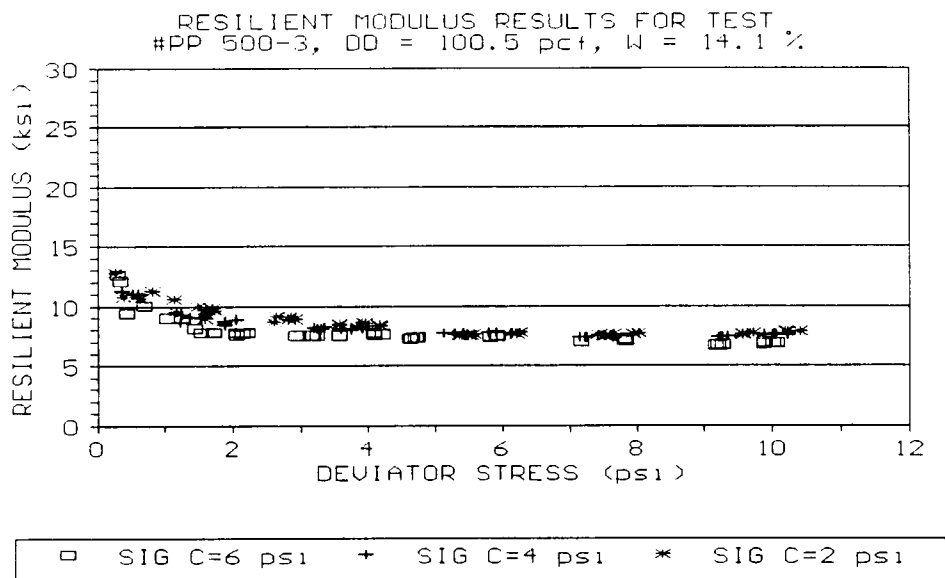


Figure A-23. Resilient Response For Pellissippi Parkway Station 500 Test No. 3

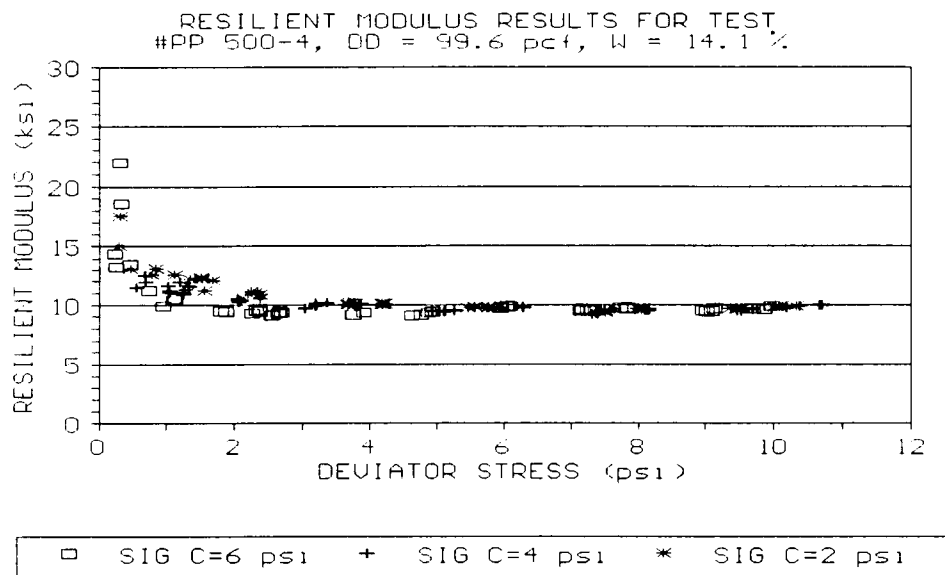


Figure A-24. Resilient Response For Pellissippi Parkway Station 500 Test No. 4

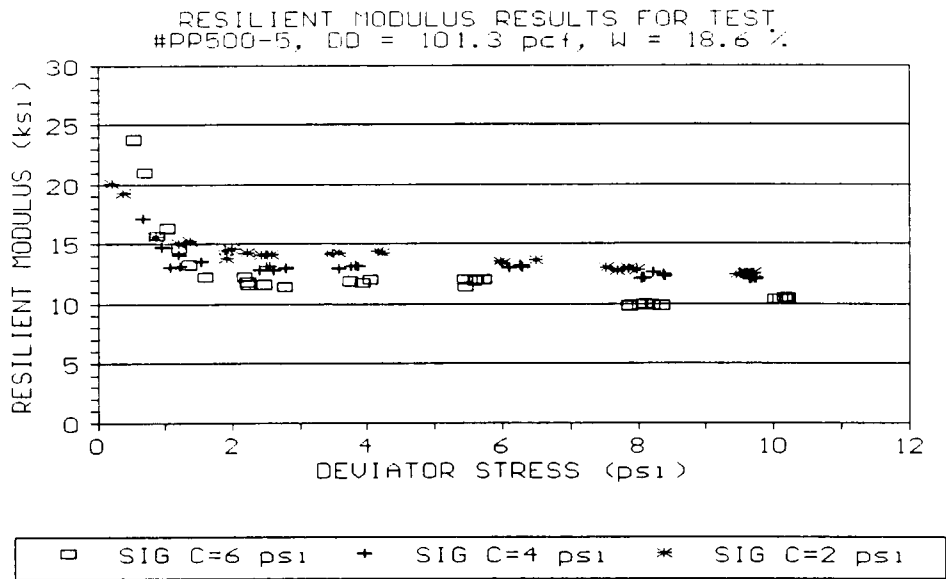


Figure A-25. Resilient Response For Pellissippi Parkway Station 500 Test No. 5

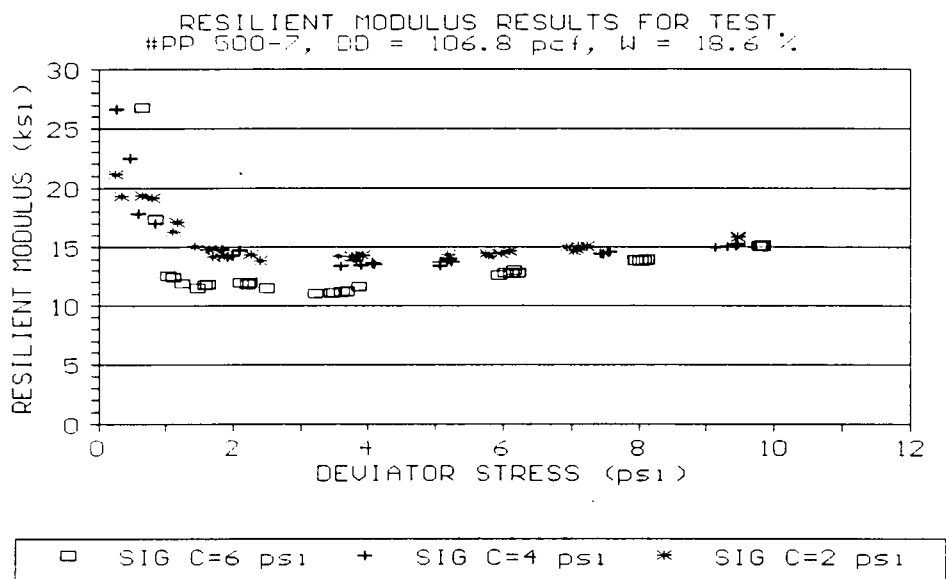


Figure A-26. Resilient Response For Pellissippi Parkway Station 500 Test No. 7

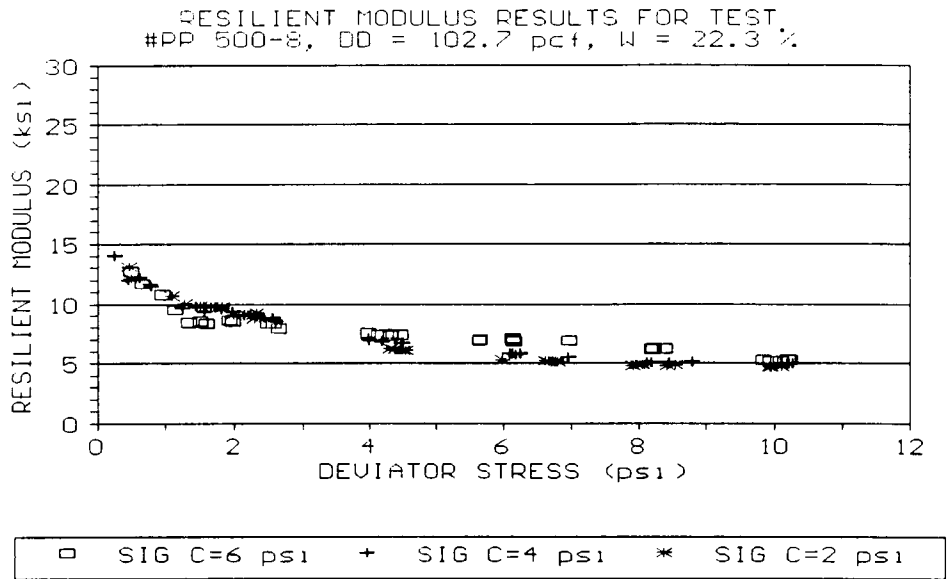


Figure A-27. Resilient Response For Pellissippi Parkway Station 500 Test No. 8

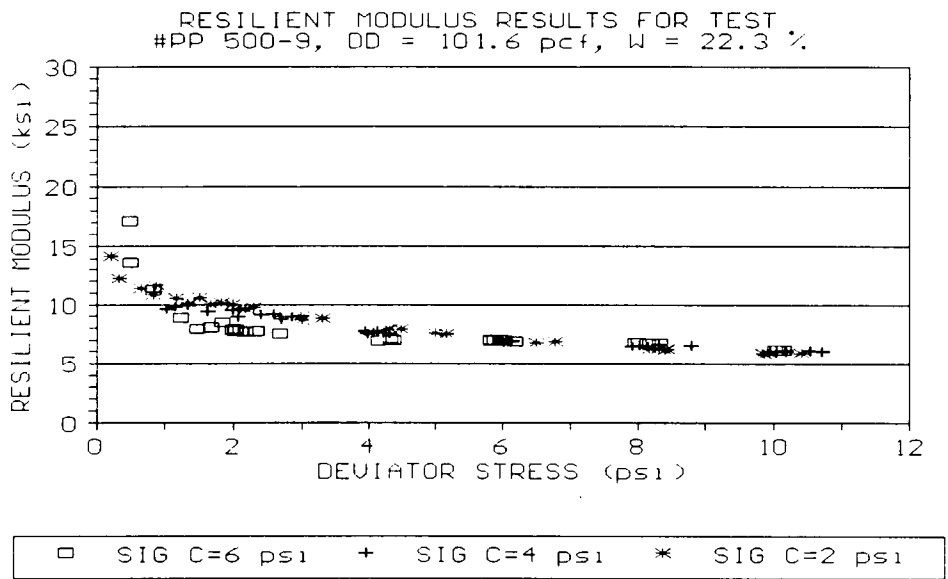


Figure A-28. Resilient Response For Pellissippi Parkway Station 500 Test No. 9

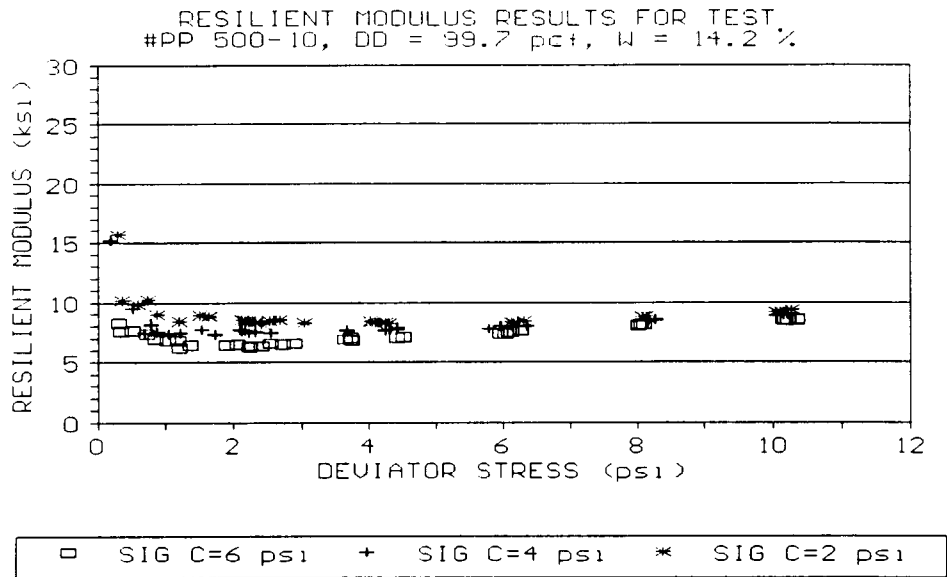


Figure A-29. Resilient Response For Pellissippi Parkway Station 500 Test No. 10

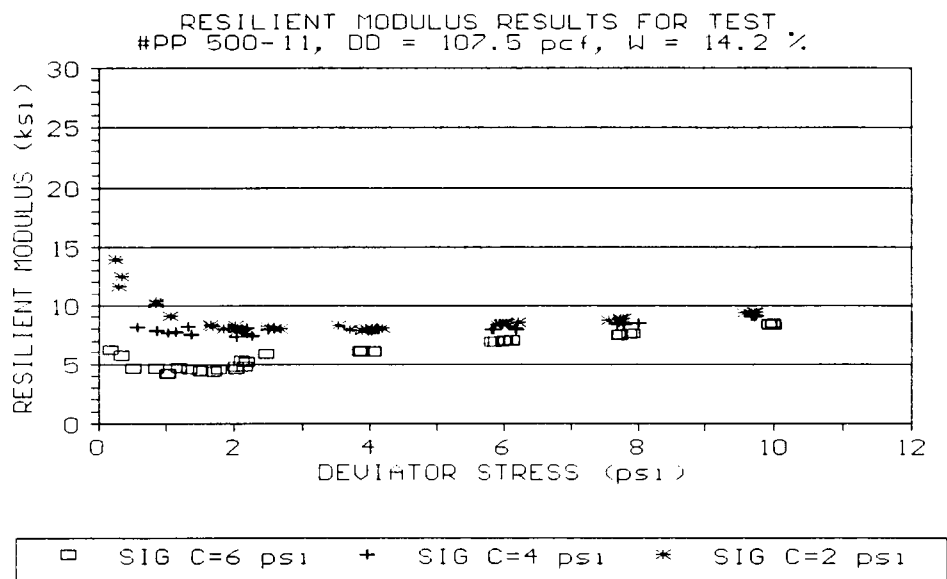


Figure A-30. Resilient Response For Pellissippi Parkway Station 500 Test No. 11

Airport Connector Station 47

**Model Parameters
and
Resilient Modulus Plots**

Table A-4. Hyperbolic and Log-Log Model Parameters For Airport Connector Station 47 Resilient Modulus Tests

TEST NO.	DRY DENSITY (pcf)	WATER CONTENT (%)	HYPERBOLIC MODEL		LOG-LOG MODEL	
			a	b	K ₁	K ₂
3	104.8	19.5	1.8823	5.1458	6.1696	-.0992
6	102.6	14.2	0.3321	5.4681	5.4862	.0421
7	108.6	17.3	2.3986	5.2127	5.9035	-.0706
8	111.2	17.3	4.1252	6.3146	9.2982	-.3055
9	103.1	17.9	3.5478	3.7733	6.4020	-.2759
10	110.3	17.9	2.7474	8.1537	10.0081	-.1895
11	105.3	21.1	1.6265	1.6165	3.6634	-.2440
12	107.8	21.1	1.7843	1.8307	3.7818	-.2242
13	97.1	13.8	2.1127	4.9159	7.0443	-.2431
14	103.9	13.8	2.4312	8.7457	11.4633	-.3230
15	101.5	13.1	1.4789	6.0618	8.4349	-.2997
16	104.7	13.1	2.1179	5.2268	7.6012	-.2828
17	104.3	13.3	1.2631	6.6482	9.1826	-.3281
18	110.2	13.3	0.6641	7.0828	8.5724	-.0653

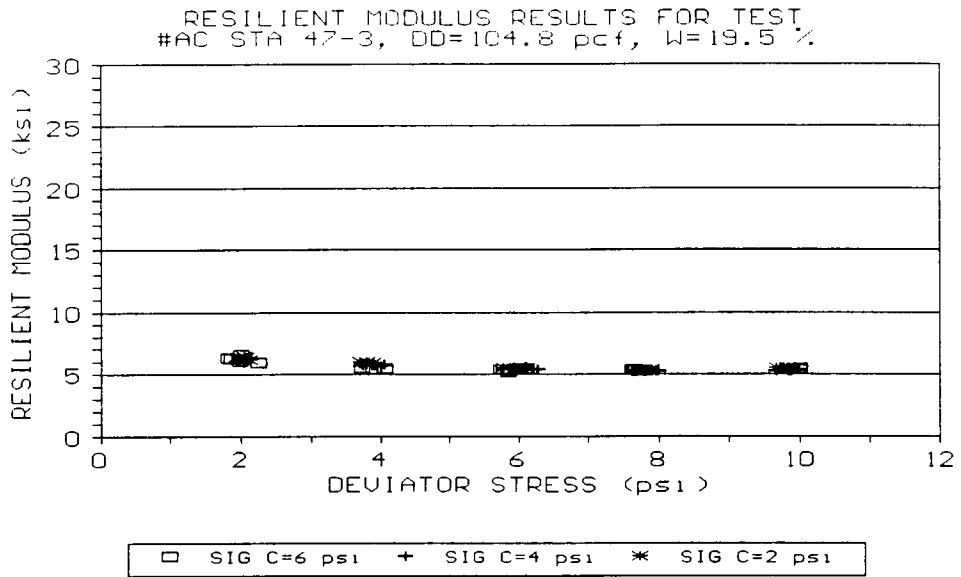


Figure A-31. Resilient Response For Airport Connector Station 47 Test No. 3

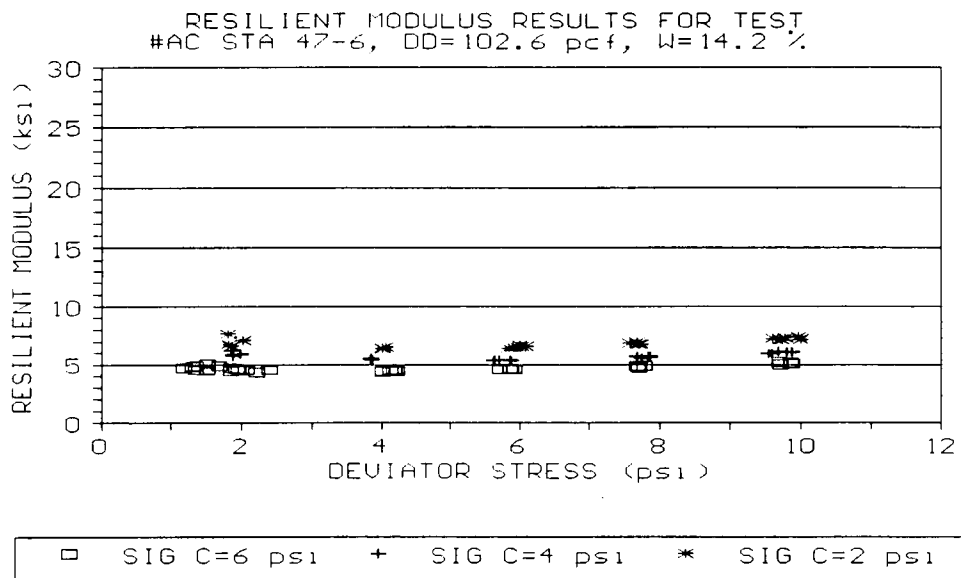


Figure A-32. Resilient Response For Airport Connector Station 47 Test No. 6

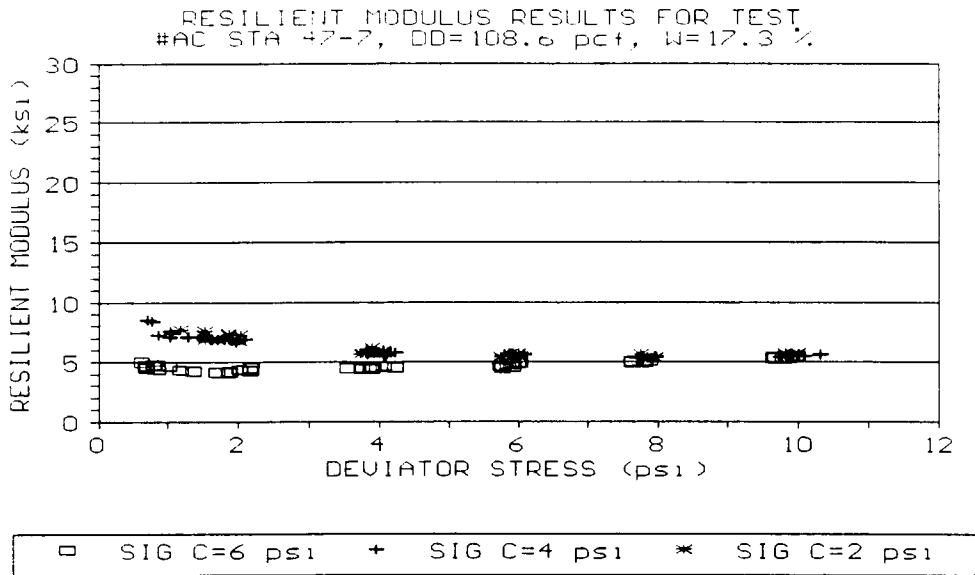


Figure A-33. Resilient Response For Airport Connector Station 47 Test No. 7

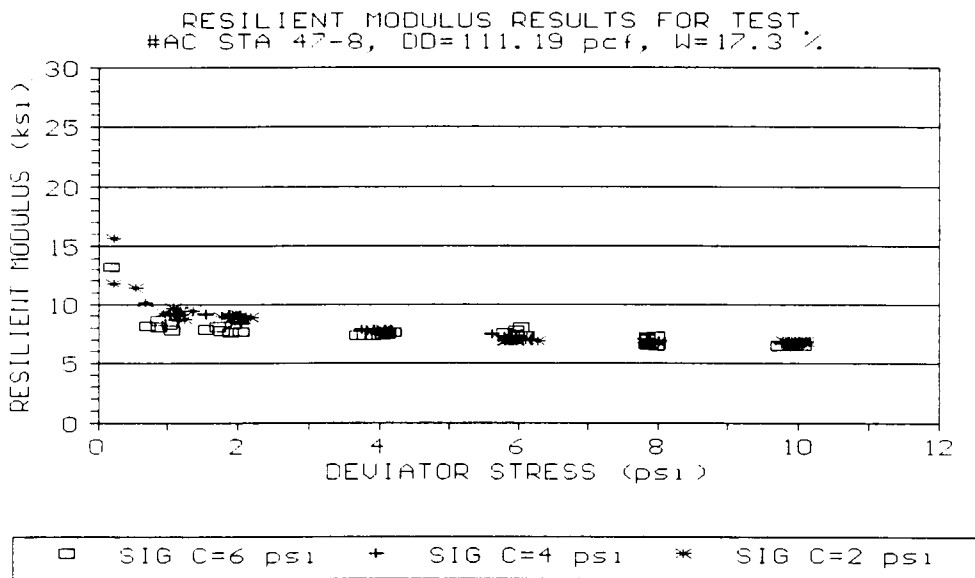


Figure A-34. Resilient Response For Airport Connector Station 47 Test No. 8

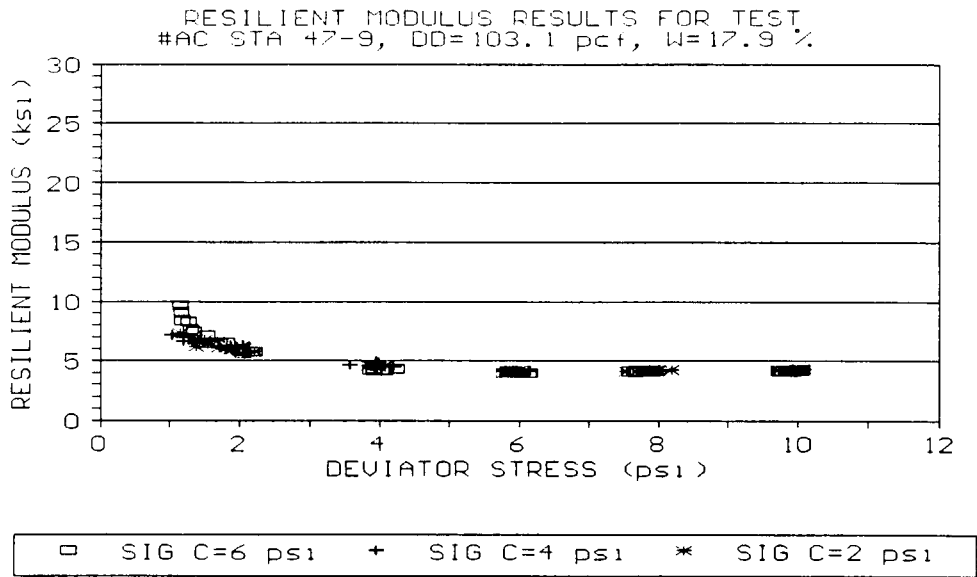


Figure A-35. Resilient Response For Airport Connector Station 47 Test No. 9

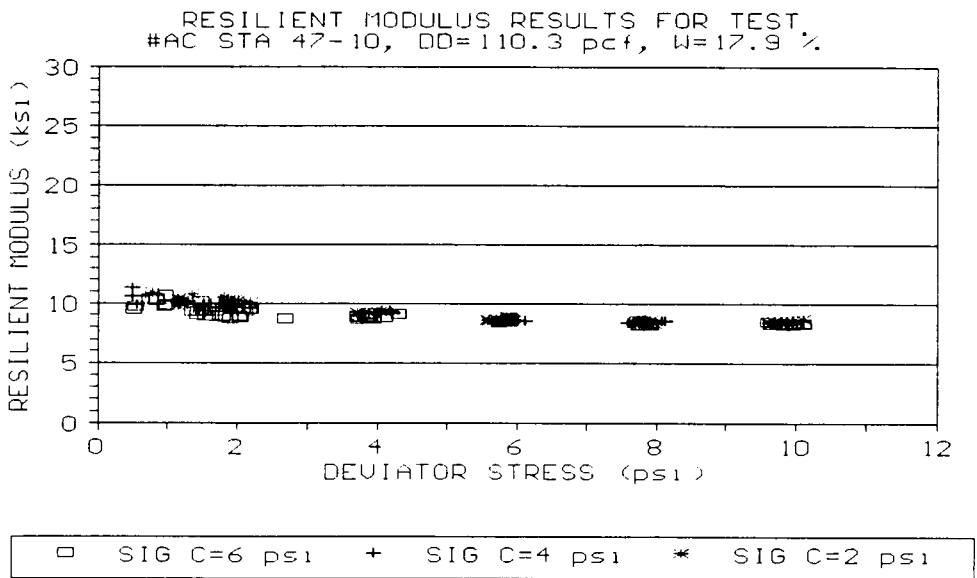


Figure A-36. Resilient Response For Airport Connector Station 47 Test No. 10

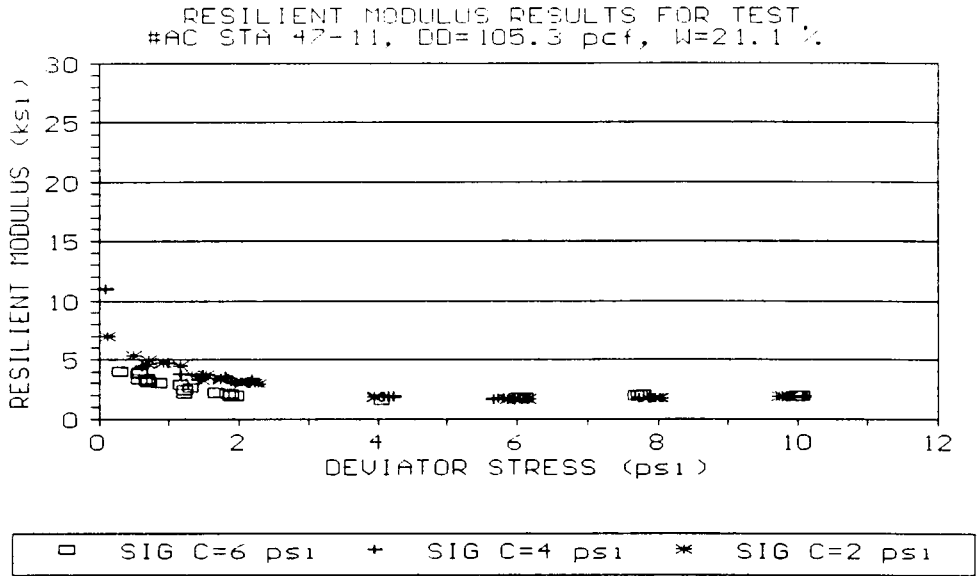


Figure A-37. Resilient Response For Airport Connector Station 47 Test No. 11

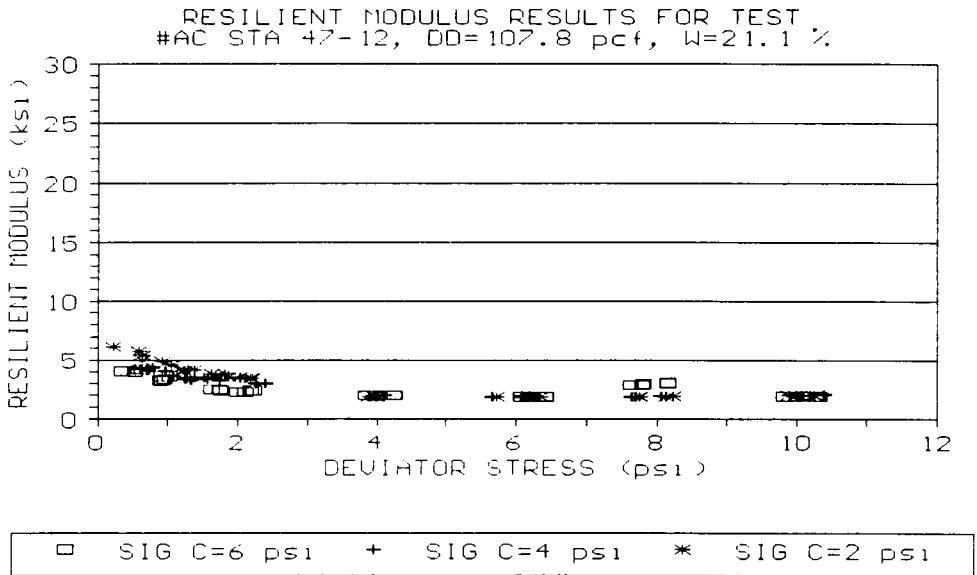


Figure A-38. Resilient Response For Airport Connector Station 47 Test No. 12

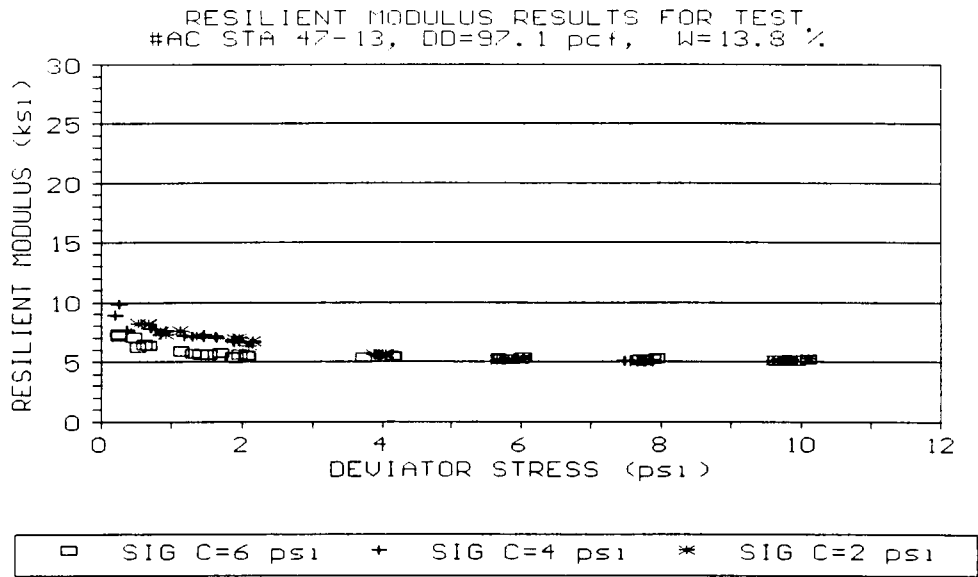


Figure A-39. Resilient Response For Airport Connector Station 47 Test No. 13

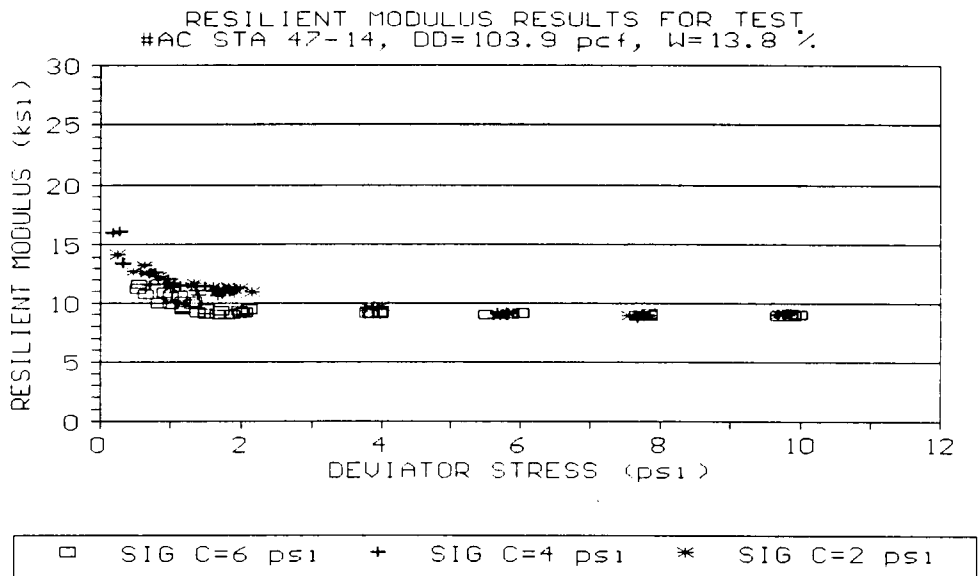


Figure A-40. Resilient Response For Airport Connector Station 47 Test No. 14

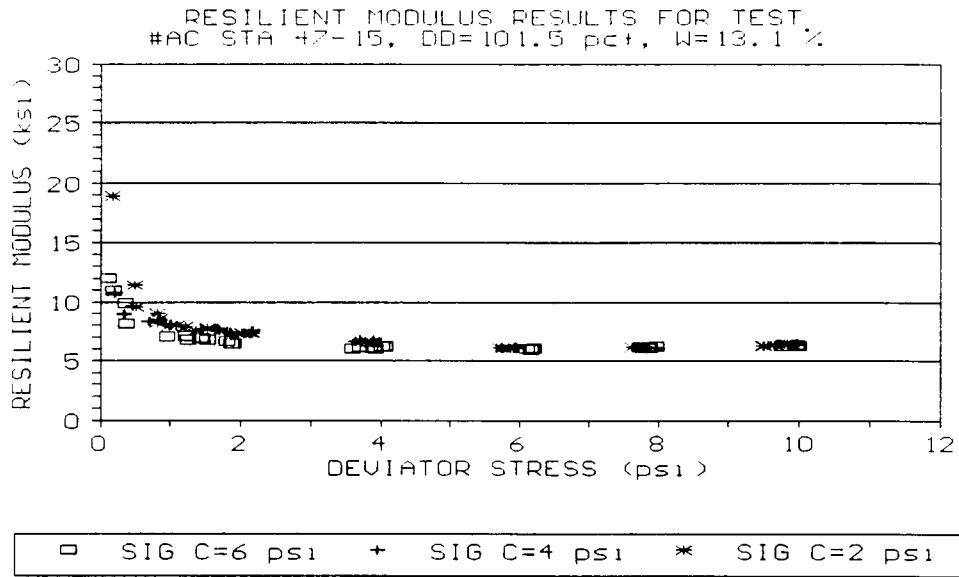


Figure A-41. Resilient Response For Airport Connector Station 47 Test No. 15

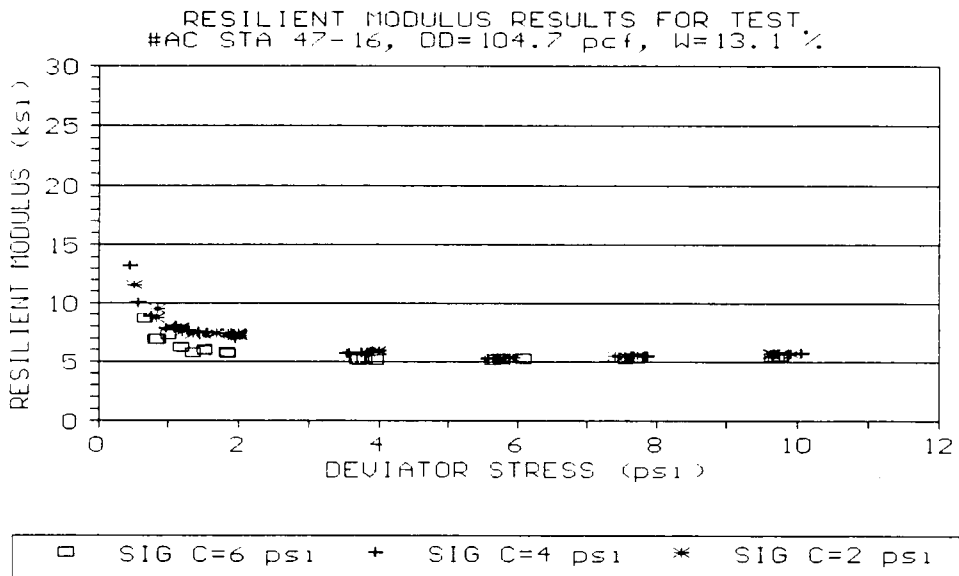


Figure A-42. Resilient Response For Airport Connector Station 47 Test No. 16

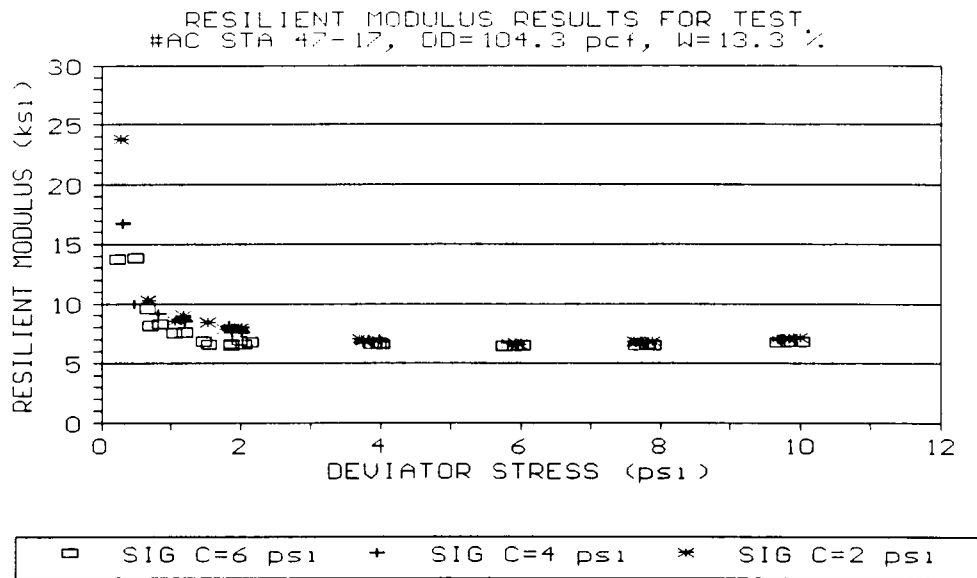


Figure A-43. Resilient Response For Airport Connector Station 47 Test No. 17

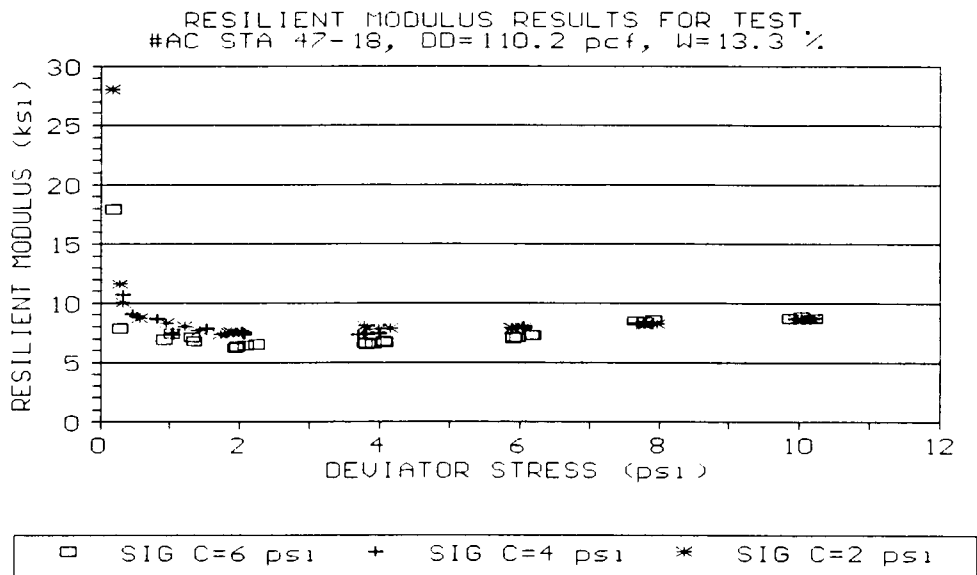


Figure A-44. Resilient Response For Airport Connector Station 47 Test No. 18

Airport Connector Station 85

**Model Parameters
and
Resilient Modulus Plots**

Table A-5. Hyperbolic and Log-Log Model Parameters For Airport Connector Station 85 Resilient Modulus Tests

TEST NO.	DRY DENSITY (pcf)	WATER CONTENT (%)	HYPERBOLIC MODEL		LOG-LOG MODEL	
			a	b	K ₁	K ₂
1	115.5	13.5	2.8833	5.9806	8.7099	-.3346
2	115.5	13.5	2.5410	5.5604	8.9439	-.4173
3	113.8	10.1	0.5654	5.4728	6.2427	.1805
4	114.1	10.1	0.3690	6.6849	8.1582	-.0479
5	116.4	13.8	3.5629	4.8385	9.9482	-.6313
6	112.4	10.1	0.7400	4.6201	5.7433	.4131
7	117.6	15.0	0.3500	0.9607	1.3262	.0328
8	113.3	15.0	0.4594	2.0007	2.4095	.0025
9	113.0	13.5	1.3944	5.7018	6.9803	-.1547

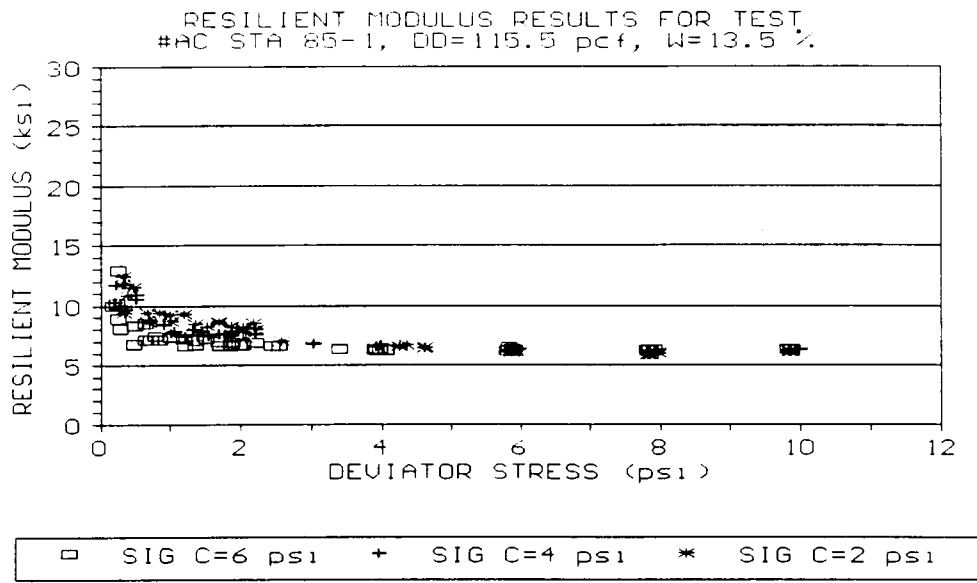


Figure A-45. Resilient Response For Airport Connector Station 85 Test No. 1

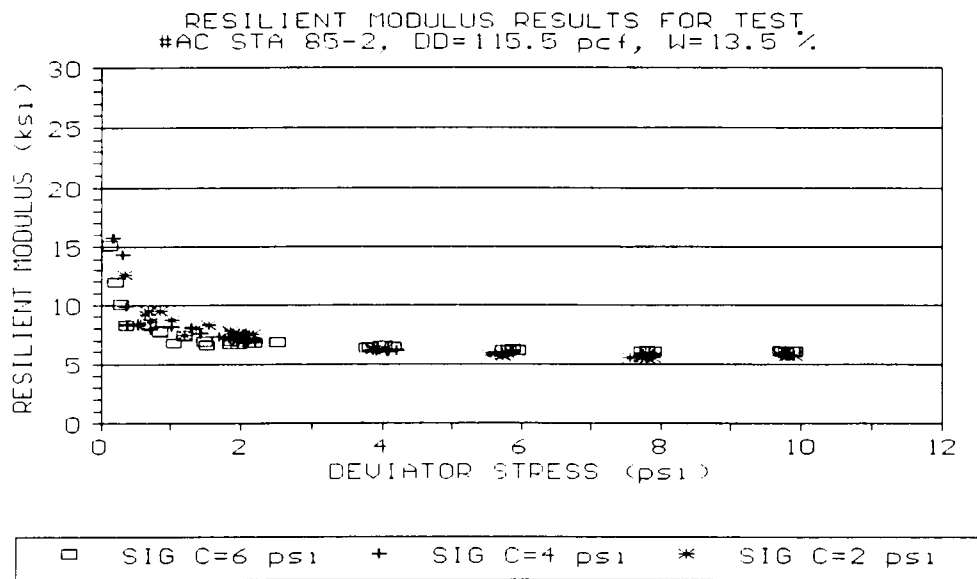


Figure A-46. Resilient Response For Airport Connector Station 85 Test No. 2

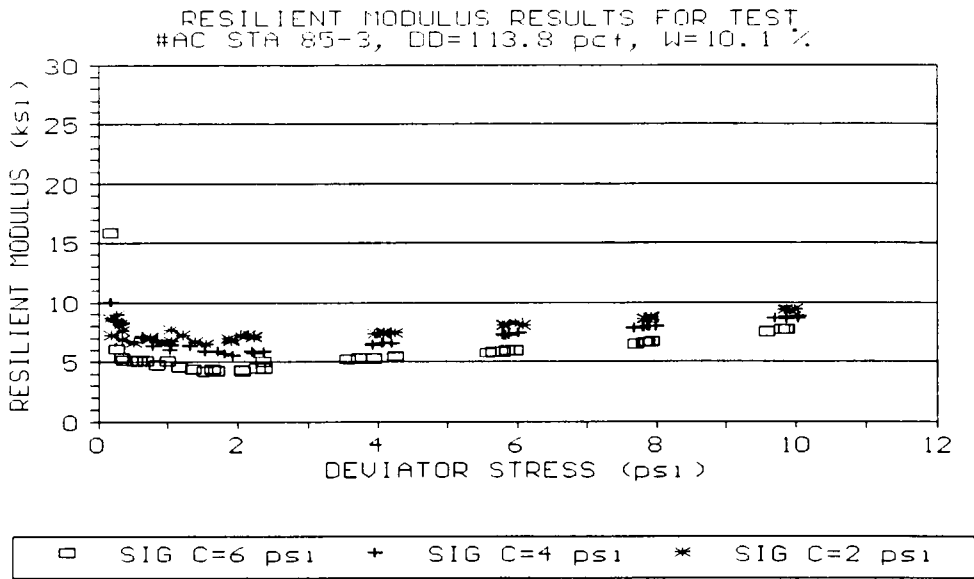


Figure A-47. Resilient Response For Airport Connector Station 85 Test No. 3

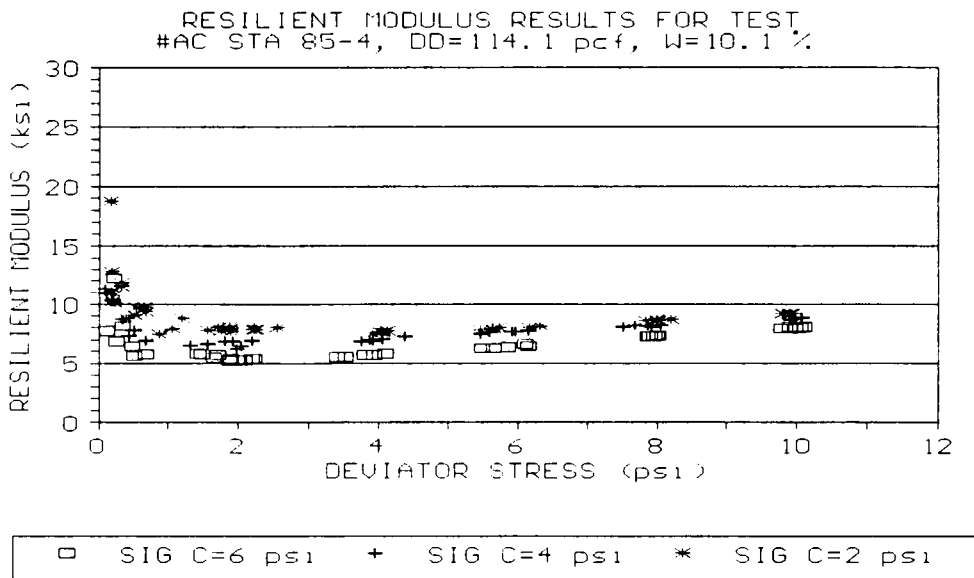


Figure A-48. Resilient Response For Airport Connector Station 85 Test No. 4

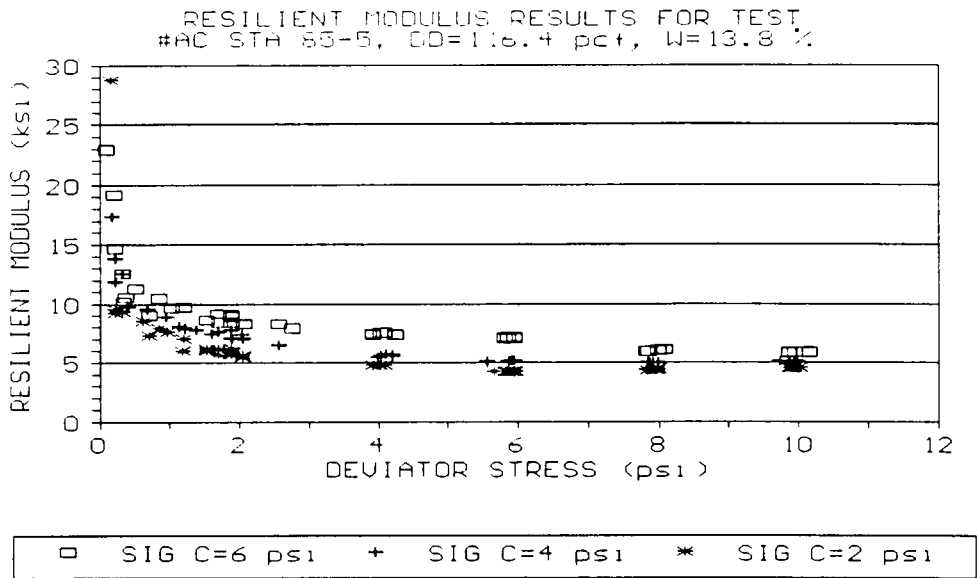


Figure A-49. Resilient Response For Airport Connector Station 85 Test No. 5

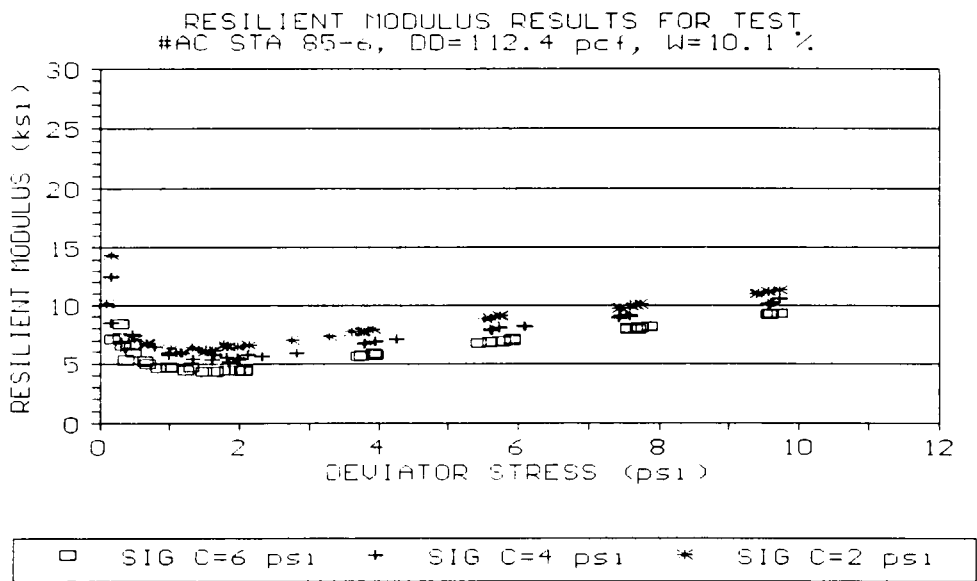


Figure A-50. Resilient Response For Airport Connector Station 85 Test No. 6

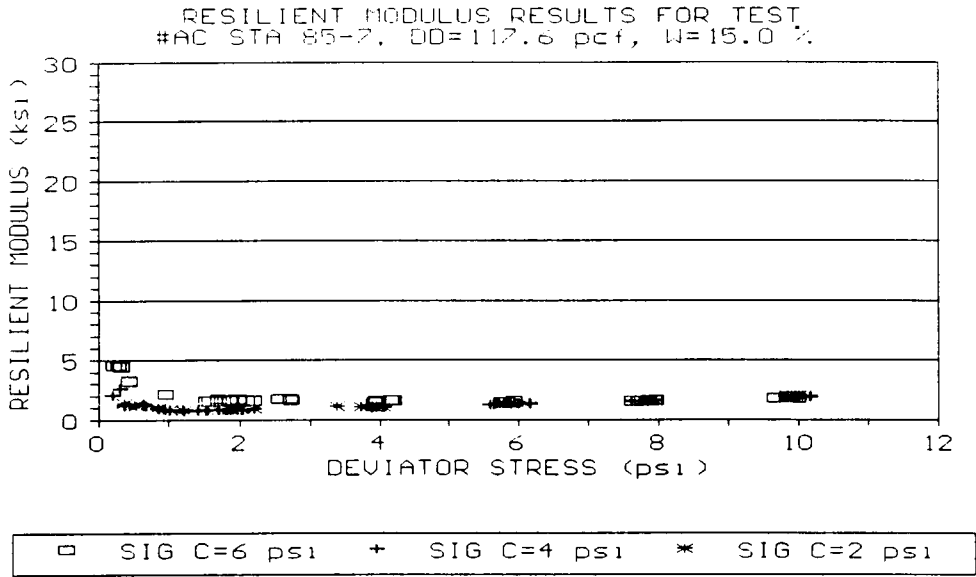


Figure A-51. Resilient Response For Airport Connector Station 85 Test No. 7

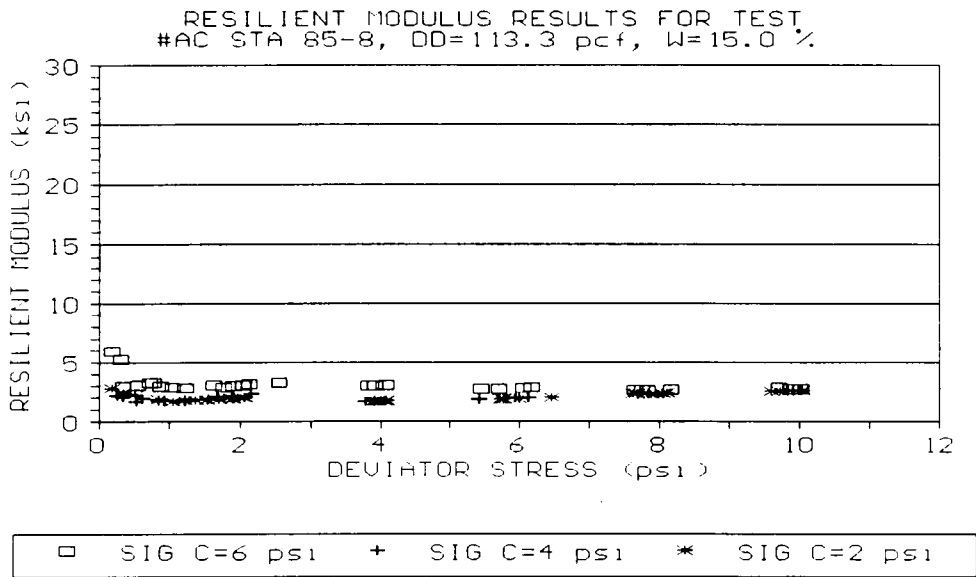
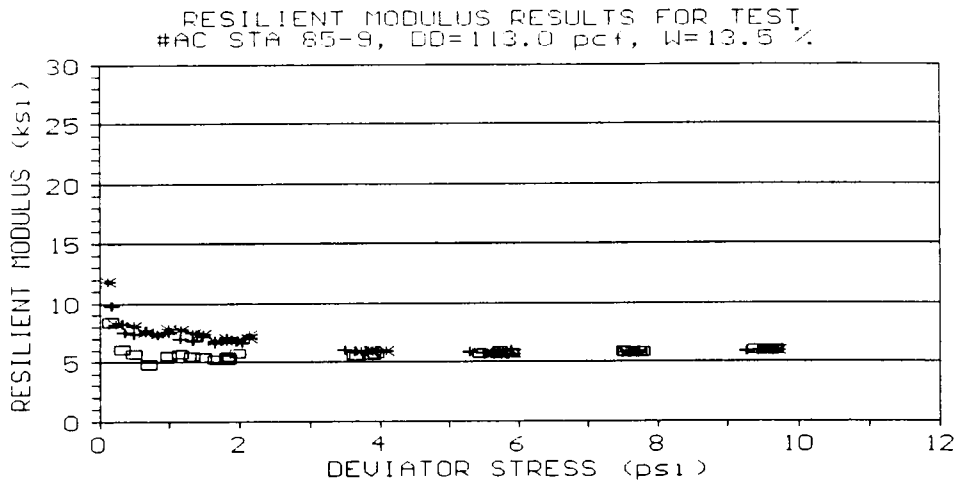


Figure A-52. Resilient Response For Airport Connector Station 85 Test No. 8



□ SIG C = 6 ps + SIG C = 4 ps * SIG C = 2 ps

Figure A-53. Resilient Response For Airport Connector Station 85 Test No. 9

State Route 20 Station 781+75

**Model Parameters
and
Resilient Modulus Plots**

Table A-6. Hyperbolic and Log-Log Model Parameters For State Route 20 Station 781+75 Resilient Modulus Tests

TEST NO.	DRY DENSITY (pcf)	WATER CONTENT (%)	HYPERBOLIC MODEL		LOG-LOG MODEL	
			a	b	K ₁	K ₂
1	101.4	20.8	0.1645	3.1633	3.5627	.0706
2	101.2	20.8	0.2422	3.9773	2.8263	.1499
3	97.9	12.8	0.1463	4.5233	5.1024	.0322
4	101.8	12.8	0.3059	5.1552	5.3168	.1151
5	101.6	18.1	0.4527	5.0173	5.4660	.0298
6	101.9	18.1	0.2252	5.4400	6.1178	-.0202
7	100.9	20.7	0.4569	4.4026	5.2426	.0141
8	102.4	20.7	0.5491	4.1717	5.0755	.0164
9	97.4	17.5	0.2763	4.6530	5.1424	-.0045

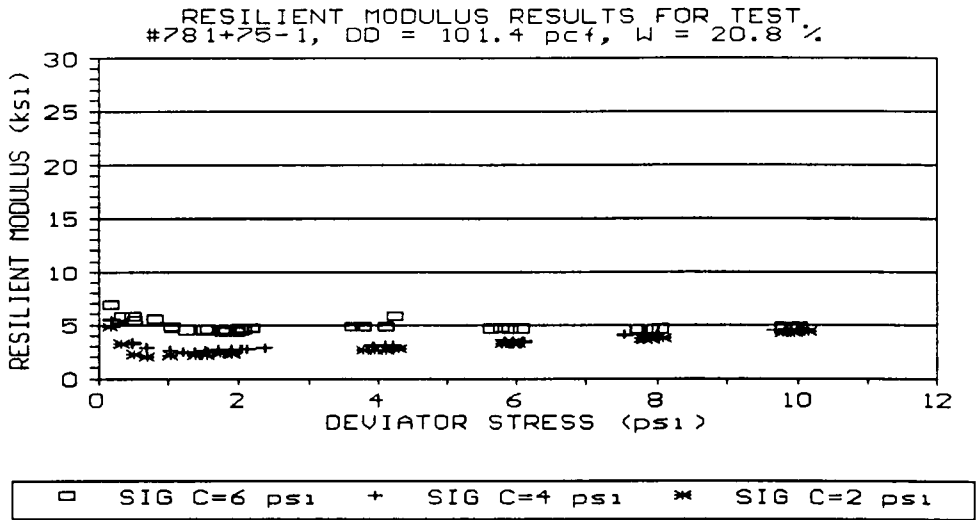


Figure A-54. Resilient Response For State Route 20 Station 781+75 Test No. 1

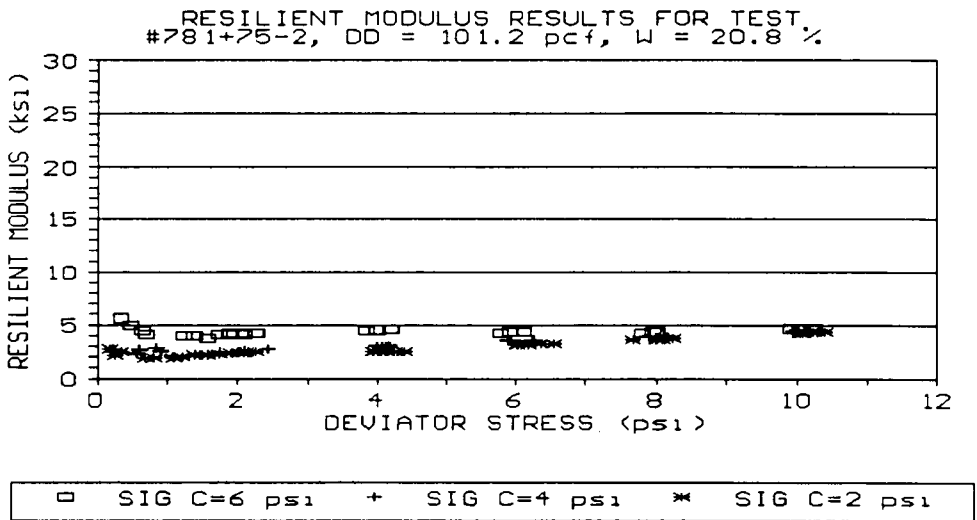


Figure A-55. Resilient Response For State Route 20 Station 781+75 Test No. 2

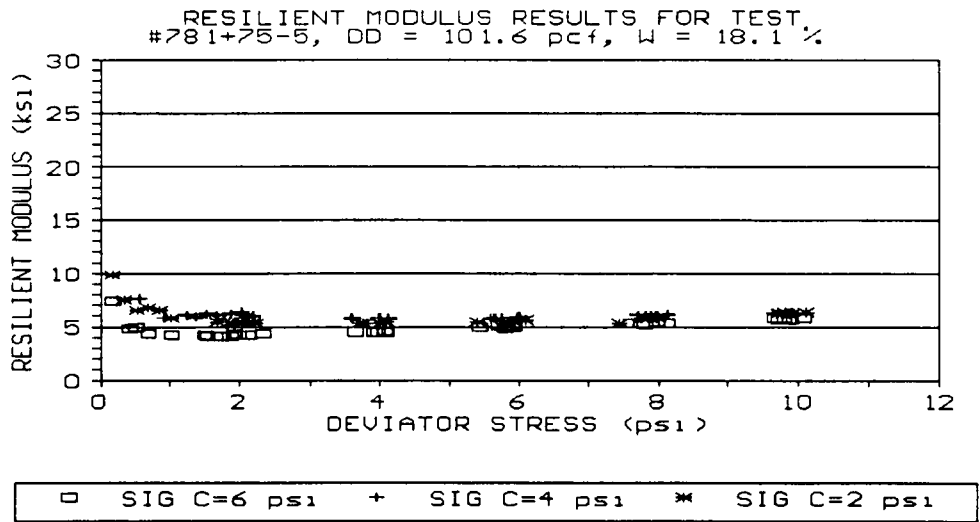


Figure A-58. Resilient Response For State Route 20 Station 781+75 Test No. 5

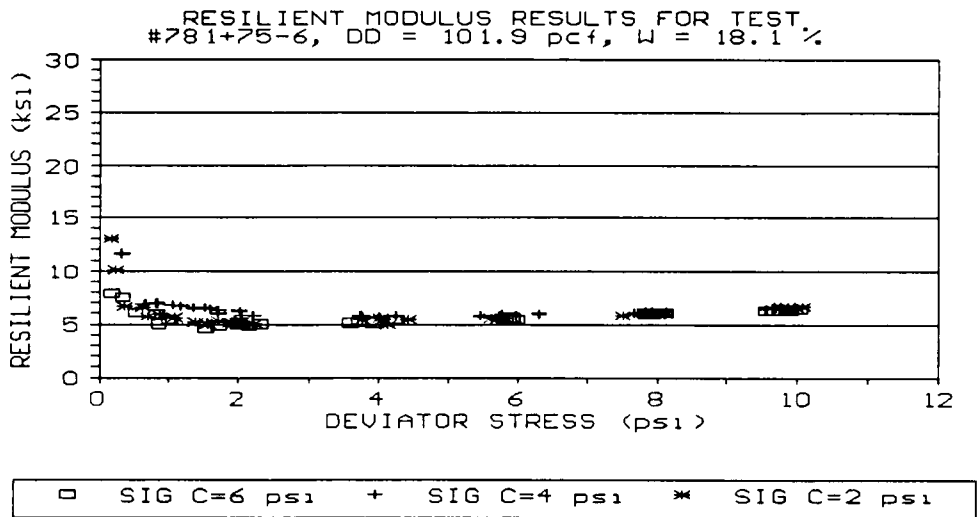


Figure A-59. Resilient Response For State Route 20 Station 781+75 Test No. 6

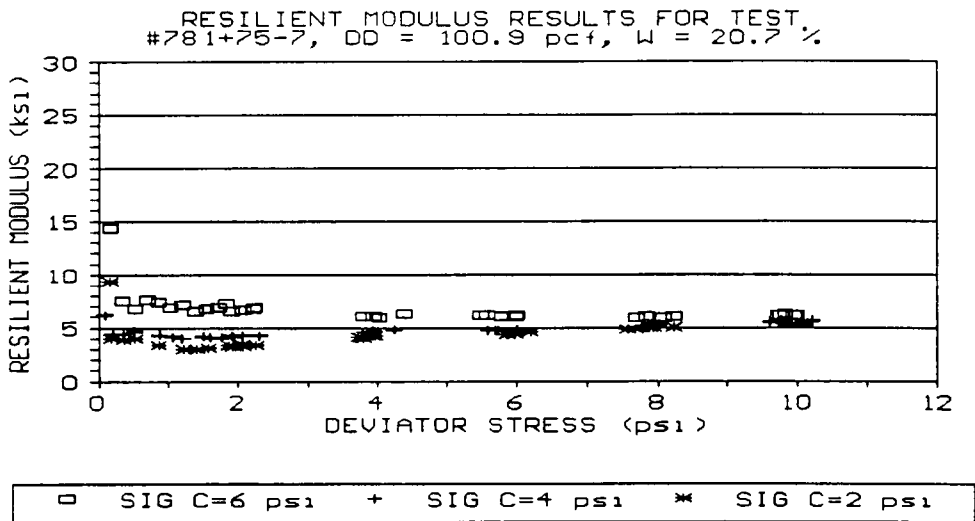


Figure A-60. Resilient Response For State Route 20 Station 781+75 Test No. 7

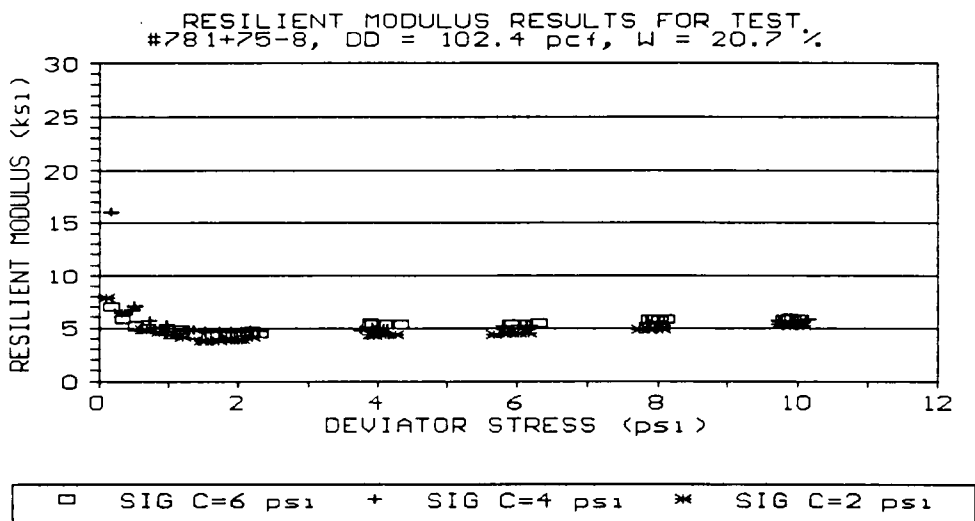


Figure A-61. Resilient Response For State Route 20 Station 781+75 Test No. 8

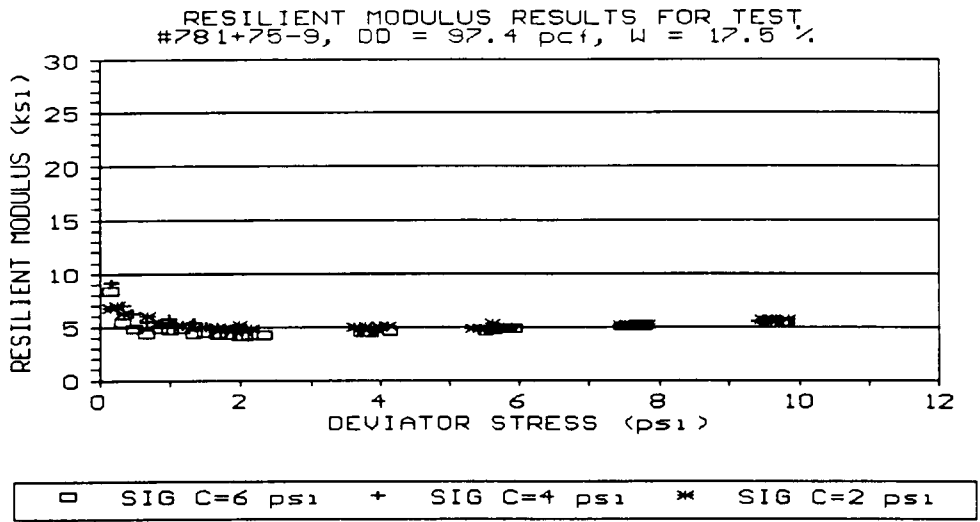


Figure A-62. Resilient Response For State Route 20 Station 781+75 Test No. 9

State Route 20 Station 1081+50

**Model Parameters
and
Resilient Modulus Plots**

Table A-7. Hyperbolic and Log-Log Model Parameters For State Route 20 Station 1081+50 Resilient Modulus Tests

TEST NO.	DRY DENSITY (pcf)	WATER CONTENT (%)	HYPERBOLIC MODEL		LOG-LOG MODEL	
			a	b	K ₁	K ₂
1	106.6	17.4	0.5801	9.6109	10.6955	-.1640
2	105.6	17.4	0.7368	6.2415	7.1393	.0028
3	105.1	18.1	2.9689	7.7811	11.1668	-.4093
4	99.8	13.7	0.4364	8.6874	10.2252	-.1166
5	105.2	14.0	0.9028	8.3186	8.8657	.3690
6	102.5	22.2	1.7996	1.3286	3.6812	-.2818
7	101.2	22.2	2.9888	1.9279	4.7011	-.3077
8	100.5	18.3	0.7460	4.5934	5.6919	-.1058

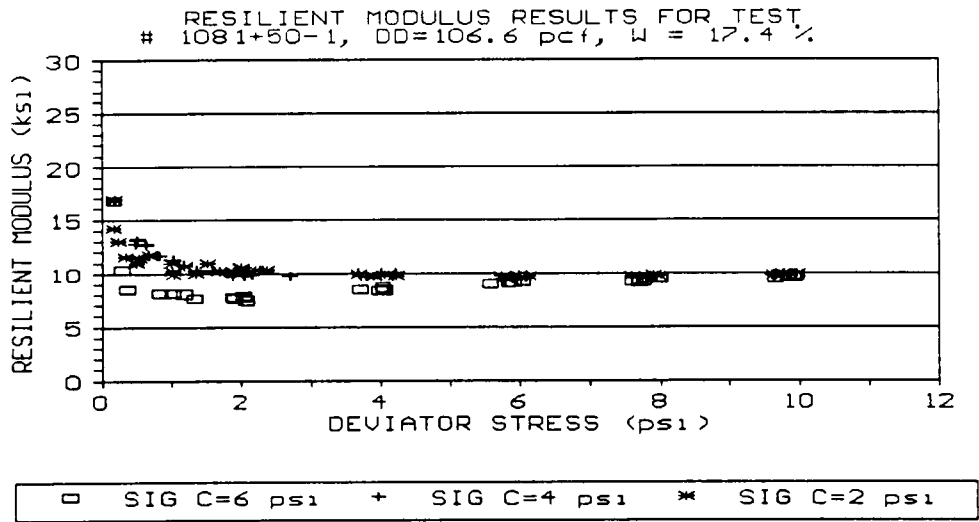


Figure A-63. Resilient Response For State Route 20 Station 1081+50 Test No. 1

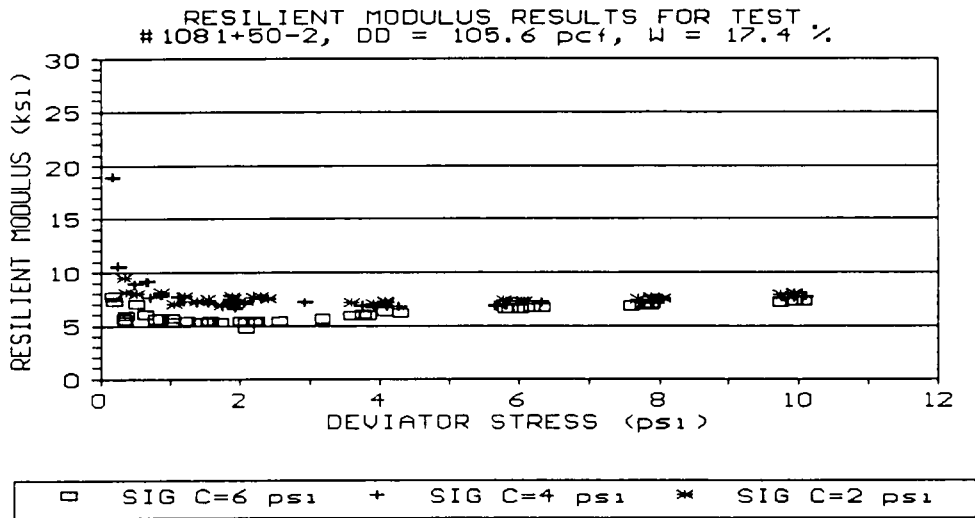


Figure A-64. Resilient Response For State Route 20 Station 1081+50 Test No. 2

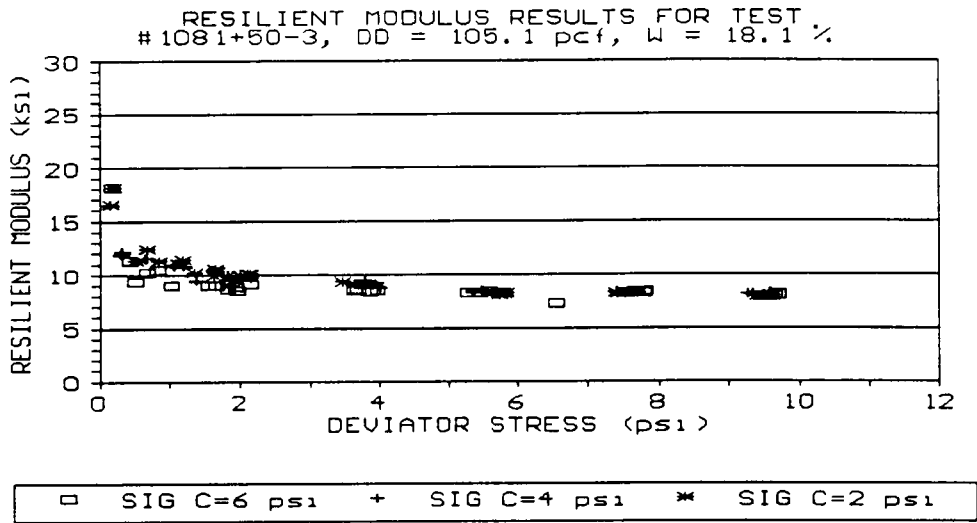


Figure A-65. Resilient Response For State Route 20 Station 1081+50 Test No. 3

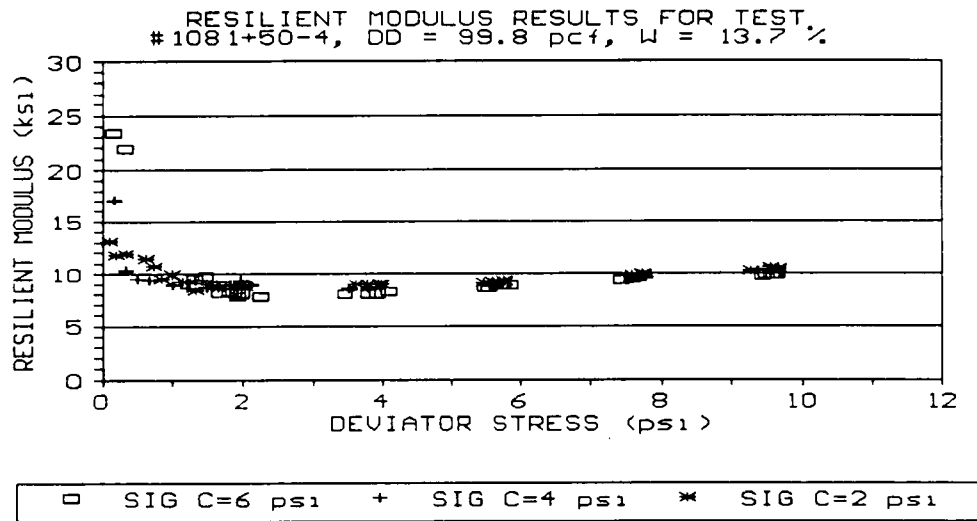


Figure A-66. Resilient Response For State Route 20 Station 1081+50 Test No. 4

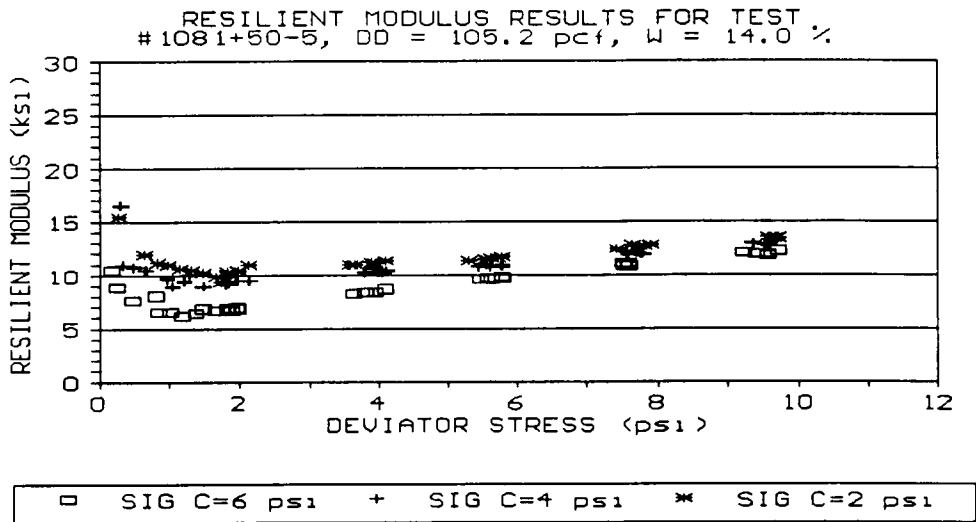


Figure A-67. Resilient Response For State Route 20 Station 1081+50 Test No. 5

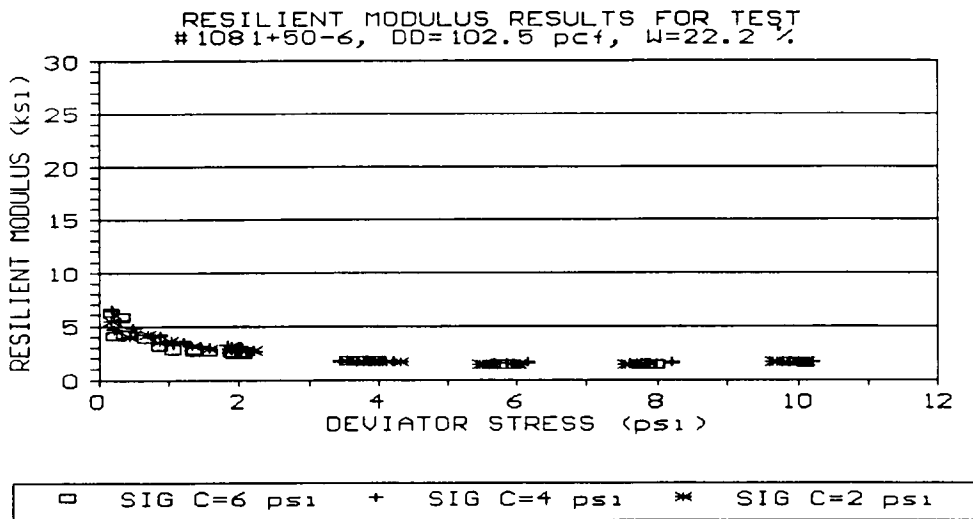


Figure A-68. Resilient Response For State Route 20 Station 1081+50 Test No. 6

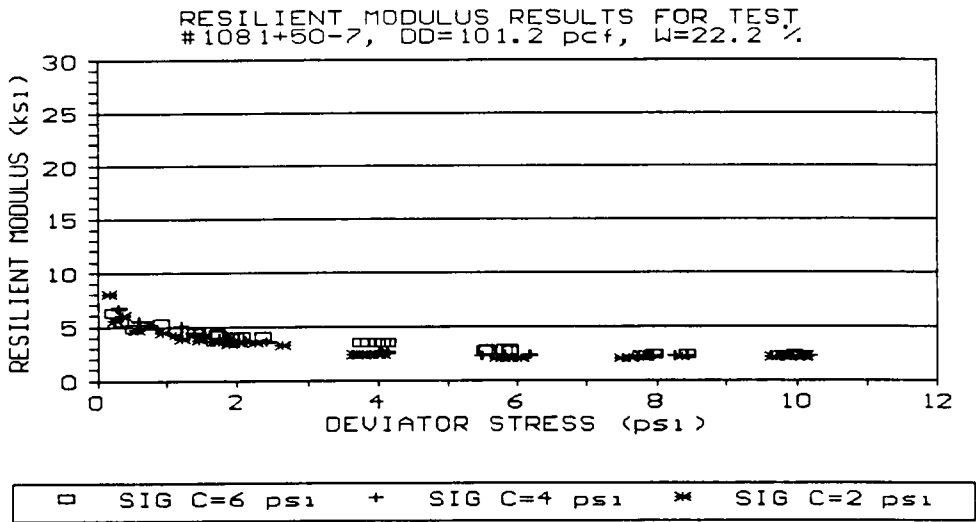


Figure A-69. Resilient Response For State Route 20 Station 1081+50 Test No. 7

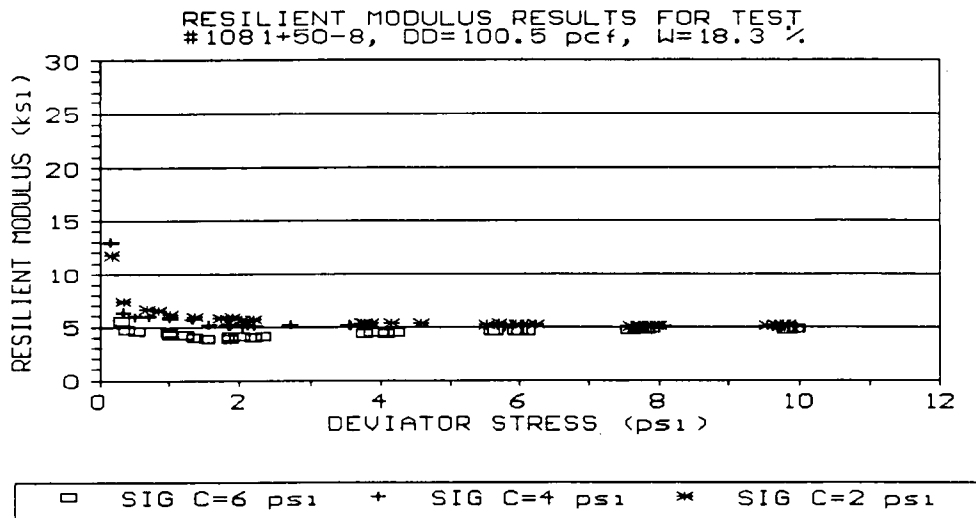


Figure A-70. Resilient Response For State Route 20 Station 1081+50 Test No. 8

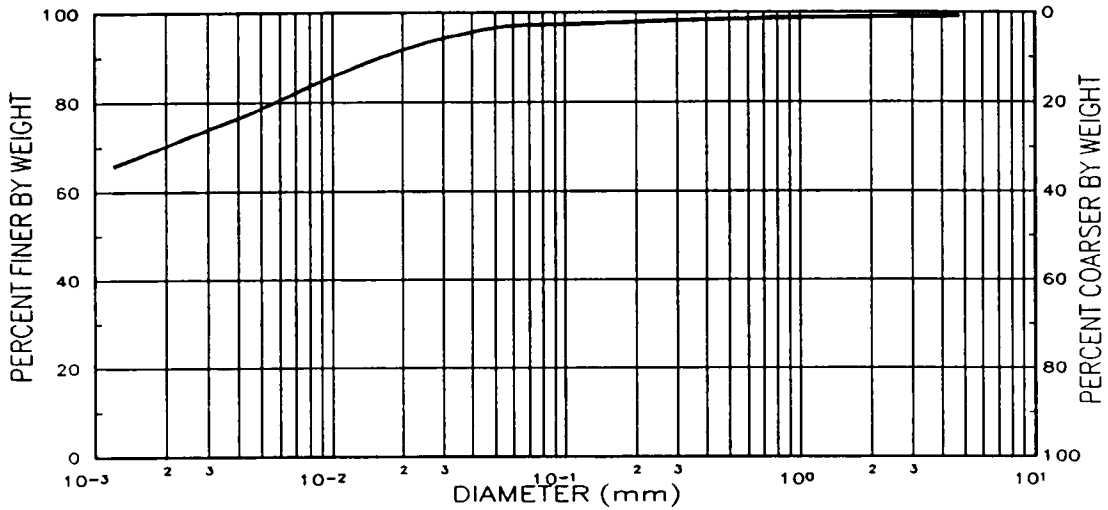
APPENDIX B
DESIGN HANDBOOK OF RESILIENT RESPONSE

**Rutledge Pike
Design Handbook**

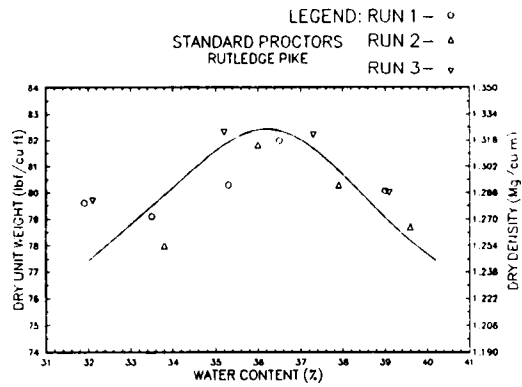
LOCATION: RUTLEDGE PIKE	
SOIL CLASSIFICATION	
AASHTO	USCS
A-7-6 (50)	CH

CLAY CONTENT (%)	PASSING #200 SIEVE (%)	ATTERBERG LIMITS			SPECIFIC GRAVITY OF SOLIDS	CBR VALUE	
		LL	PL	PI		0.1"	0.2"
70.3	97.8	71	28	43	2.60	3.3	3.0

GRAIN SIZE DISTRIBUTION
RUTLEDGE PIKE



Grain Size Distribution

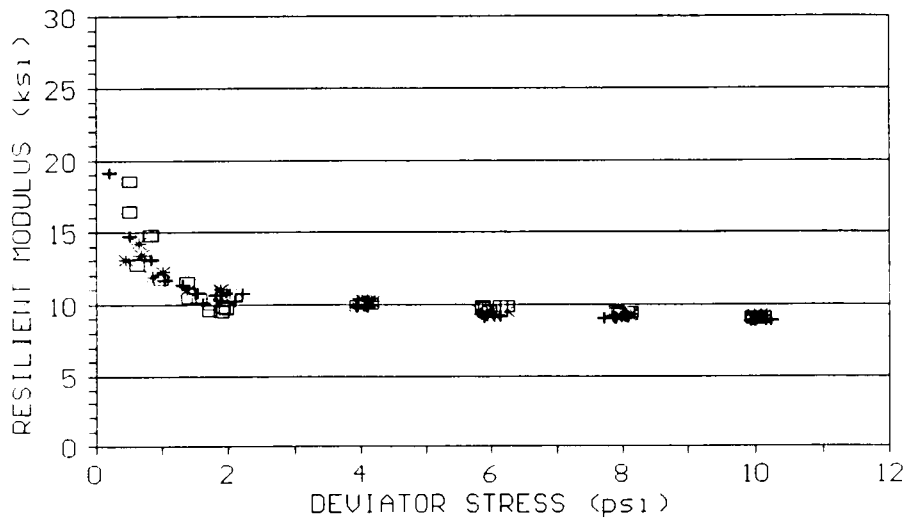


Standard Proctor Moisture-Density Relationship

Hyperbolic and Log-Log Model Parameters

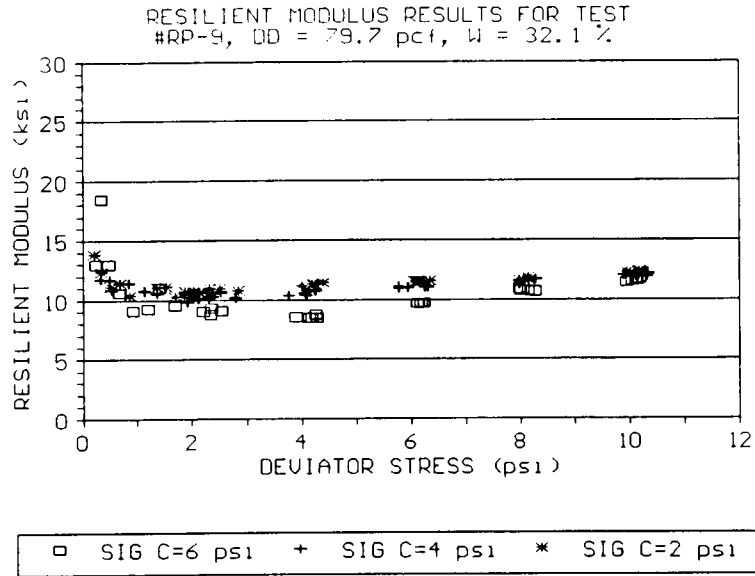
TEST NO.	DRY DENSITY (pcf)	WATER CONTENT (%)	HYPERBOLIC MODEL		LOG-LOG MODEL	
			a	b	K ₁	K ₂
4	82.4	32.4	3.7475	8.7295	12.2786	-.3909
9	79.7	32.1	0.2389	10.0799	10.6158	.0713
5	82.2	35.7	5.7173	5.1267	9.0876	-.4016
6	79.4	35.7	5.4376	4.5213	8.3214	-.3859
2	79.6	39.4	5.5570	2.9230	6.7198	-.3839

RESILIENT MODULUS RESULTS FOR TEST #RP-4, DD = 82.4 pcf, W = 32.4 %

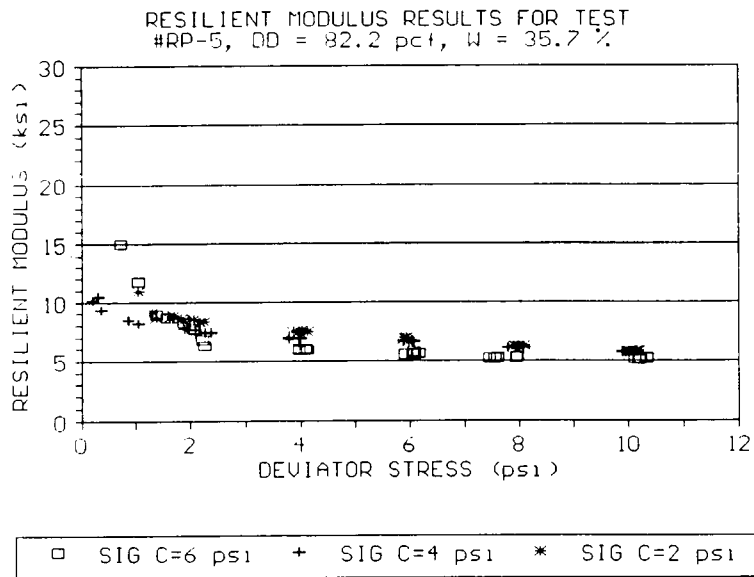


□ SIG C=6 psi + SIG C=4 psi * SIG C=2 psi

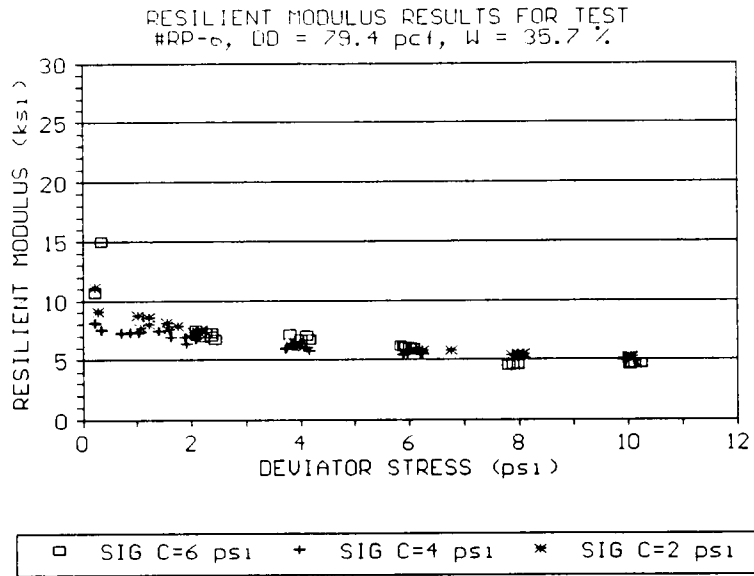
Resilient Response at Low Water Content, High Density



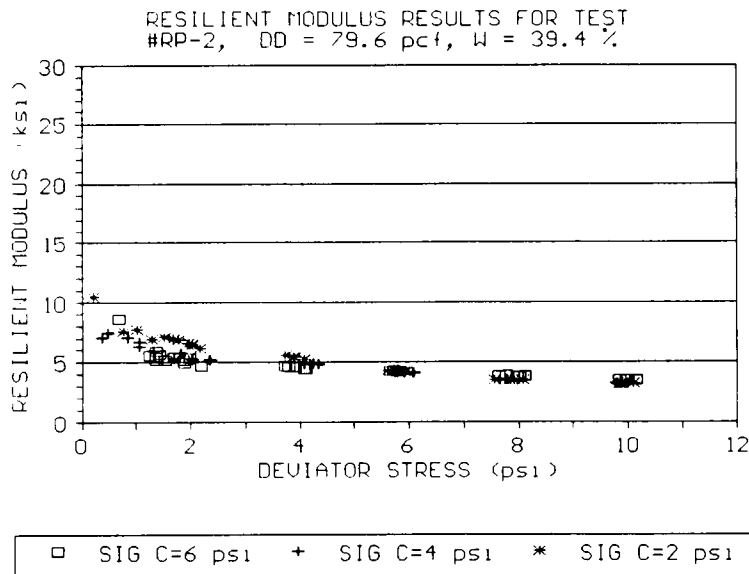
Resilient Response at Low Water Content, Low Density



Resilient Response at Optimum Water Content, High Density



Resilient Response at Optimum Water Content, Low Density



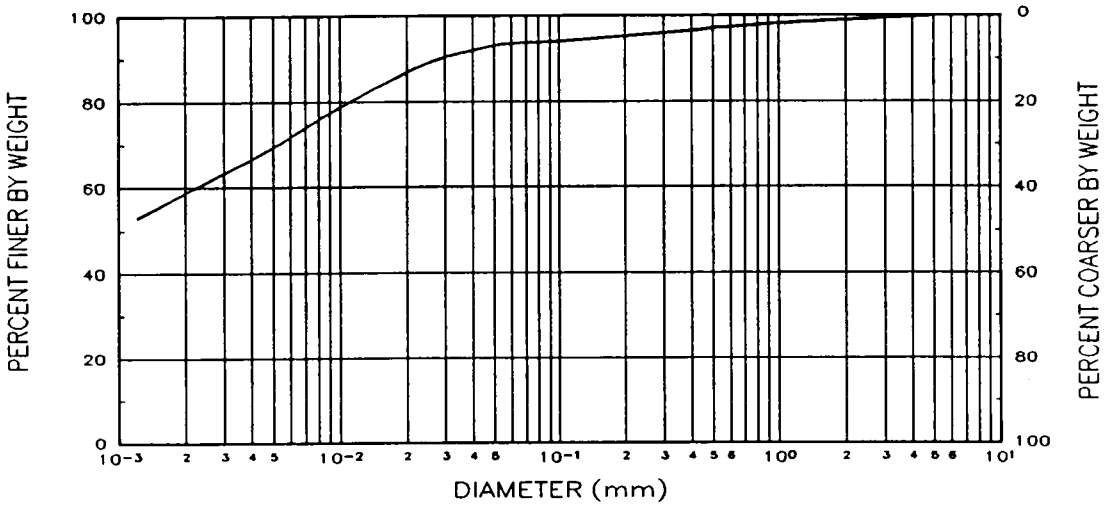
Resilient Response at High Water Content, Low Density

Pellissippi Parkway Station 400
Design Handbook

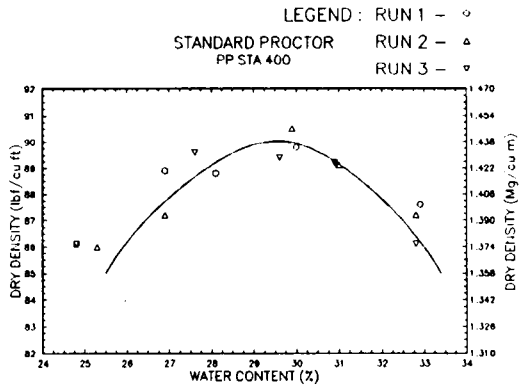
LOCATION: PELLISSIPPI PARKWAY STATION 400	
SOIL CLASSIFICATION	
AASHTO	USCS
A-7-5 (36)	MH

CLAY CONTENT (%)	PASSING #200 SIEVE (%)	ATTERBERG LIMITS			SPECIFIC GRAVITY OF SOLIDS	CBR VALUE	
		LL	PL	PI		0.1"	0.2"
58.6	94.2	70	41	29	2.61	6.2	5.3

GRAIN SIZE DISTRIBUTION
PELLISSIPPI PARKWAY STA 400



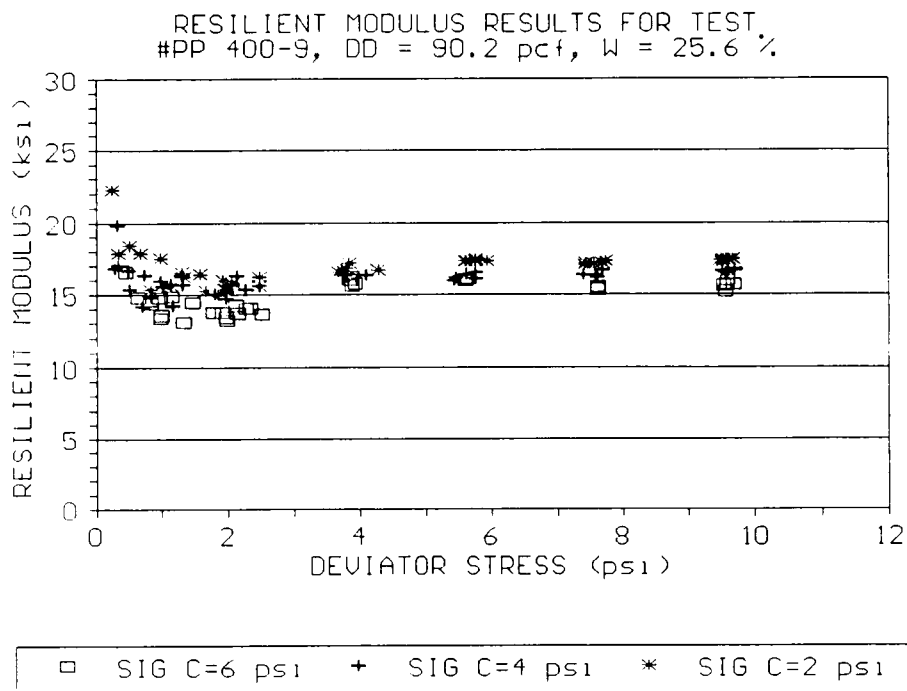
Grain Size Distribution



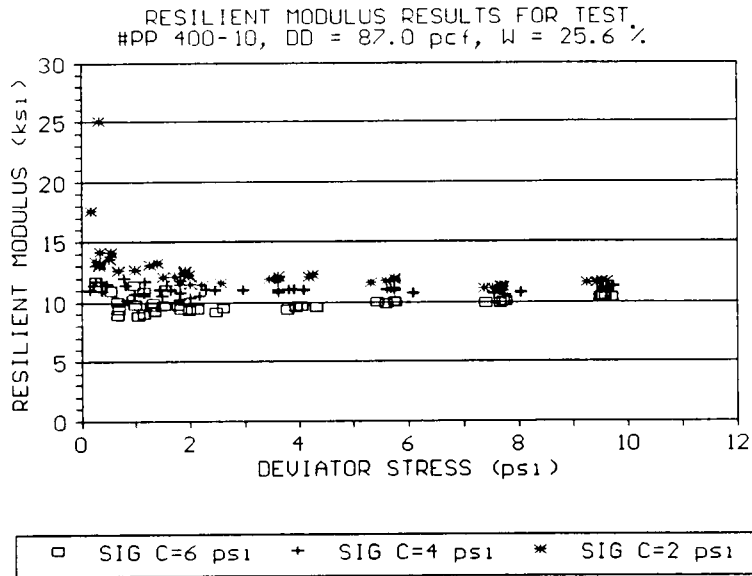
Standard Proctor Moisture-Density Relationship

Hyperbolic and Log-Log Model Parameters

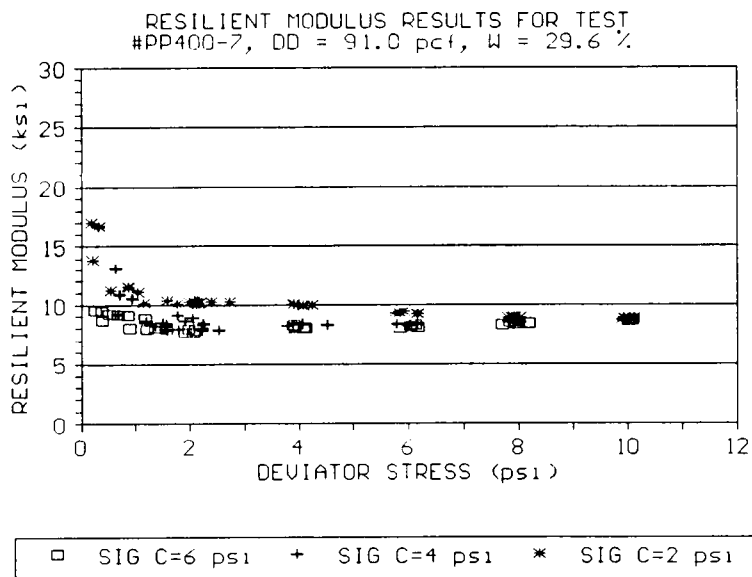
TEST NO.	DRY DENSITY (pcf)	WATER CONTENT (%)	HYPERBOLIC MODEL		LOG-LOG MODEL	
			a	b	K ₁	K ₂
9	90.2	25.6	0.8619	14.5811	15.6214	.0948
10	87.0	25.6	0.6270	10.5517	11.5623	-.1066
7	91.0	29.6	1.4153	8.2548	9.8835	-.1710
2	86.4	29.8	2.7282	6.3962	8.7345	-.2545
5	86.0	33.6	1.3472	5.3055	5.8074	-.0804



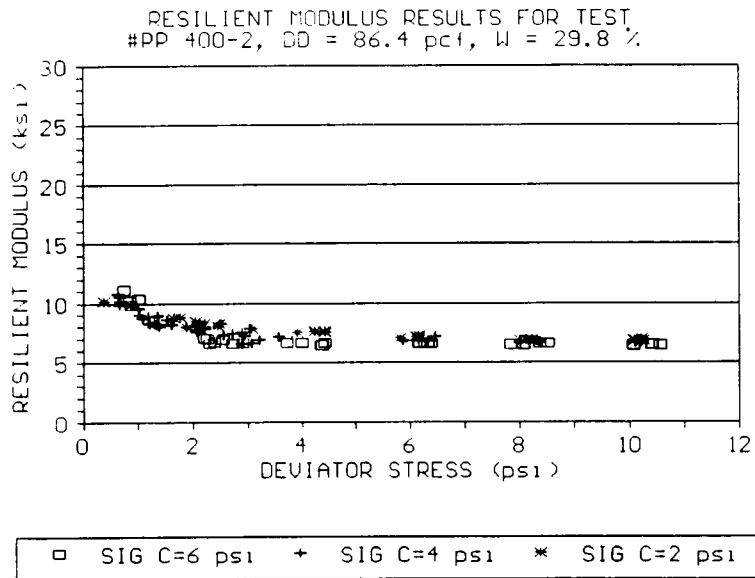
Resilient Response at Low Water Content, High Density



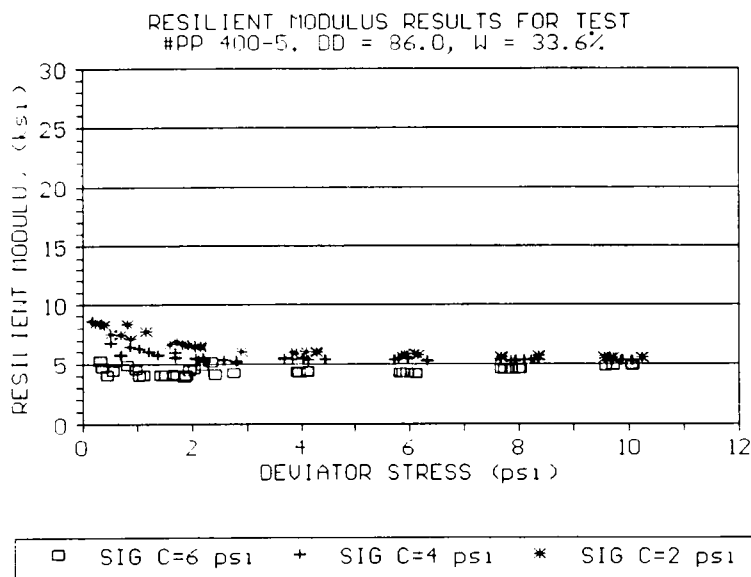
Resilient Response at Low Water Content, Low Density



Resilient Response at Optimum Water Content, High Density



Resilient Response at Optimum Water Content, Low Density



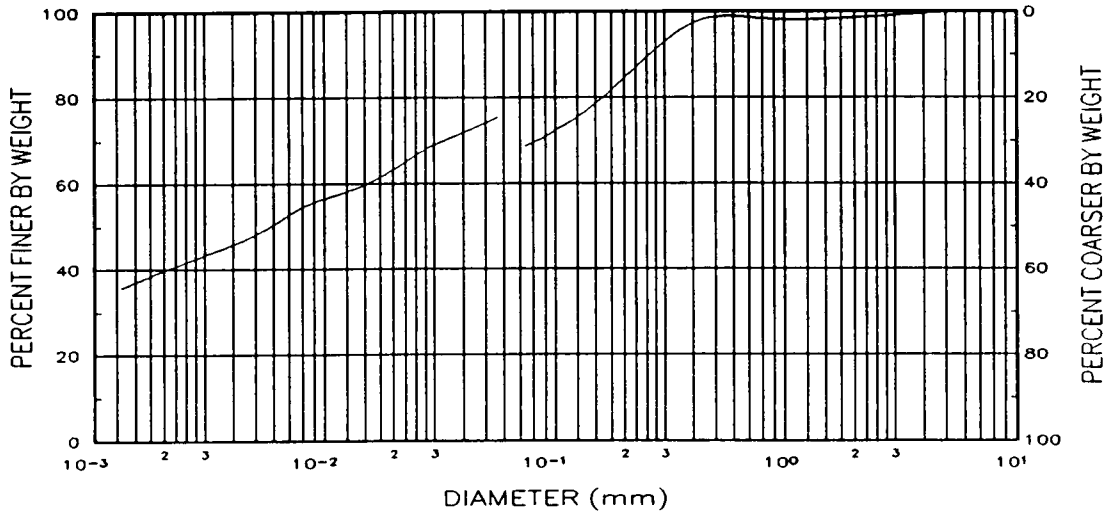
Resilient Response at High Water Content, Low Density

Pellissippi Parkway Station 500
Design Handbook

LOCATION: PELLISSIPPI PARKWAY STATION 500	
SOIL CLASSIFICATION	
AASHTO	USCS
A-7-6 (15)	CL

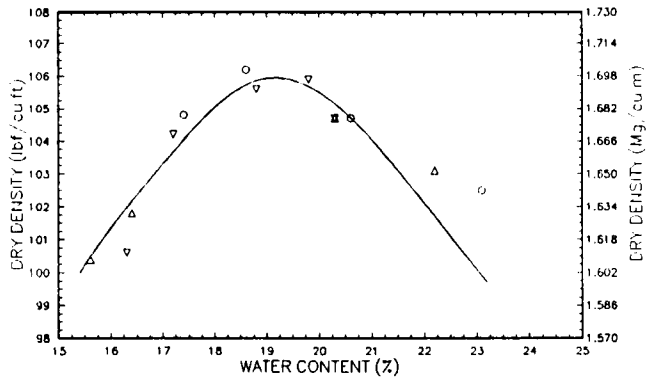
CLAY CONTENT (%)	PASSING #200 SIEVE (%)	ATTERBERG LIMITS			SPECIFIC GRAVITY OF SOLIDS	CBR VALUE	
		LL	PL	PI		0.1"	0.2"
39.9	70.4	45	22	23	2.70	4.5	3.1

GRAIN SIZE DISTRIBUTION
PELLISSIPPI PARKWAY STA 500



Grain Size Distribution

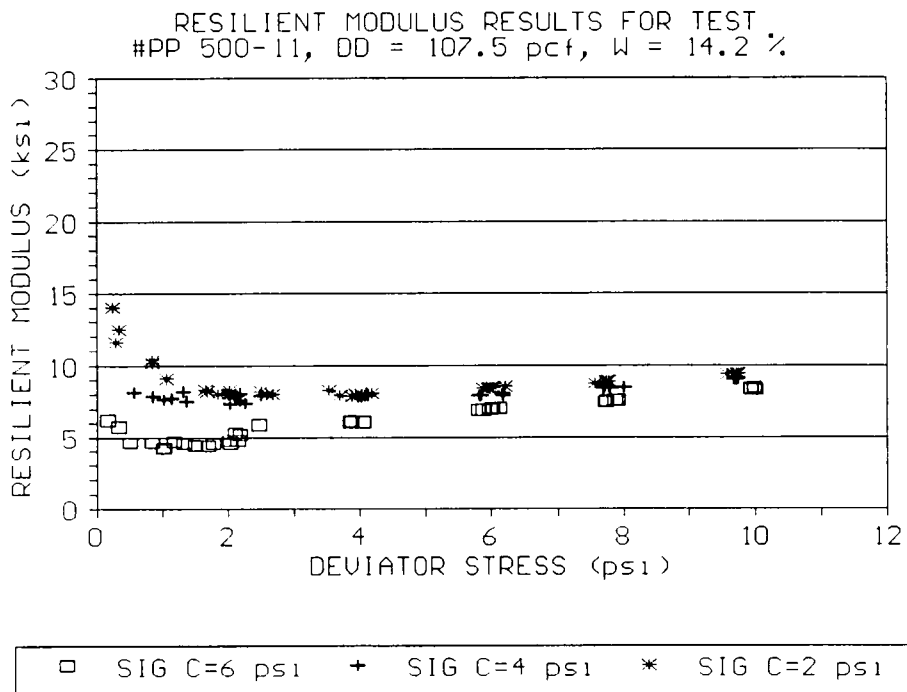
LEGEND: RUN 1 - ○
STANDARD PROCTORS RUN 2 - △
PP STA 500 RUN 3 - ▽



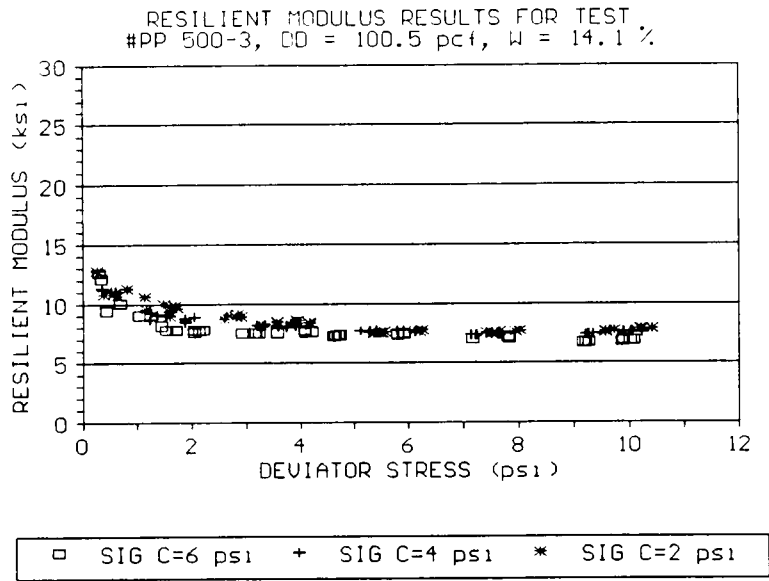
Standard Proctor Moisture-Density Relationship

Hyperbolic and Log-Log Model Parameters

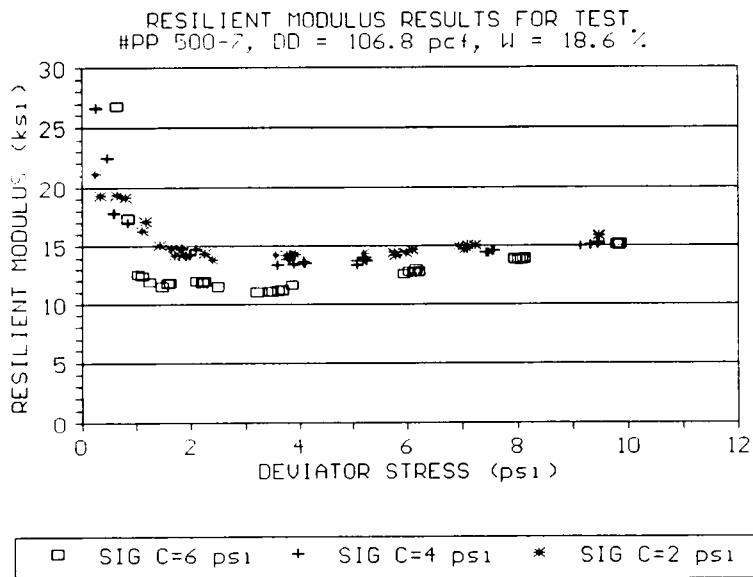
TEST NO.	DRY DENSITY (pcf)	WATER CONTENT (%)	HYPERBOLIC MODEL		LOG-LOG MODEL	
			a	b	K ₁	K ₂
11	107.5	14.2	.7695	7.6365	6.9751	.1664
3	100.5	14.1	2.8599	7.0657	9.5198	-.2714
7	106.8	18.6	3.0519	12.3001	15.3235	-.1423
5	101.3	18.6	5.0636	11.2551	15.2328	-.4319
9	101.6	22.3	6.6993	5.5799	10.4411	-.4992



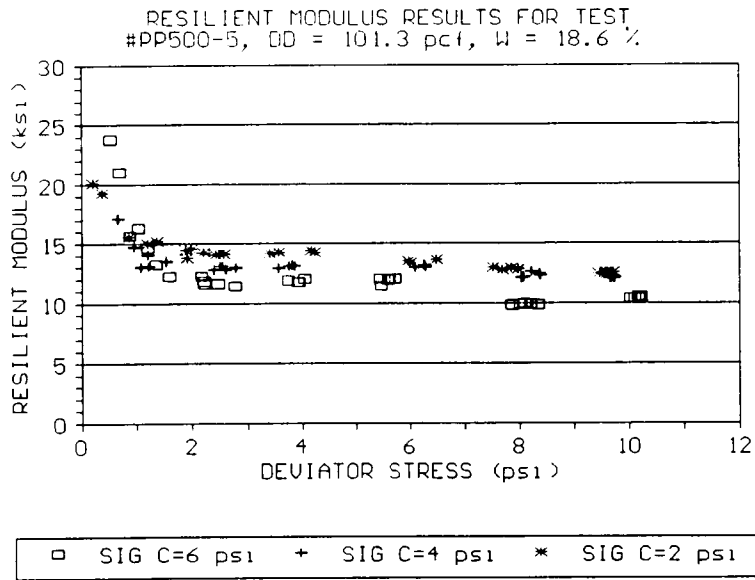
Resilient Response at Low Water Content, High Density



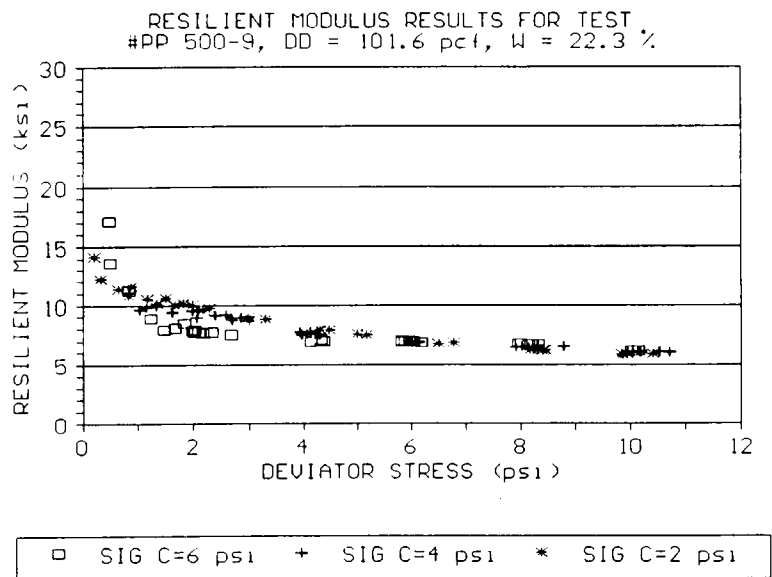
Resilient Response at Low Water Content, Low Density



Resilient Response at Optimum Water Content, High Density



Resilient Response at Optimum Water Content, Low Density



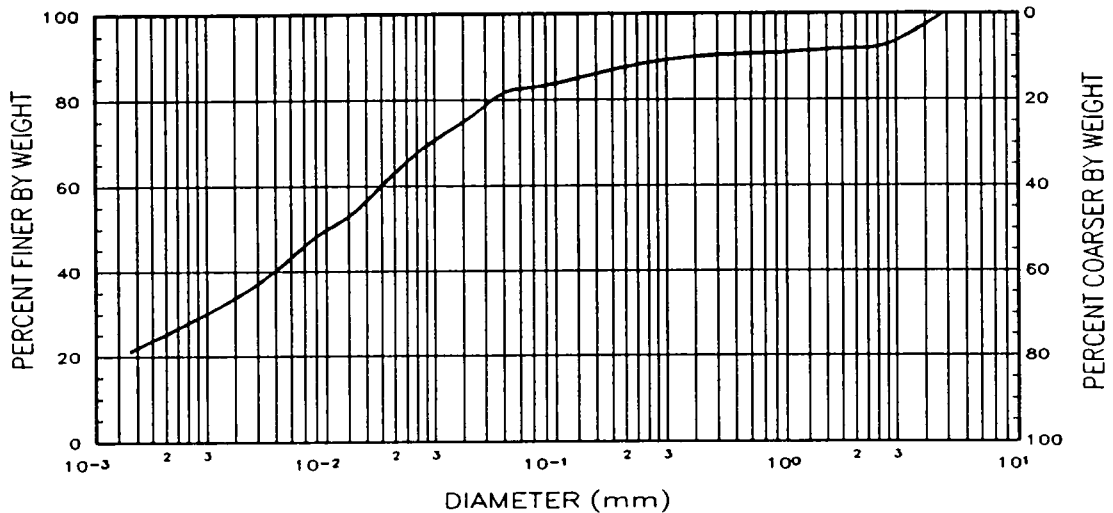
Resilient Response at High Water Content, Low Density

Airport Connector Station 47
Design Handbook

LOCATION: AIRPORT CONNECTOR STATION 47	
SOIL CLASSIFICATION	
AASHTO	USCS
A-6 (8)	CL

CLAY CONTENT (%)	PASSING #200 SIEVE (%)	ATTERBERG LIMITS			SPECIFIC GRAVITY OF SOLIDS	CBR VALUE	
		LL	PL	PI		0.1"	0.2"
25.4	72.3	34	21	13	2.65	3.9	3.3

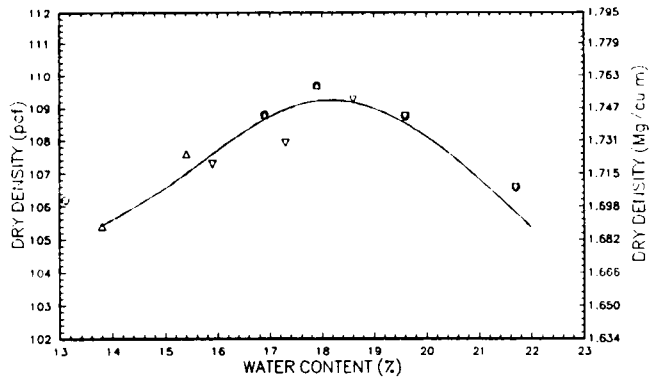
GRAIN SIZE DISTRIBUTION
AIRPORT CONNECTOR STATION 47



Grain Size Distribution

STANDARD PROCTORS
1-40 AIRPORT CONNECTOR STA 47

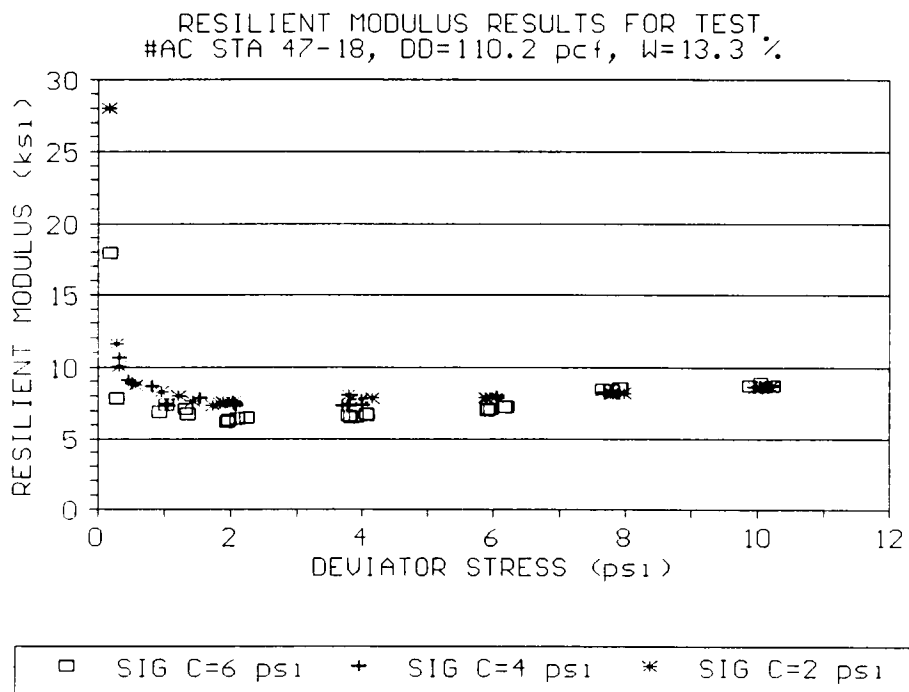
RUN 1 - ○
RUN 2 - △
RUN 3 - ▽



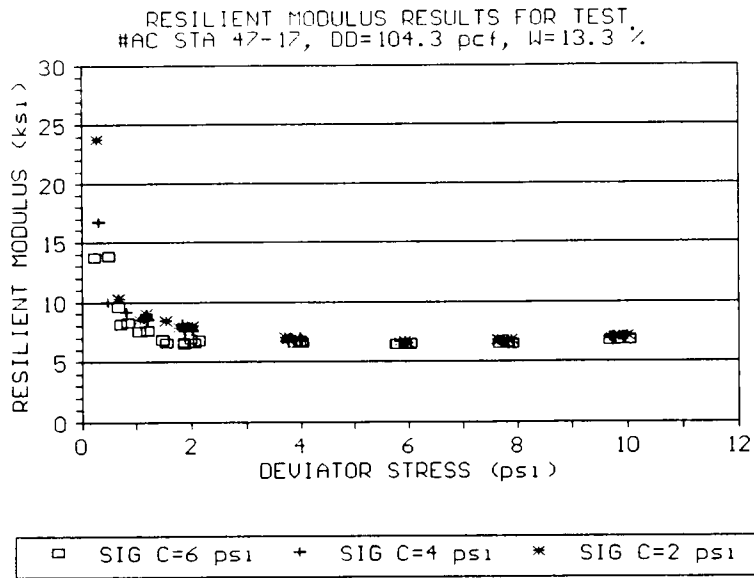
Standard Proctor Moisture-Density Relationship

Hyperbolic and Log-Log Model Parameters

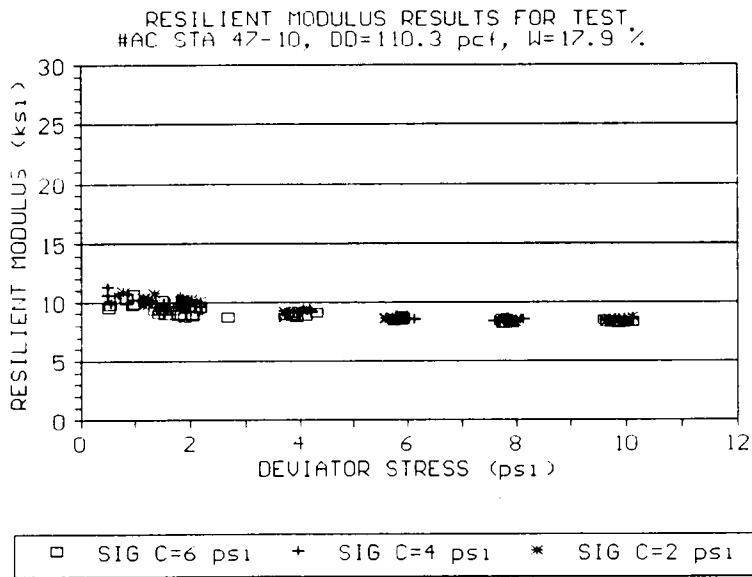
TEST NO.	DRY DENSITY (pcf)	WATER CONTENT (%)	HYPERBOLIC MODEL		LOG-LOG MODEL	
			a	b	K ₁	K ₂
18	110.2	13.3	0.6641	7.0828	8.5724	-.0653
17	104.3	13.3	1.2631	6.6482	9.1826	-.3281
10	110.3	17.9	2.7474	8.1537	10.0081	-.1895
9	103.1	17.9	3.5478	3.7733	6.4020	-.2759
11	105.3	21.1	1.6265	1.6165	3.6634	-.2440



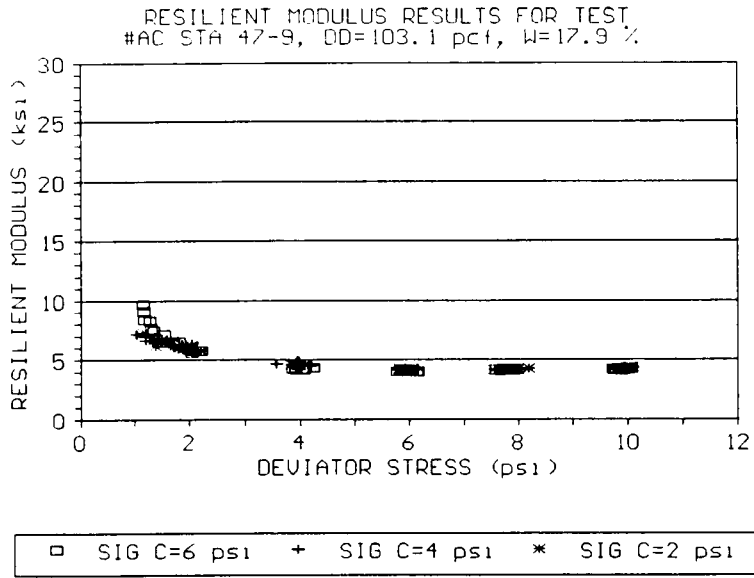
Resilient Response at Low Water Content, High Density



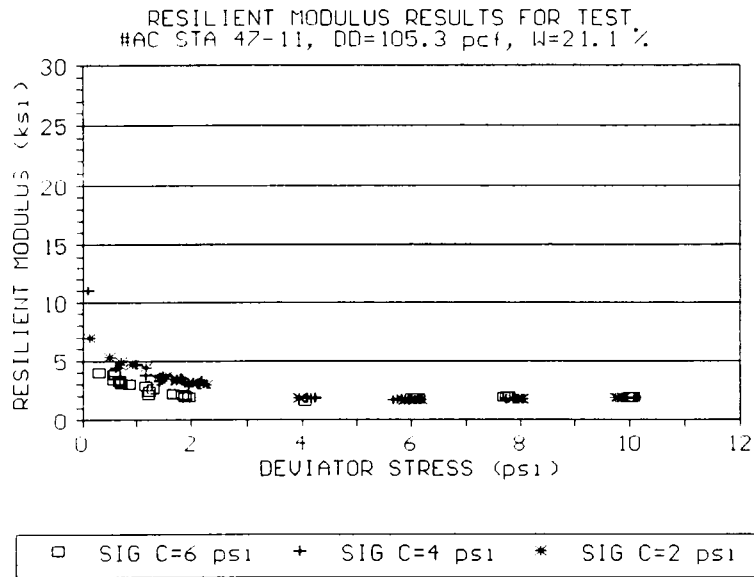
Resilient Response at Low Water Content, Low Density



Resilient Response at Optimum Water Content, High Density



Resilient Response at Optimum Water Content, Low Density



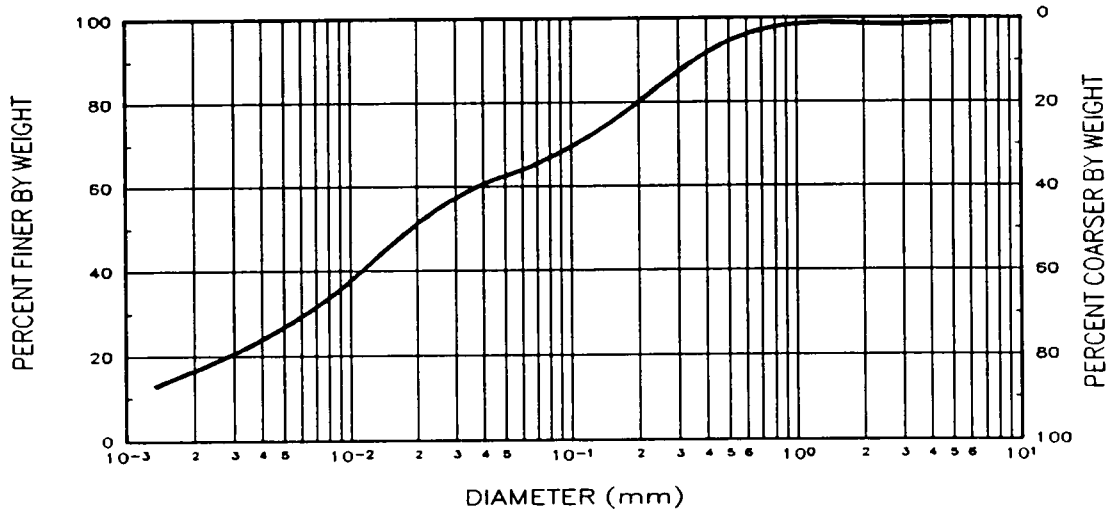
Resilient Response at High Water Content, Low Density

Airport Connector Station 85
Design Handbook

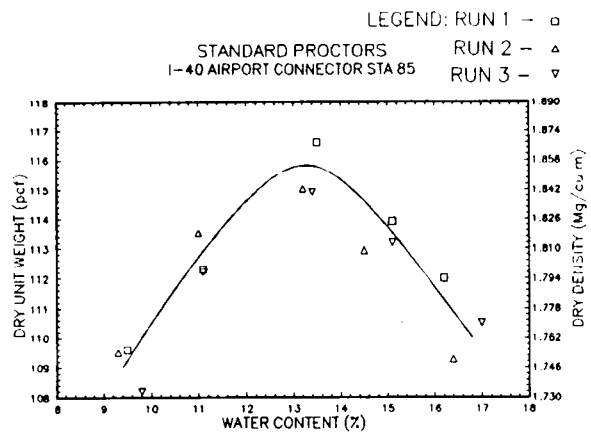
LOCATION: AIRPORT CONNECTOR STATION 85	
SOIL CLASSIFICATION	
AASHTO	USCS
A-4 (0)	CL-ML

CLAY CONTENT (%)	PASSING #200 SIEVE (%)	ATTERBERG LIMITS			SPECIFIC GRAVITY OF SOLIDS	CBR VALUE	
		LL	PL	PI		0.1"	0.2"
16.7	56.1	21	16	5	2.60	5.0	4.6

GRAIN SIZE DISTRIBUTION
AIRPORT CONNECTOR STATION 85



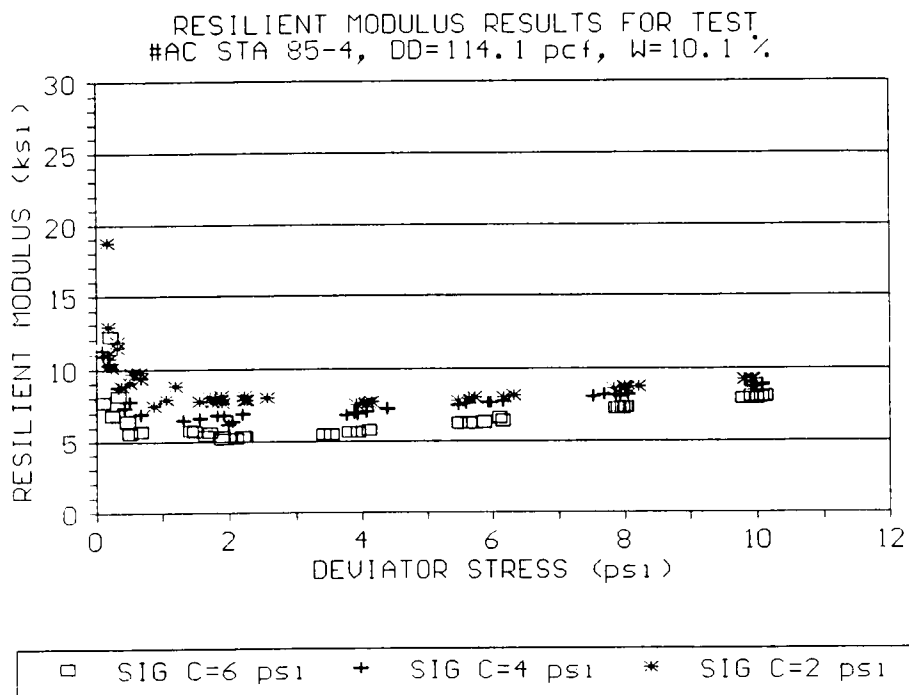
Grain Size Distribution



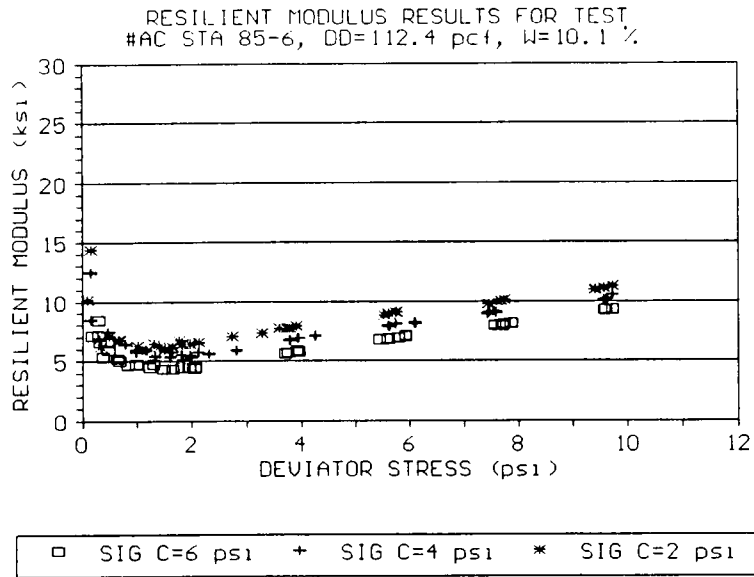
Standard Proctor Moisture-Density Relationship

Hyperbolic and Log-Log Model Parameters

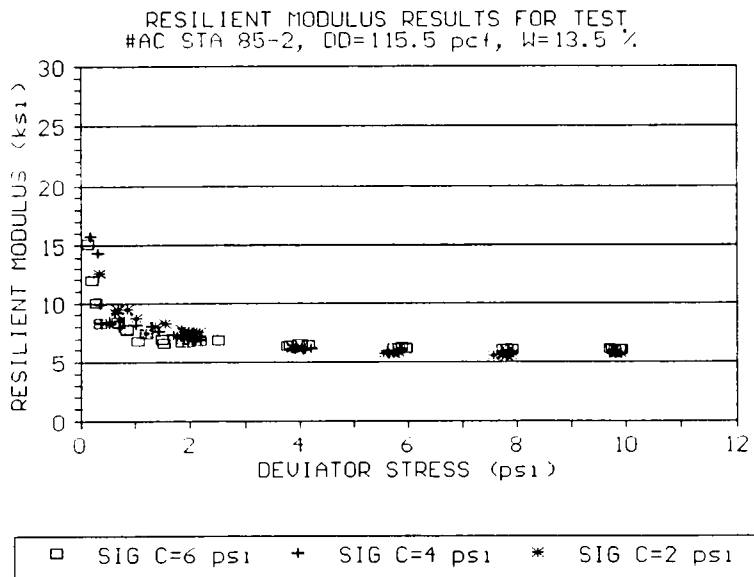
TEST NO.	DRY DENSITY (pcf)	WATER CONTENT (%)	HYPERBOLIC MODEL		LOG-LOG MODEL	
			a	b	K ₁	K ₂
4	114.1	10.1	0.3690	6.6849	8.1582	-.0479
6	112.4	10.1	0.7400	4.6201	5.7433	.4131
2	115.5	13.5	2.5410	5.5604	8.9439	-.4173
9	113.0	13.5	1.3944	5.7018	6.9803	-.1547
8	113.3	15.0	0.4594	2.0007	2.4095	.0025



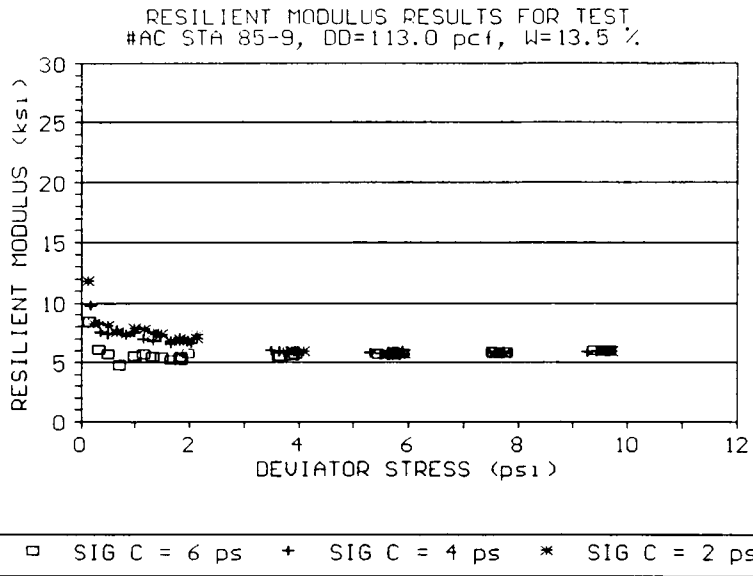
Resilient Response at Low Water Content, High Density



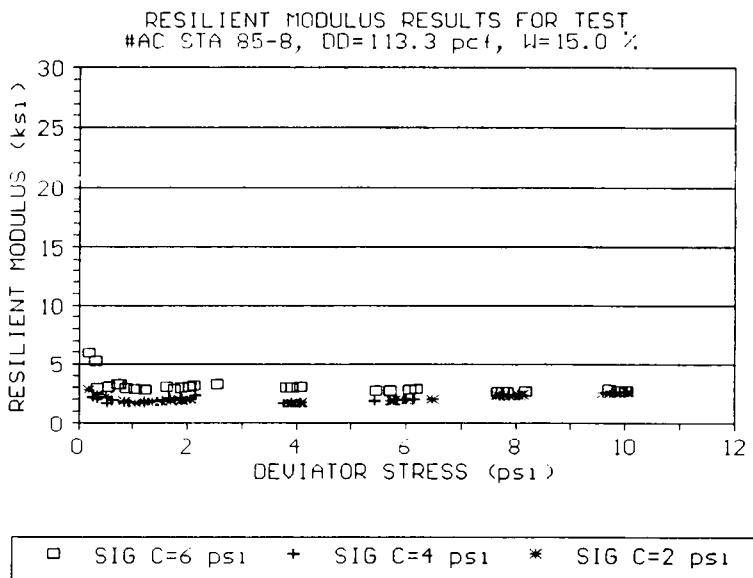
Resilient Response at Low Water Content, Low Density



Resilient Response at Optimum Water Content, High Density



Resilient Response at Optimum Water Content, Low Density



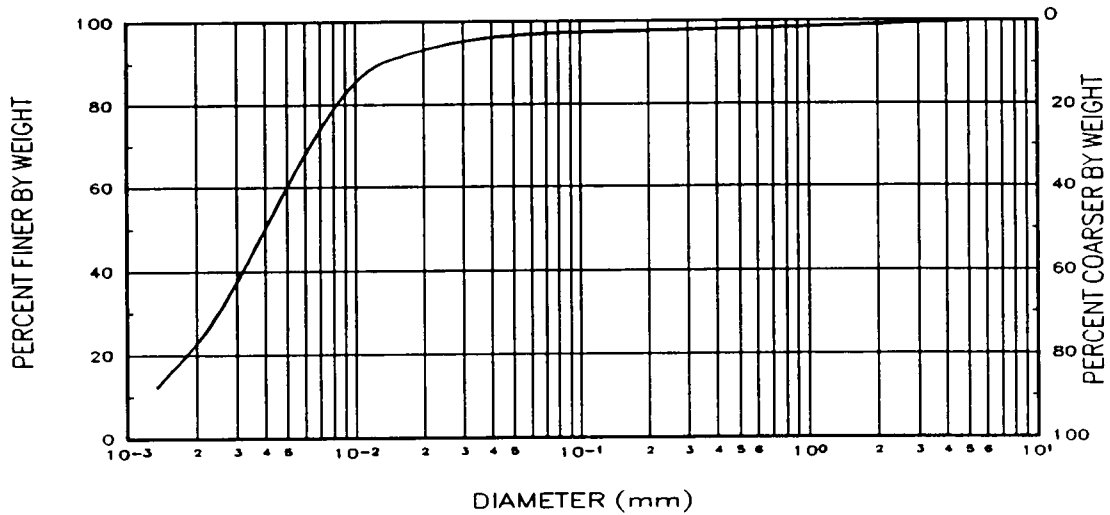
Resilient Response at High Water Content, Low Density

State Route 20 Station 781+75
Design Handbook

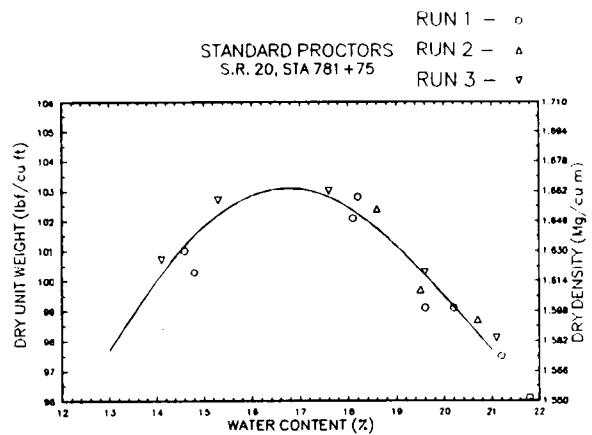
LOCATION: STATE ROUTE 20 STATION 781+75	
SOIL CLASSIFICATION	
AASHTO	USCS
A-4 (0)	ML

CLAY CONTENT (%)	PASSING #200 SIEVE (%)	ATTERBERG LIMITS			SPECIFIC GRAVITY OF SOLIDS	CBR VALUE	
		LL	PL	PI		0.1"	0.2"
22.9	97.2	24	22	2	2.59	11.2	13.6

GRAIN SIZE DISTRIBUTION
S.R. 20 STA 781 +75



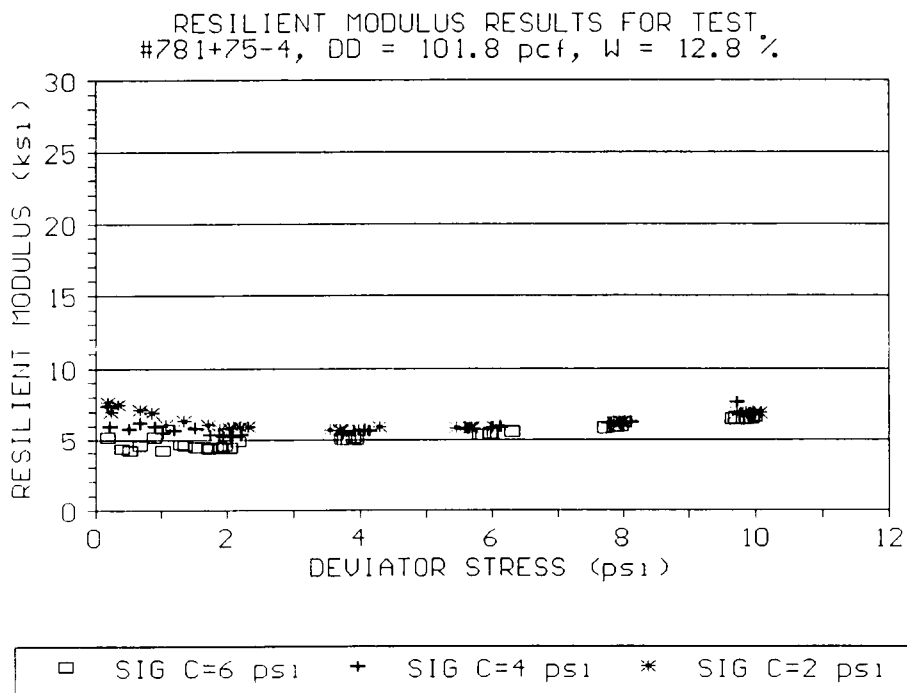
Grain Size Distribution



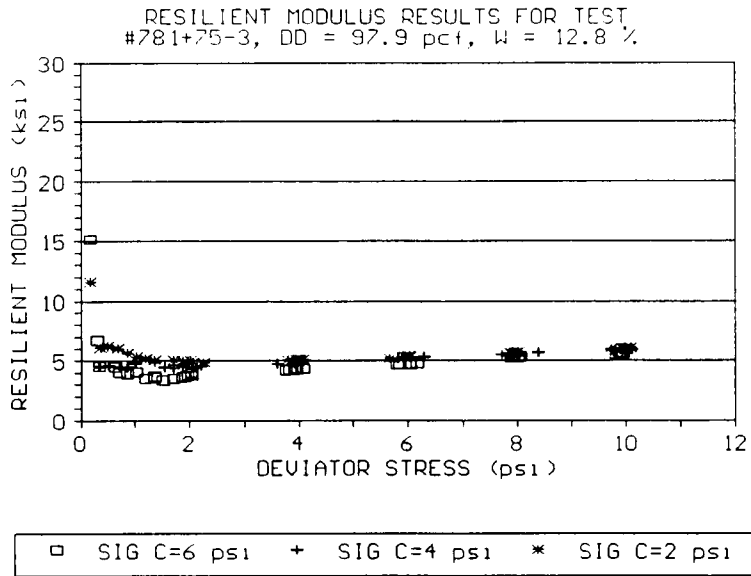
Standard Proctor Moisture-Density Relationship

Hyperbolic and Log-Log Model Parameters

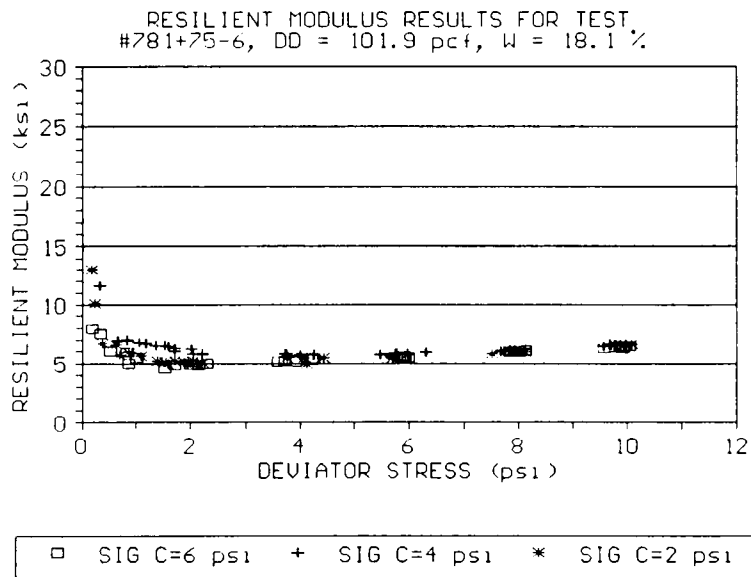
TEST NO.	DRY DENSITY (pcf)	WATER CONTENT (%)	HYPERBOLIC MODEL		LOG-LOG MODEL	
			a	b	K ₁	K ₂
4	101.8	12.8	0.3059	5.1552	5.3168	.1151
3	97.9	12.8	0.1463	4.5233	5.1024	.0322
6	101.9	18.1	0.2252	5.4400	6.1178	-.0202
9	97.4	17.5	0.2763	4.6530	5.1424	-.0045
7	100.9	20.7	0.4569	4.4026	5.2426	.0141



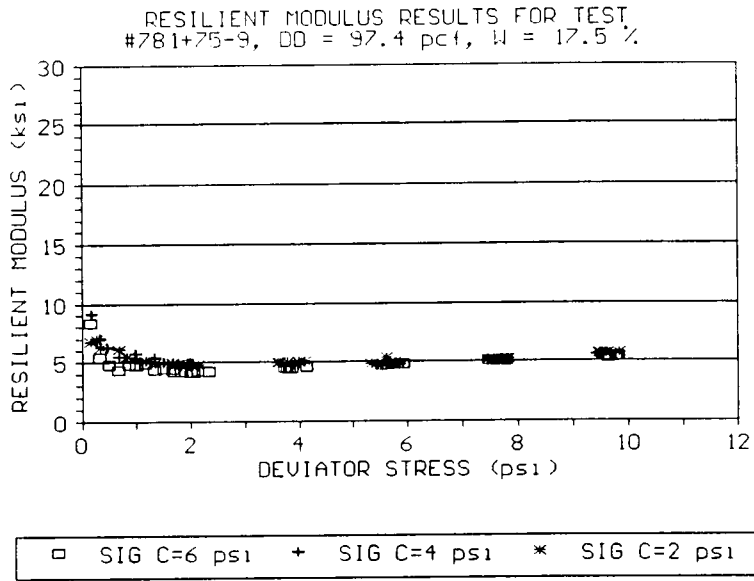
Resilient Response at Low Water Content, High Density



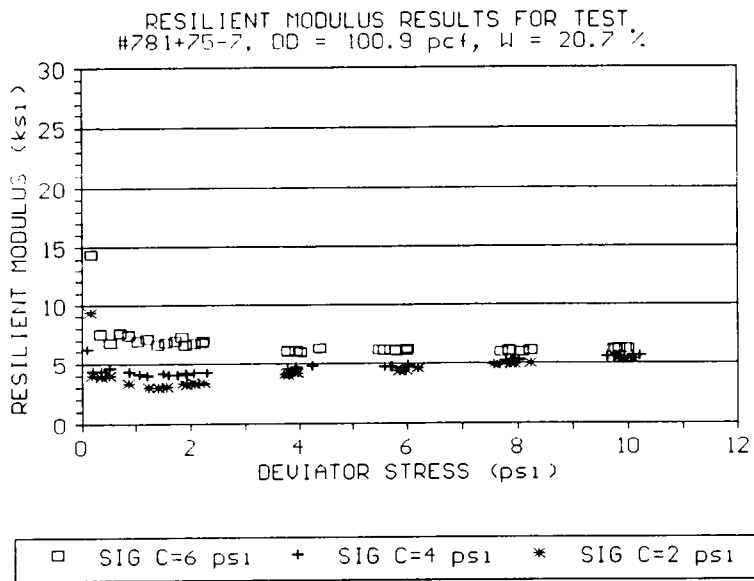
Resilient Response at Low Water Content, Low Density



Resilient Response at Optimum Water Content, High Density



Resilient Response at Optimum Water Content, Low Density



Resilient Response at High Water Content, Low Density

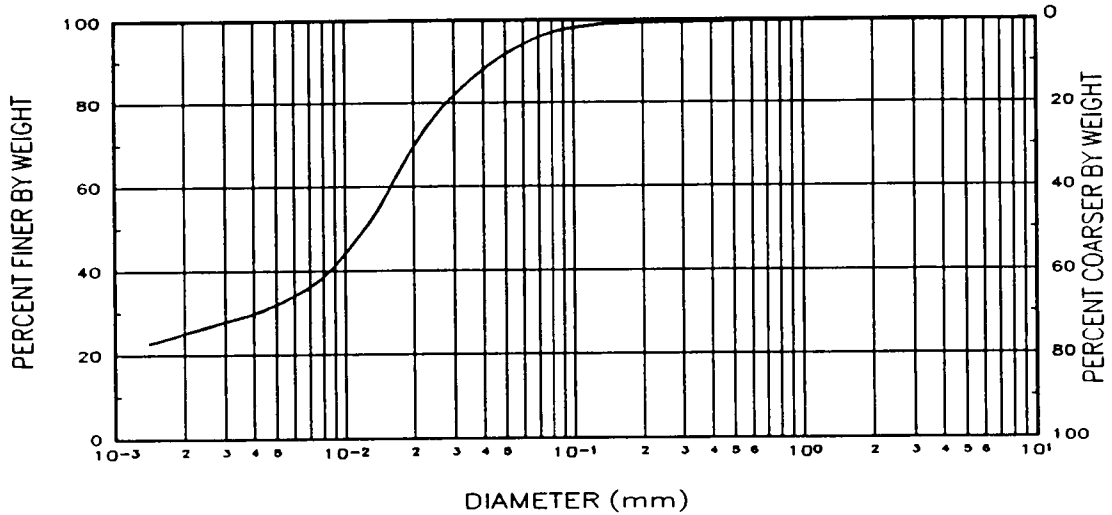
State Route 20 Station 1081+50

Design Handbook

LOCATION: STATE ROUTE 20 STATION 1081+50	
SOIL CLASSIFICATION	
AASHTO	USCS
A-6 (13)	CL

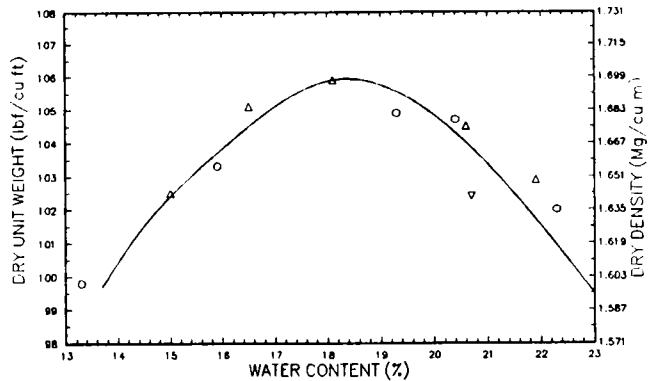
CLAY CONTENT (%)	PASSING #200 SIEVE (%)	ATTERBERG LIMITS			SPECIFIC GRAVITY OF SOLIDS	CBR VALUE	
		LL	PL	PI		0.1"	0.2"
25.4	98.9	36	22	14	2.62	3.4	3.0

GRAIN SIZE DISTRIBUTION
S.R. 20 STA 1081+50



Grain Size Distribution

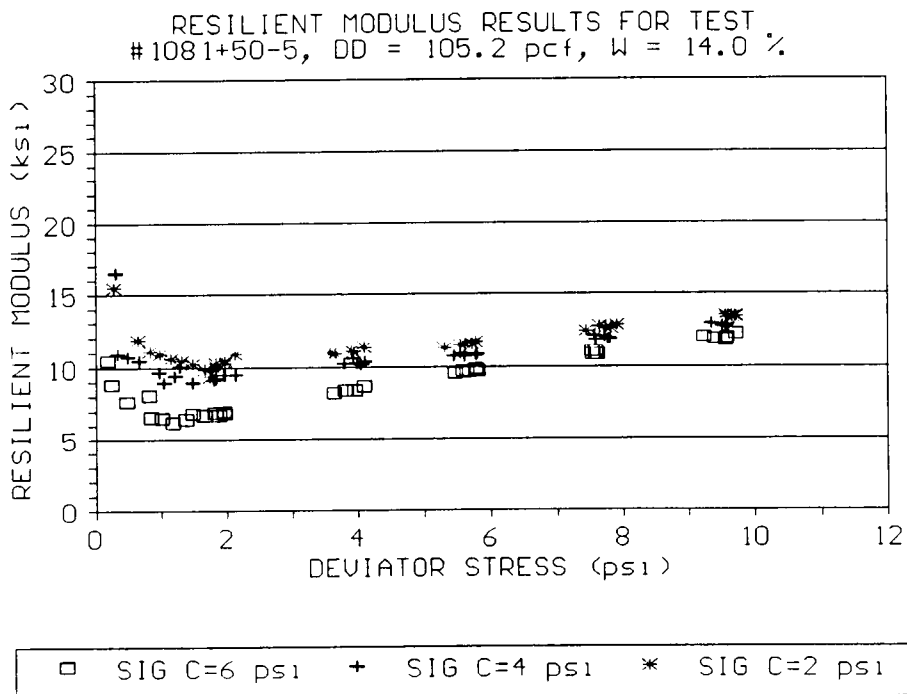
RUN 1 - o
STANDARD PROCTORS RUN 2 - Δ
S.R. 20, STA 1081+50 RUN 3 - ▽



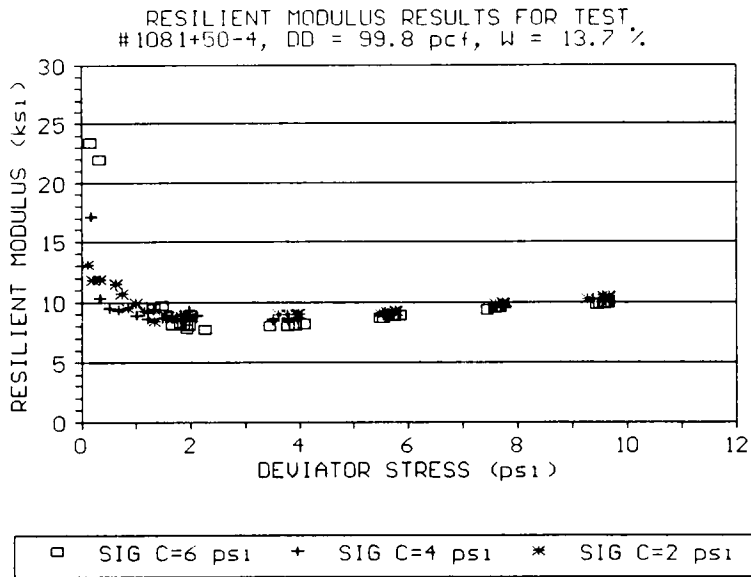
Standard Proctor Moisture-Density Relationship

Hyperbolic and Log-Log Model Parameters

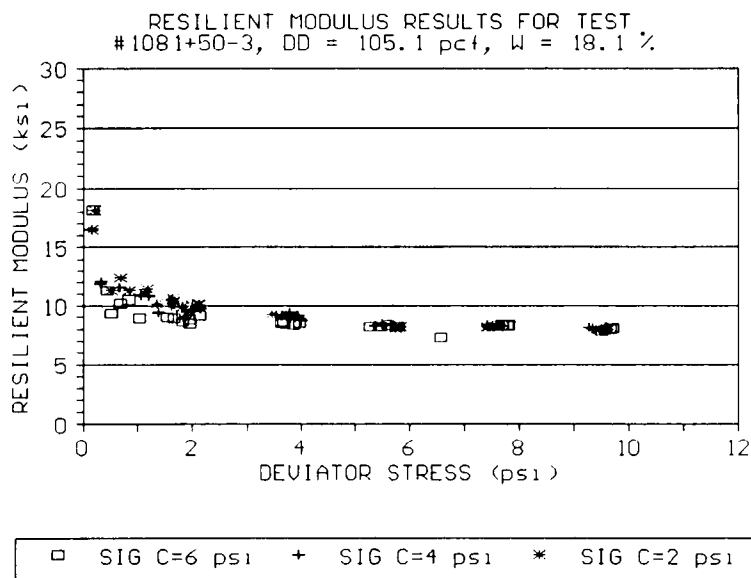
TEST NO.	DRY DENSITY (pcf)	WATER CONTENT (%)	HYPERBOLIC MODEL		LOG-LOG MODEL	
			a	b	K ₁	K ₂
5	105.2	14.0	0.9028	8.3186	8.8657	.3690
4	99.8	13.7	0.4364	8.6874	10.2252	-.1166
3	105.1	18.1	2.9689	7.7811	11.1668	-.4093
8	100.5	18.3	0.7460	4.5934	5.6919	-.1058
7	101.2	22.2	2.9888	1.9279	4.7011	-.3077



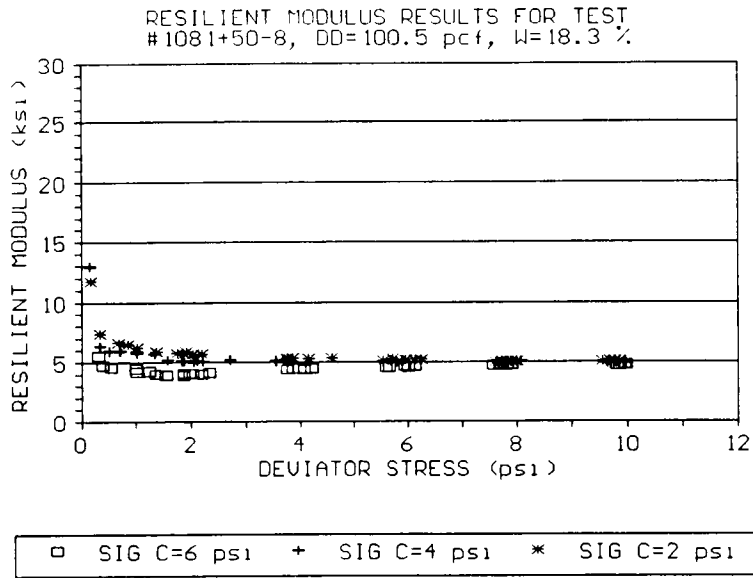
Resilient Response at Low Water Content, High Density



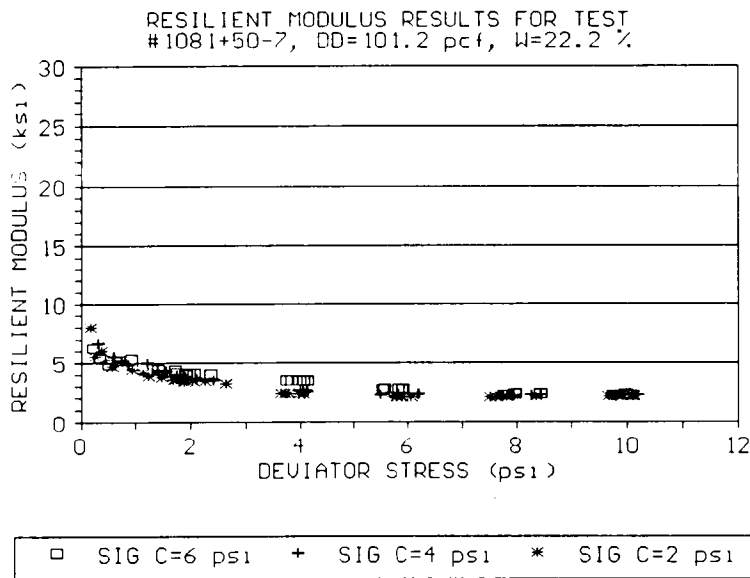
Resilient Response at Low Water Content, Low Density



Resilient Response at Optimum Water Content, High Density



Resilient Response at Optimum Water Content, Low Density



Resilient Response at High Water Content, Low Density

Examples of How Handbook May be Used to Estimate M_r

Example I

Known Soil Properties:

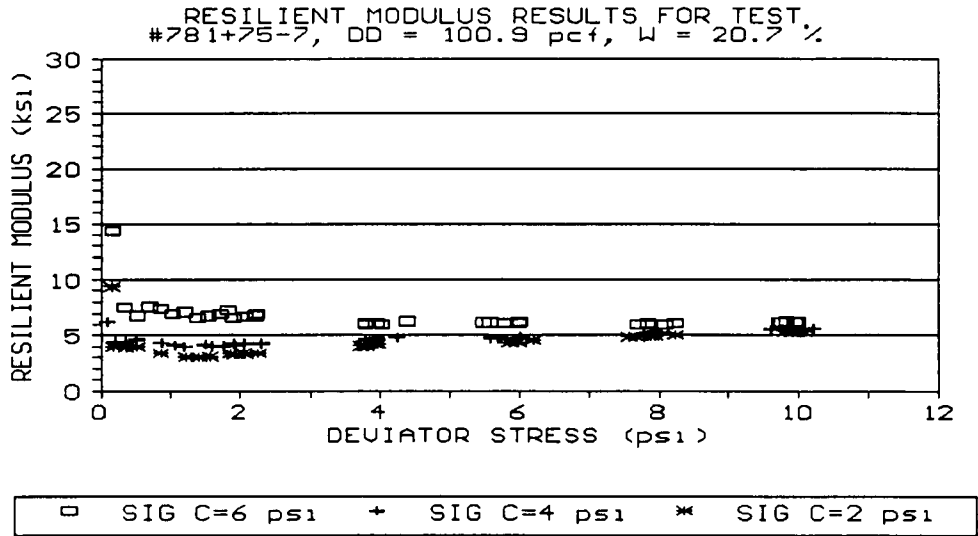
USCS Classification:	CL
AASHTO Classification:	A-4
Clay Content (%):	17
Passing #200 Sieve (%):	95
Liquid Limit:	30
Plastic Limit:	22
Plasticity Index:	8
Standard Proctor Maximum Dry Density (pcf):	103.5
Optimum Water Content (%):	18.0

Properties of A-4 Soils Tested:

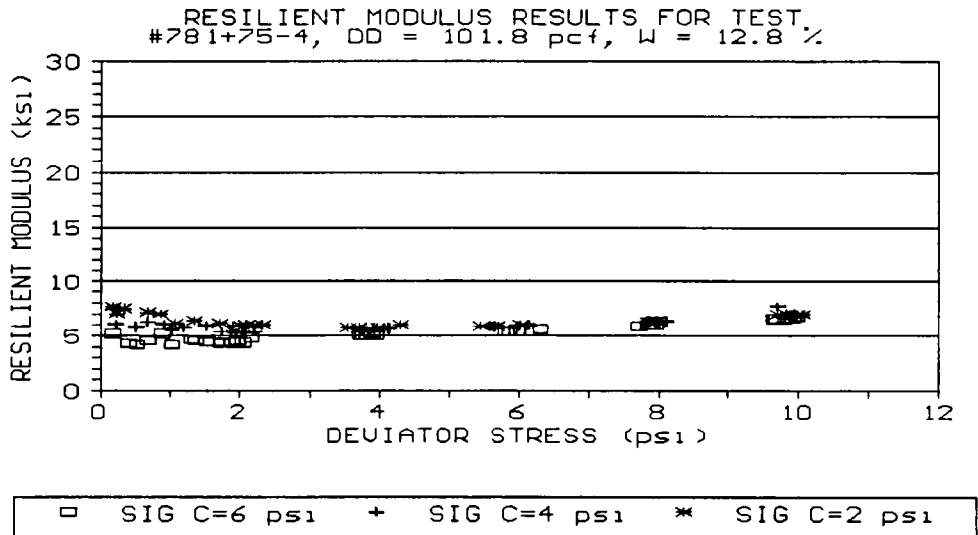
	<u>A.C. Sta. 85</u>	<u>Sta.781+75</u>
Clay Content (%):	16.7	22.9
Passing #200 Sieve (%):	56.1	97.2
Liquid Limit:	21	24
Plastic Limit:	16	22
Plasticity Index:	5	2
Max. Dry Density (pcf):	115.8	102.8
Optimum Water Content (%):	13.3	17.6

Since most of the properties of the new soil are closer to those of Sta. 781+75, use the Sta. 781+75 soil to get a range of resilient behavior. Since the dry density was found to have a negligible effect on the resilient response of the

A-4 soils tested, an estimation of the resilient modulus can be made based on water content using tests no. 7 and 9 for the Sta. 781+75 soil as shown below.



Resilient Modulus = 4 ksi



Resilient Modulus = 6 ksi

Interpolate for Optimum Water Content of 18% : $M_r = 4.7$ ksi

Example II

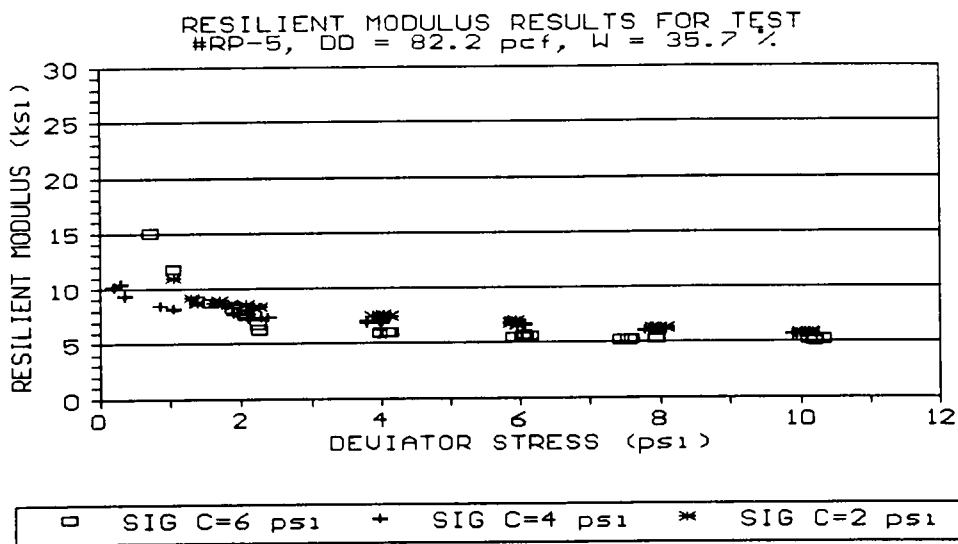
Known Soil Properties:

USCS Classification:	CL
AASHTO Classification:	A-7-6
Clay Content (%):	35
Passing #200 Sieve (%):	93
Liquid Limit:	37
Plastic Limit:	27
Plasticity Index:	10
Standard Proctor Maximum Dry Density (pcf):	94.6
Optimum Water Content (%):	23.1

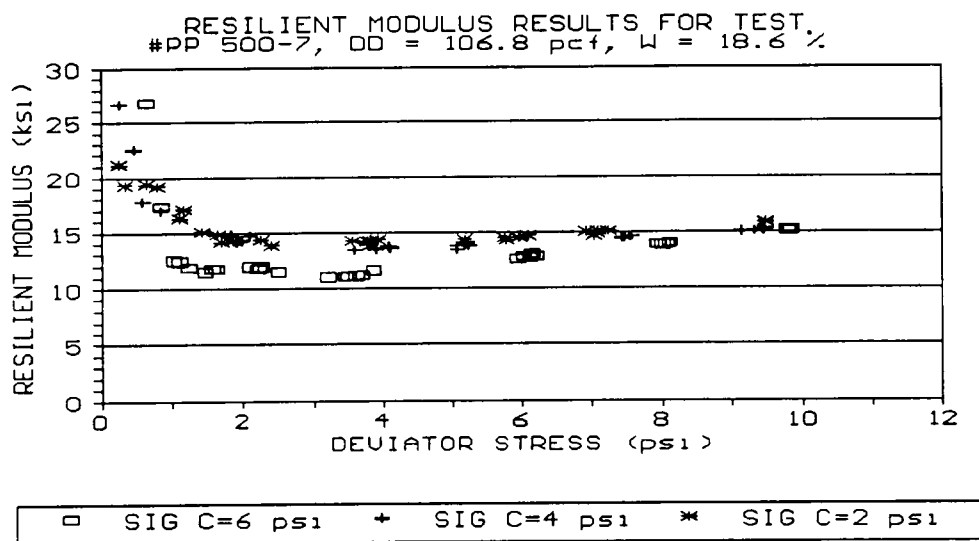
Properties of A-7-6 Soils Tested:

	<u>Rutledge Pike</u>	<u>P.P. Sta. 500</u>
Clay Content (%):	70.3	39.9
Passing #200 Sieve (%):	97.8	70.4
Liquid Limit:	71	45
Plastic Limit:	28	22
Plasticity Index:	43	23
Max. Dry Density (pcf):	82.5	106.0
Optimum Water Content (%):	36.2	18.7

The new soil has properties similar to both of the A-7-6 soils tested, so both soils will be used to get a range of resilient response at optimum water content and maximum dry density as shown below.



Resilient Modulus = 6 ksi



Resilient Modulus = 11 ksi

Interpolate on basis of dry density: $M_r = 8.5$ ksi
 Interpolate on basis of water content: $M_r = 11$ ksi
Average $M_r = 9.1$ ksi

VITA

Jamie Manis Hudson was born on December 25, 1961 in Chattanooga, Tennessee. She attended Senter and Boyd Buchanan Schools for an elementary education and graduated from Lookout Valley High School in June 1979. After working and being self-supporting for several years, she began attending evening classes at Chattanooga State Technical Community College. In January 1988 she entered Chattanooga State on a full time basis as a Civil Engineering Technology major. She transferred to the University of Tennessee, Knoxville in August 1988 and received a Bachelor of Science degree in Civil Engineering in May 1991. She entered graduate school as a Research Assistant in June 1991 and began working toward a Master of Science degree in Civil\Geotechnical Engineering. The Master of Science degree was conferred in December 1992.

The author is a member of Chi Epsilon, the American Society of Civil Engineers and the National Society of Professional Engineers. As an undergraduate she was awarded Tennessee Road Builders Association scholarships, served as treasurer of the Associated General Contractors student chapter and was active in the American Society of Civil Engineers student chapter. She also worked as a research assistant for the University of Tennessee Institute for Geotechnology from January 1990 to May 1991. The author received her Engineer-in-Training certification in December 1991.